Copyright Warning & Restrictions

The copyright law of the United States (Title 17, United States Code) governs the making of photocopies or other reproductions of copyrighted material.

Under certain conditions specified in the law, libraries and archives are authorized to furnish a photocopy or other reproduction. One of these specified conditions is that the photocopy or reproduction is not to be "used for any purpose other than private study, scholarship, or research." If a, user makes a request for, or later uses, a photocopy or reproduction for purposes in excess of "fair use" that user may be liable for copyright infringement,

This institution reserves the right to refuse to accept a copying order if, in its judgment, fulfillment of the order would involve violation of copyright law.

Please Note: The author retains the copyright while the New Jersey Institute of Technology reserves the right to distribute this thesis or dissertation

Printing note: If you do not wish to print this page, then select "Pages from: first page # to: last page #" on the print dialog screen

Kuo, Ted Lai-che

CRIMP-TYPE ELECTRICAL CONNECTORS

New Jersey Institute of Technology D.ENG.SC. 1982

PLEASE NOTE:

In all cases this material has been filmed in the best possible way from the available copy. Problems encountered with this document have been identified here with a check mark __✓__.

1. Glossy photographs or pages _____
2. Colored illustrations, paper or print _____
3. Photographs with dark background _____
4. Illustrations are poor copy _____
5. Pages with black marks, not original copy _____
6. Print shows through as there is text on both sides of page _____
7. Indistinct, broken or small print on several pages __✓__
8. Print exceeds margin requirements _____
9. Tightly bound copy with print lost in spine _____
10. Computer printout pages with indistinct print _____
11. Page(s) _____ lacking when material received, and not available from school or author.
12. Page(s) _____ seem to be missing in numbering only as text follows.
13. Two pages numbered _____. Text follows.
14. Curling and wrinkled pages _____
15. Other _____

CRIMP-TYPE ELECTRICAL CONNECTORS

BY

TED LAI-CHE KUO

A DESSERTATION

PRESENTED IN PARTIAL FULFILLMENT OF THE

REQUIREMENTS FOR THE DEGREE OF

DOCTOR OF ENGINEERING SCIENCE IN

MECHANICAL ENGINEERING

AT

NEW JERSEY INSTITUTE OF TECHNOLOGY

NEWARK, NEW JERSEY
1982

ABSTRACT

Three types of surface conditions (plain surface, plain surface with oxidation inhibitor, and toothed surface) and four types of environmental gases (air, nitrogen, hydrogen, and oxygen) were used to study the performance of electrical connectors installed on aluminum conductors. All of the connectors were placed insealed vessels which allowed the desired type of gas to flow at a steady rate. The connectors were then current cycled.

For the connections prepared with plain surfaces, the connectors deteriorated equally fast in air, nitrogen and hydrogen. Only the connectorsexposed to oxygen showed a higher deterioration rate than the others.

Connections prepared withhaving plain surface and oxidation inhibitor were not influenced by air, nitrogen, hydrogen, or oxygen. The deterioration rates for the connections of these groups were generally lower than those with plain surfaces without inhibitor.

The deterioration rates for connectors with toothed surface were found to be the lowest among the groups of connectors tested.

The teeth on the surface of the connector in this study had the configuration of a cone. The transient heat transfer characteristics of the cone-shaped tooth was investigated analytically. On-off heat generation at the cone surface due to contact resistance and heat loss through convection at the cone base were investigated. A control-volume approach was used to

formulate the energy equations which were solved by numerical methods.

The study shows that during the heating process the temperature rise of the solid is proportional to the heat generating intensity and inversely proportional to the convective heat transfer coefficient and that the temperature rise decreases with increasing conductivity. The time required to reach steady state is independent of the intensity of the heat generation and decreases with increasing conductivity. The transient temperature distributions along the centerline of the cone, at the apex of the cone, at the center of the cone base and along the circumference of the cone base are presentedgraphically and approximate expressions for them were found. The time required to reacha certain percentage of the steady state temperature was also determined.

During the cooling process the temperature distribution becomes one-dimensional in nature within a very short time. An approximated expression for the apex transient temperature and the time required for cooling were also obtained.

Closed form solutions for one dimensional transient heat transfer in plate, cylinder, and sphere were also derived using an integral method.

APPROVAL OF DISSERTATION

CRIMP-TYPE ELECTRICAL CONNECTORS

BY

TED LAI-CHE KUO

DEPARTMENT OF MECHANICAL ENGINEERING

NEW JERSEY INSTITUTE OF TECHNOLOGY

BY

FACULTY COMMITTEE

APPROVED: .....CHAIRMAN

.....

.....

.....

.....

NEWARK, NEW JERSEY

1982

ACKNOWLEDGEMENTS

The author wishes to express his sincere gratitude to his advisor, Dr. Rong-Yaw Chen, who provided many valuable suggestions, constant supervision, continuous guidance and encouragement throughout the course of investigation.

The author wishes also to express his sincere gratitude to Dr. Jui S. Hsieh, Dr. Hans E. Pawel, Dr. Manuel Perez and Dr. Richard C. Progelhof who have kindly read through the original manuscript and provided valuable suggestions. My sincere thanks also to Mr. Raymond J. Chen for his assistance with the graphic computer programs for the Apple computer used to create figures presented in this dissertation.

The aothor is grateful to the Thomas & Betts Co. of Raritain, N. J. for financial and technical support of this project.

TABLE OF CONTENTS

LIST OF TABLES

LIST OF FIGURES

NOMENCLATURES

If symbols are not defined under each equation, they take the following meanings:

A coefficient of difference equation

B coefficient of difference equation

b radial distance of a control surface

C coefficient of difference equation

c thermal diffusivity

D coefficient of difference equation

d diameter

E thermal emissivity

e electrical charge of an electron

F Fourier modulus, dimensionless time $\tau c/r_o^2$

h convective heat transfer coefficient

I electrical current

K reciprocal of Biot modulus, dimensionless parameter k/hr_o

k thermal conductivity

R dimensionless radius r/r_o

r radial distance or coordinate

r_o radius of the sphere

T dimensionless temperaure $k(t-t_o)/qr_o$

T^o dimensionless temperature at time before increment Δ F

t temperature

V coefficient of difference equation

Subscripts

i line (or column) number of a control volume (i.e. grid point)

j row number of a control volume

o ambient or solid boundary

Greek Letters

θ angle between centerline and nodal point

ϕ angle between centerline and control surface

τ time

1. INTRODUCTION

Every electrical apparatus or system, whatever its purpose, and even when vaguely described as "electric" or "electronic", incorporates many electrical connectors. When electric conductors are used to carry electronic current, one of the most efficient and inexpensive methods of connecting the conductor is the use of crimp-type electrical connectors. Splice connectors are used to join two conductors while terminal connectors are used to provide terminals at the ends of conductors so that they can be joined to the equipment.

Both splice connectors and terminal connectors are the essential and vital linkage for all the devices in which electricity is utilized. Their performance not only contributes to the overall efficiency of the device, but also controls the reliability of the device. High resistance in a hydraulic system can hardly fail the whole system. However, if an electrical joint has high resistance, it not only means loss of power at the connection, but also a high possibility of failure of the connection. This is because the electrical energy lost at the connection is transformed into heat which in turn further accelerates the deterioration of the connection. Because of the numerous electrical equipment failures attributed to faulty connectors, the properties of contacts and connectors have been widely investigated [12,26,27].

The material commonly used for conductors and connectors has

been copper or copper alloy. However in recent years, the use of aluminum as a substitute for copper has accelerated. Unfortunately, due to the fact that the properties of aluminum differ from those of copper, the rather successful performance of the crimp-type solderless connections involving copper and copper alloy as conductors cannot be duplicated for those electrical connections involving aluminum as conductors. It is commonly believed that the difficulties encountered in connecting aluminum conductors arise from the following facts: (1) aluminum as metal is often covered with a layer of aluminum oxide film which is highly non-conductive; (2) when aluminum is used as a conductor, it tends to creep away from pressure which plays an important role in the contact resistance; (3) aluminum as conductor inside a copper connector can expand so much as to over-stress the connector and destroy it, and (4) aluminum is more susceptible to chemical corrosion than copper [11,16,20].

Chapter 2 of this study is devoted to a presentation of the physical properties of electrical connectors and aluminum conductors and their theoretical effects on the performance of connections. Variations of surface conditions of connectors and their effects on the basic aspects of the problems encountered in electrical connections are also discussed in detail in this chapter.

Recently Kuo [25] developed an electrical connector with a multiplicity of cone-shaped teeth and cavities on the connecting surfaces. The connectors have been widely used to solve the

problems of aluminum to copper connectors.

The first objective of the research presented in this dissertation is to verify quantitatively the performance of the developed connector by experimentally comparing it with other types of connectors. It has been reported [16,17] that one of the possible reasons why the connectors with the cone-shaped teeth can successfully connect aluminum conductors is their ability to keep the environmental gases from penetrating into the contacting surfaces. In order to study the effects of the environmental gas on the performance of a connector, three types of surface conditions and four types of gases were used to conduct the current cycling. The results of the experiments are presented in Chapter 3.

It has been long recognized that the life expectancy of an electrical connection is closely related to the temperature. Since the connector interface can be viewed as a rather "porous" zone consisting of peaks of contact surrounded by valleys or channels through which gaseous contaminants can diffuse, increased heating can gradually decrease the area of contact by increasing the chemical reaction. It is a very rough empirical rule that reactions double their speed with an increase in temperature of 10 C [1]. This means that whereas for the first-order process, an increase in the concentration of 100 per cent is required to double the specific rate, the same effect can be achieved by a 10 C increase intemperature. The Anrhenius relationship has been verified for a large number of

processes. These include solid, liquid, and gas phase reactions or more specifically, the processes which are thermally activated. Specific types of reactions which have been shown to exhibit this type of temperature dependency include oxidation, diffusion, creep and stress relaxation. All of these processes are considered to be contributing factors to the degradation of the electric connectors.

The second objective of this dissertation is to study the temperature distribution within the cone-shaped teeth which is the part of sphere cut out by a 30-degree cone with the apex at the center of the sphere. The theoretical transient heat transfer analysis has been carried out using a finite difference method. The effects of heat generation at the cone surface and that of theconductivity of the solid and the heat dissipation through surface convection at the cone base (spherical surface) on the transient temperature distribution during the heating and cooling process are investigated and presented in Chapter 4.

It is an industrial standard to current cycle the electrical connector to evaluate the life expectancy of the connector. The current cycling usually consists of an "on" period and an "off" period, the connectors are heated by the current to observe the effect of chemical reaction, metal creep, stress-relaxation and other time and temperature dependent factors. A plenty of time period is usually allotted to observe these time and temperature dependent factors. The "off" period is for the

connectors to cool down to the ambient temperature so that the connectors can be heated again. Any excessive time in the "off" period does not contribute to the systematic artificial destruction of the connectors.

It is also the purpose of this study to develop expressions to calculate the transition time required for heating as well as cooling so that the total heat cycling time can be optimized. Approximated expressions based on the numerical analysis for transient temperature distributions at the apex of the cone, at the center of the convective surface (cone base), and along the circumference of the cone base during heating process and that at the apex during cooling are also obtained.

Some closed form solutions for constant-temperature heating of flat-plate, infinite cylinder and sphere are also developed in Appendix D.

Conclusions are presented in Chapter 5 and suggested recommendations for future study are presented in Chapter 6.

2. PRELIMINARY INVESTIGATIONS

In recent years, the contact between metal surfaces has been extensively studied, and a number of publications[12] have been of particular relevance to the electrical resistance of the contact.

The failure of an electrical connector can generally be attributed to a contact-resistance value in excess of some limiting value. In determining this value, consideration must be given to the circuit resistance, temperature rise, and service life requirements of each application.

2.1 Contact Resistance

The two components of contact resistance are constricting resistance and film resistance. For a circular area of actual contact, semiinfinite contact members, and the absence of thermoelectric effects, the constriction resistance is given by

$$R_c = \rho / 2a \qquad (2.1)$$

where ρ is the volume resistivity of the contact material, and a is the radius of the circular contact area.

If perfectly clean metal contact members are assumed, the total contact resistance R is equal to the contriction resistance. However, the contaminant films that are usually present on metal surfaces give rise to another component of contact resistance called film resistance R_f. If the film is assumed to be uniformly distrubuted over the actual area of

contract, the following relationship obtains:

$$r = \rho_f \, d \tag{2.2}$$

$$R_f = \frac{r}{\pi a^2} = \frac{\rho_f \, d}{\pi a^2} \tag{2.3}$$

where r is the resistance across a unit area of the film, ρ_f is the volume resistivity of the film. Hence, Holm states that conduction in quasimetallic contacts is due primarily to tunneling of electrons through the thin insulating film between the contact members [13]. For the quasimetallic contact, ρ_f is the tunnel resistivity of the film. For thicker contaminant films, ρ_f is the volume resistivity of the film material. In the conventional model,

$$R = R_c + R_f = \frac{\rho}{2a} + \frac{\rho_f \, d}{\pi a^2} \tag{2.4}$$

When two surfaces are brought together, plastic and/or elastic defomation of the asperities occurs at the points of contact. It was noted earlier that the relationship of actual contact area to load varies for a given contact material as a function of size, shape, and distribution of asperities. Bowden and Tabor[2] have shown that for purely plastic deformation of all asperities, the constriction resistance R_c is related to the load force P by

$$R_c \sim P^{-0.5} \qquad (2.5)$$

and for purely elastic deformation

$$R_c \sim P^{-1/3} \qquad (2.6)$$

Holm [12] points out that Equations (2.5) and (2.6) are applicable only for clean metal surfaces having a sufficient degree of smoothness.

It is established that real surfaces are not flat, and mechanical contact takes place at regions where the surface undulations meet. Thus, of the area over which the surfaces are apparently in contact, only a small proportion is actually in contact. Within these mechanical-contact regions, even smaller regions of metal-metal contact exist, where the surface oxide film have been fractured under the contact load. If the oxide films are insulating, as are those on aluminum, these metal-metal contact bridges are the only electrically conducting paths.

2.2 Contact Heating

The passage of current causes the temperature of the conducting regions to increase above the bulk temperature of the metal. The temperature of the metal-metal contact spots is related to the voltage U across the interface by the relation [12]

$$L(T_m^2 - T_o^2) = U^2/4 \qquad (2.7)$$

where L is the Wiedman-Franz-Lorenz number with the value $2.45 \times 10^{-8}\ V^2/K^2$, T_m the temperature in kelvins of the conducting regions in the interface, and T_o is the bulk temperature in kelvins. The amount by which the temperature of contact spots is above the bulk, i.e. $T_m - T_o$, is called the super-temperature and has been shown theoretically [12] to have the same value at all contact spots in the interface.

The Wiedeman-Franz law states that the product of the resistivity p and thermal conductivity k of a metal is equal to a constant L times the absolute temperature of the metal T_m. That is,

$$p\,k = L\,T_m \qquad (2.8)$$

For most metals, T_m is great enough compared with T_o that T_o^2 can be neglected in Eq.(2.7). Thus, T_m is given approximately by

$$T_m = (V_c/2)\ L^{-0.5}\ (3200\ V_c) \qquad \text{(in kelvins)} \qquad (2.9)$$

Equation (2.9) enables one to quickly approximate the maximum contact temperature when the contact voltage is known.

Temperature plays a vital role in determining the life of a connector. One of the most widely suggested mechanism of degradation occuring in mechanical connectors [11,20] is the oxidation of the metal-metal contact within the interface. Spofford [22] has produced a model based upon the erosion of contact spots by an electrically heated process. His model shows

that continuous erosion by a process such as current cycling could cause the resistance of a connector to increase very rapidly to a high value after remaining constant for a long peroid of time. However, the evidence which supports the oxidation mechanism of degradation has predominantly been obtained on copper contact in oxygen containing atmospheres.

It is obvious that oxidation of the contact is just one of the factors contributing to the degradation of the contact. Other degradation factors such as stress relaxation and thermal expansion are also highly temperature dependent.

The experiment in this dissertation has been designed to investigate the mechanical and chemical degradation of the connections by current cycling. Three kinds of connections were prepared by using three kinds of connectors which were only different in their surface conditions. Each kind of connection was then sealed inside various gases. They were air, oxygen, hydrogen, and nitrogen. The connections were then current cycled by passing current for thirty minutes and allowed to cool for another thirty minutes.

The current cycling causes physical expansion and contraction for both the connectors and the conductors to accelerate the mechanical degradation. The various kinds of gases in which the connectors were expanding or contracting were to chemically influence the connector and conductor interfaces.

2.3 The Connectors and the Installing Tools

In making a crimp type electrical connection, electrical

conductors are usually first stripped off the outer insulation jacket. A connector, usually in the form of a cylindrical shell or an U-shaped channel is then placed over the conductors in such a way that the connector is completely housing the conductors. The connector is then mechanically compressed to reduce its original cross-sectional area to exert pressure on the conductors. This process of deforming the connector to mechanically hold the connector is called crimping.(Fig 2.1-2.2)

The crimping action not only makes the conductors and the connector to be held together mechanically, but also causes the conductors and the connector to be electrically connected. The purpose of electrical contact is to allow electrons to flow freely from the atomic lattice of one conductor metal to the atomic lattice of another conductor metal. The connectors used in this investigation were of the open seam U-shaped crimp type connectors made of special copper alloy. Their basic configuration before the installation are shown in Fig 2.2.

Two 12 AWG aluminum conductors were placed through the opening of the U-shaped connectors and then compressed into the rectangular shape with the predetermined finishing configuration as shown in Fig 2.2. The constant finished configuration was achieved by using a set of spring loaded crimping dies as shown in Fig 2.3. The compressional crimping operation was performed with hydrantic tools.

2.4 Aluminum Conductor and Copper Connector

Round alumium conductors of the size 12 AWG were used in this

investigation to expect faster joint deterioration.

It is well known that the electrical joint composed of aluminum conductor and copper connector deteriorates faster than the joint composed of copper conductor and copper connector.

This higher rate of deterioration of connecting aluminum conductor to copper connector arises from the following factors: [16, 21, 22] (1) aluminum oxide film on the aluminum conductor is less conductive than the copper oxide film on the copper conductor; (2) aluminum has higher creep rate than copper, (3) aluminum has higher coefficient of expansion than copper, and (4) aluminum is more susceptible to chemical corrosion than copper. The various effects of these facts are as follows:

(1) Oxidation Film: An oxide film approximately 20 Angstroms thick is formed within seconds after bare metal is exposed to air. Unlike many metallic oxides which are either conductors or semiconductors, aluminum oxide is a good insulator. The oxidation film is believed to be the major factor responsible for the difference between aluminum and other base metal contact such as copper. Industrially, electroplating, grease, and other surface preparations are used to modify this factor.

Many experiments have shown that the growth of an oxidation film depends on both ionic and electronic conductivity. The resistance to the passage of both ions and electrons will be proportional to the thickness, y, so that:

$$\frac{dy}{dt} = \frac{k}{y} \qquad \text{where k is a constant} \qquad (2.10)$$

or $y^2 = 2kt + c$ where c is a constant, giving the well known parabolic law of oxidation [2]. Wagner [3] showed that the constant k could be calculated to be:

$$k = \frac{J\ n_1\ (n_2 + n_3)\ K\ E}{D\ F} \qquad (2.11)$$

where F is Faraday's number.

D is the oxide density.

J is the equivalent weight of the tarnish film, n_1, n_2, n_3 are the transport numbers of the electrons, anions, and cations.

K is the specific conductivity of the film.

E is the E. M. F. of the cell Metal/ Metal oxide/oxygen.

This relationship shows that films which grow slowly do so because of their poor ability to conduct electricity by some mechanism. From this it follows that although aluminum forms thin oxide films, the conductivity of such films is no better than that of much thicker films on some other metals. On the other hand, the initial stages of the formation of the oxidation film cannot be governed by the parabolic law because this implies an infinite rate when no film is present. In addition, the theory involves the movement of particles through the film, and this

theory cannot apply until the film has formed. Experimental results show that the initial formation of the film may reach 20Å in a few seconds on aluminum, in several minutes on copper, but may require half an hour on nickel.

The low electronic conductivity of aluminum oxide may be associated with the perfection of the lattice. Metals such as iron, copper and zinc form oxides, FeO, Cu_2O, ZnO, which can be non-stoichiometric, and may conduct by virtue of the defect lattice.

The effect of the growth of oxidation films on the resistance of the connection has been studied by Muller-Hillebrand [13]. He showed that when contacts of size 0.6 x 0.12 in. were loaded under 550 lb_f (250 kg.) after storage for various periods, the resistance was markedly influenced by the atmosphere in which the pieces were stored. It was also shown that both greased and ungreased, stored contacts made by wire brushing, continued to deteriorate even if no current was passed through them. The best conditions were obtained with contacts filed under a grease before assembly. In this experiment, connectors were first filled with grease containing metallic particles and then crimped on the conductors to simulate this condition.

(2) Creep: Another effect of temperature on an electrical contact involves changes in mechanical properties, particularly stress relaxation. Creep or cold flow has long been recognized as a major problem in causing the stress relaxation. Bond [3] has shown that the increase in contact resistance is caused by interfacial movement that destroys the initial contact points

established during the installation of the connector. The residual stresses maintained by any connector are, by definition, lower than the yield strength of the conductor. Therefore, it seems valid to assume that the interfacial movement must be caused by creep, because creep is the classic mechanism that accounts for the time-dependent dimensional change of metals stressed at less than the yield strength. When aluminum is subjected to stress it tends to deform or flow away from the stressed area(Fig.2.4). In the electrical connection this acts to reduce the effective normal force at the contact interface. The reduction of contact pressure results in a high-resistance joint which causes further heating. The heating, in turn, causes the creep to accelerate. This sequence of events has a cascading effect, which ultimately results in the failure of the joints.

The rate of stress relaxation is quite dependent on the metallurgical history of the material. For example, the creep strain of EC-grade aluminum at room temperature and constant stress may vary as much as 30:1 between fully annealed and highly cold worked material. However, it is also important to note that the creep rate of a competitive material such as ETP copper may be as much as 80 times lower than that of EC aluminum for the annealed condition. This points to one of the difficulties which has been encountered in the use of "pure" aluminum, particularly in applications where it must be terminated to a copper alloy. These represent nearly the extremes of mis-match in mechanical properties.

(3) Thermal Expansion: Another factor which aggravates the

creep problem is the differences in thermal-expansion rates of other materials used with aluminum. When aluminum is heated in close conjunction with copper, for example, an aluminum wire crimped in a solid copper connector, the aluminum expands more than the copper. This differential expansion can cause a permanent set to be induced in the aluminum. When the joint cools, the cross-sectional area of the aluminum is effectively reduced, which results in a poor electrical joint.

(4) Corrosion: Traditionally electrolytic or galvanic corrosion presents a severe set of problems to the aluminum-copper joints. Galvanic corrosion occurs when dissimilar metals are used in contact with each other and are in the presence of water and electrolyte.

Chemical deterioration of the joint is also induced by various type of environmental condition. In this investigation, various types of gasas were used to react on the joints.

2.5. Connector Surface Conditions

Three kinds of surface characteristics were employed in this investigation:

(1) Plain smooth surface with electro-tin deposit of 0.0001" in thickness.

(2) Plain smooth surface with electro-tin deposit of 0.00001" with oxidation inhibitor. (Thomas and Betts Co. Cat. No 21059). The compound is a mixture of fine metallic zinc particles suspended in a hih temperature grease. The fine metallic zinc particles can penetrate both the connector and the

conductor surfaces. When the surface of the conductor is ruptured and compressed, some vergin metal will exposed to get in contact with the connector surface. The petroleum base grease is provided for sealing out the environmental atmosphere.

(3) Connector surface with sharp projections with electro tin deposit of 0.0001" all over the surfaces. As shown in Fig 2.5 the size of the projections is very substantial in comparison with the thickness of the base metal of the connector. The projections were formed in such a way that the cone-shaped top had a very sharp point and its hardness could be higher than that of the base metal [25] (U.S. patent 3,549,786). The projections were distributed on the connector surface with the density of approximately (90) projections per square inch. Since the connector had the surface area of 0.7 square inches, there were approximately 63 projections on each connector surfaces.

2.6 Effects of Surface Conditions

(1) Effects of Surface Conditions on Initial Contact Resistances: The practical surfaces are quite rough when compared to atomic or molecular dimensions. A magnified metallic surface, ideally clean, will appear as shown in Fig 2.6. In visualizing this surface, in this case, the vertical magnification is ten times that of the horizontal. This means that the actual slopes on the hills and the valleys are more gradual than pictured. When two surfaces similar to this are brought together, they will touch on just a few asperities, as

pictured in Fig. 2.7. Even as the asperities deform due to localized high pressures as crimping force between the connector and the conductor is increased the majority is occupied by air or the gas of the local environment.

Starting with the condition in which some asperities just barely touch, the crimping force P is gradually increased. The asperities will deform and new asperities will begin to touch. At first the deformation is elastic. The sum of the areas of all these tiny spots will be just large enough to support the applied load. In the cases where the macroscopic shape of the members would tend to produce round strained areas (assuming for a moment that perfect contours are present with asperities) the radius, a, of the equivalence load bearing area can be calculated by

$$a = 0.087\ P^3\ r\ \left(\frac{1}{E_1} + \frac{1}{E_2}\right) \qquad (2.12)$$

where the metric system a = radius in millimeters

r = contact radius in millimeters

P = force in grams

E_1 , E_2 = Modulus of elasticy in kg/m

Since the equivalent area is a^2 , we see that the load supporting area is proportional to $P^{2/3}$ when deformation is wholly elastic. As the crimping force is increased, the deformation will also increase. When the applied stress exceeds the elastic limit of a material, plastic deformation occurs. In common practice, most of the solderless crimp type connectors are crimped beyond elastic deformation to obtain the

plastic deformation to increase the equivalent contact area.

This equivalent area is one of the major factors influencing the contact resistance. The greater the contact area the more paths for current flow and the less the resistance. This fact can be confirmed by the phenomenon that when a newly prepared connection is subjected to heat cycling, the joint resistance often decreases during the initial heat cycle due to the softening of the material. Films of oxides, sulfides, carbonates formed on the conductor or the connector surfaces are insulators or at least semi-conductors whenever they are of sufficient thickness. They can interfere with the free flow of electrons between the mating contacts.

The surfaces of connectors or conductors are usually plated with softer metal such as tin to resist formation of high resistant films and also to enhance the plastic deformation of the asperities to increase the equivalent contact area. For the connectors which have only plain roll-finished surface, the initial contact value have to depend on the nunmber of the asperities *exis*ting on the connector surface. (Fig 2.8a)

When terminals are joined such that one terminal rubs across the other, the mating terminals only touch intimately at the "peaks" of the metallic surface asperities. The "valleys" effectively do not enter into electrical conduction. Mating of the terminals tend to level out the peaks; the softer the materials coming in contact the better the leveling. The better the leveling the more contact area is created and the lower the contact resistance, all other things

being equal. Tin plating provides better leveling economically.

For the connectors which have plain roll-finished surface and is also provided with fine metallic particles suspended in grease, the asperities are thus created by the metallic particles. Depending on the density of the metallic particles the equivalent contact area can be greatly increased to decrease the initial contact resistance. (Fig 2.8b) When the connectors with particle containing grease is installed on conductor, it is intended to achieve the condition that the contact is filled under a grease before assembly.

As can be seen from Fig 2.5, the configulation of the corn-shaped sharp projections on the connector are to be used to create maximum contacting areas between the conductor and the connector.

This is due to the fact that the sliding action between the entire surfaces of the projection and the conductor metal can create the electrical contact like the contact between the individual asperites. Moreover, due to the conical configulation of the projection, the overall contact area can be much larger than that of the connectors with plain roll-finished surface. (Fig 2.8c). The initial resistance of this kind of connection should be the lowest of the three kinds of surface conditions.

(2) Effects of Surface Conditions on Creep: One of the unfavorable effects of heat generated at the electrical contact involves changes in mechanical properties, particularly stress relaxation at the contact. Creep or cold flow has long been recognized as a major problem in causing the stress relaxation. It will act to reduce the effective normal force at the contact interface with the possible consequences outlined earlier.

Even though creep is highly dependent on temperature, this author [16,17] believes that certain mechanical configulation of the connector surface condition could arrest the damaging effect of the creep of the conductor material.

For the connectors which have only plain smooth surface, as can be seen from Fig. 2.4, the normal forces exerted by the connector are such that the conductor material can gradually creep out of the pressured region. Even at room temperature this process of cold flow takes place. Heat generated at the connection enhances the process.

For the connectors which have plain smooth surfaces but are also provided with fine metallic particles suspended in grease, the movement of the material in the direction normal to the applied connector forces could be discouraged by the existance of the metallic particles between the conductor and the connector interface. The metalic particles imbeded between the conductor material interlock both metals and offer a high resistance to flow out of the pressurized region.

The connectors with conical projections on their contact

surfaces have been believed to have entirely different mechanism in arresting the damaging effects of creep. As can be seen in Fig. 2.9, the normal compressional force F exerted by the connector is decomposed into F_1's or F_2's due to the conical projections. These decomposed forces F_1's and F_2's which are perpendicular to the surfaces of the adjacent conical projections should be less effective in causing the conductor metal to flow in the direction perpendicular to the original normal compressional force F.

(3) Effects of Surface Conditions on Thermal Expension: In practice the loss of contact face can occur much more rapidly than that associated with the rather long-term creep process. This is due to the deformation developed from differential thermal expansion between the conductor metal and the connector metal. The source of temperature variations may be cyclic I^2R heating of the connector or ambient tempeature variations. For example, the thermal-expansion coeffiient of pure aluminum is 40 to 45 per cent greater than that of the copper. During heating of an aluminum wire-copper connector combination, compressive stress will develop in the wire which, if greater than the yied strangth of the aluminum, will cause permanent plastic deformation. As the joint cools, some loss of contact force must be expected unless prevented by the special design. Repeated cycles will ultimately lead to an increase in contact resistance and failure.

As was indicated by this investigator [16,17], there are two general approaches to solve the problem of differential

expansion. One approach is to construct the connector itself like a spring in holding the conductor. Since the conductor is held by spring force, the contact pressure between the conductor and the connector can be controlled by the spring.

Another approach is to provide spaces for accomodating the excessive volume so that the building up of stress can be avoided. Fig. 2.10 is a comparitave illustration of the effects of smooth surface with projections due to thermal expansion. When the connector with smooth surface is heated the connector is stressed beyond elastic limit and at the same time some of the conductor material creeps out. After heating, when it cools, a space is created between the connector and the conductor to destroy the contact. (Fig. 10 a,b) The surface configuration developed not only has the conical projections but also provides with cavities equivalent to 27.9 per cent the original volume of the connector material [16]. These cavities are formed on the process of creating the conical projection on the connector surface. When the conductor expands the increased volume is accomodated by the room in the cavities without plastically deforming the connector. The expansion and contraction of conductor metal into these cavities allows relatively active metal such as aluminum to move freely under thermal cycling without breaking the electrical contact established and held by the projection on the connector surface.

(4) Effects of Surface Conditions on Corrosion: Corrosion is another major phenomena involves the interfaces

between the connductor and the conductors. Galvanic corrosion is especially one of the most severe forms of corrosion exhibited by the aluminum copper interface because aluminum is a highly electronegative (anodic) material. This form of corrosion has apparently held responsible for numerous problems with the aluminum-copper connection. Aluminum may corrode at a faster rate when electrically connected to material more noble than itself than when in the uncoupled state.

Even though the occurrence of galvanic corrosion can be reduced by reducing the electrode potentials between the conductor metal and the conductor metal, various physical conditions of the connector surfaces can also influence this kind of chemical reactions.

The connectors which have only plain smooth surface are more susceptible to corrosions due to the fact that the conductor and the connector interface can easily be opened due to vibration, thermal expansion and loss of contact force. The environmental contaminants such as humidity and gases existing in the opened interface act as electrolyte to induce the corrosion. For the connectors which have plain smooth surfaces but are also provided with grease containing metallic particles, can be greatly reduced. When a relative motion at interface occur between the conductor and the connector to open the interface, the relatively inert grease can prevent the environmental contaminants from coming into the interface. The metallic particles suspended in the grease

can also help the interface to re-establish electrical contact by penetrating into both conductor and connector surfaces.

For the connectors which has conical projections on the surface, the relative motion between the connector and the conductor at the interface can not be induced easily. First of all, the fact that the projections on the connector surface are imbeded deep into the conductor material in staggered pattern can reduce the relative motion between the conductor and the connector along the longitudinal axis of the connector. When the relative motion is thus reduced, there is less chance that the environment contaminates can be introduced to the interface.

On the other hand, the expansion in the direction transverse to longitudinal axis can hardly induce the relative motion. The cavities on the connector surface allow the expanded portion of the conductor metal to occupy these cavities instead of sliding along the conical surfaces of the imbeding projections. The absence of the relative motion between the contacting interface can then reduce the influx of the environmental contaminants to induce the corrosion.

Due to the fact that the projections are conical, the contacting interfaces are three dimensional zig-zag in their configuration. This zig-zag contacting area also offer more resistance to the invading environmental contaminants.

(5) Effects of Surface Condition on Bulk Temperature: The heat generated at the connector and the conductor interface can immediately increase the electrical resistance at that area and

create more heat.

The chemical reactions and the stress relaxations between the connector and the conductor interface are all directly accelerated by the heat. For this reason, if the heat can be dissipated, the connector life can be prolonged.

When the connectors having conical projections penetrate into the conductor, the wiping action between the projection surface and the conductor metal tends to create some degree of cold welding between the two parts. In this case, not only the electrical resistance, but also the thermal resistance is extremely low due to the intimate contact . The imbeded conical projection also function like a fin to effectively conduct heat from the conductor to the outer surface of the connctor(Fig 2.11). All the unfavorable effect due to heat should thus be minimized due to such surface condition.

The existence of grease between the connector surface and the conductor surface should also reduce the thermal resistanc

3. EXPERIMENTAL INVESTIGATION

A familiar method of evaluating electrical components from the standpoint of reliability involves the use of accelerated heat-cycling tests. Heat-cycling tests are useful development aids because direct comparisons in performance can be made under controled conditions

In this study the three types of connectors were connected in series and then their temperature was elevated by means of electric current. Also four types of artificial environments were created for each type of connector to produce accelerated deterioration in the contact structures.

After reaching a stabilized temperature the circuit is de-energized for an interval of time. This process is repeated over 580 cycles of operation. The heating periods are thirty minutes and the cooling periods are same as the heating period. During this heats-cycling d-c resistance measurements were taken at intervals as a measure of the connector performance.

3.1 Test Current

Equations for calculating the approximate current-carrying capacity of conductor under known conditions of ambient temperature, limiting temperature rise and wind velocity formulated by Schurig and Frick are

$$I^2R = (W_c + W_r)\ A \qquad (3.1)$$

$$W_c = \frac{0.0128\ (PV)^{0.5}}{T_a^{0.123}\ d^{0.5}}\ \Delta t \qquad (3.2)$$

$$W_r = 368\ E \left(\frac{T^4}{1000^4} - \frac{T_o^4}{1000^4} \right) \qquad (3.3)$$

where

I = conductor current, amperers

R = conductor resistance, ohm/ft

W_c = watt/sq in, dissipated by convection

W_r = watt/sq in, dissipated by radiation

A = conductor surface area, sq in/ft

P = pressure, atmospheres

V = wind velocity

T_a = average of absolute temperatures of conductor and air, deg k

d = outside diameter of conductor, inches

Δt = temerature rise, deg C

E = relative emissivity of conductor surfaces. (E=1.0 for "black body" or 0.5 for average oxidized copper)

T = absolute temperature of conductor, deg K

T_o = absolute temperature of surroundings, dog K

The base for this method of approximating current-carrying capacity is that the heat developed in the conductor by I^2 R loss is dissipated by convection in the surrounding air and radiation to srrounding objects.

By calculating $(W_c + W_r)$ A, and R, it is then possible determine I from Eq. (3.1). The value of R to use is the a-c resistance at the conductor temperature (ambient temperature plus temperature rise) taking into account the skin effect.

3.2 Number of cycles

The exact number of load cycl that necessary for a reliable assessment of the long-term stability of a joint is not known yet. Spofford [22] showed that a joint which is electrically stable up to 500 cycles is likely to remain so. In this experimental investigation the connectors are to be tested up to 580 cycles. However the test would be terminated before 580 cycles, should the temperature of the connector exceed 200C. In practical application a connector may still perform its function at this temperature but in this study this temperature is used to estimate the life of the of the connector under accelerated test.

Metal creep is considered to be an important factor affecting the life of a joint, and this is a function of time and temperature. It is important, therefore, not to hurry the testing of joints, otherwise the effects of creep may not be observed.

When the cyclic test is consisted of heating cycle and cooling cycle it is in the cooling that some time could be saved.

3.3 Specimens

The three types of surface conditions i.e. plain surface, plain surface with oxidation inhibitor, and teethed surface described in the previous chapter were all employed in this investigation. All the connectors used were of the same basic dimensions except the surface conditions.

Four kinds of gas i.e. air, nitrogen, hydrogen, and oxygen were used as environmental gases. The combination of the surface conditions and the gaseous environment creates twelve groups as shown in Table 3.1.

Each group of connectors was made up of four connectors of same type. The four connectors were connected in series (Fig.3.1). A cardboard separators was used to divide the four connectors into two sides so that the heat generated from one connector can not affect the other connectors. Each connector in series had the center distance of fifteen inches from the other to minimize the influence of one connector to the other.

After the four connectors were connected in series to form a group, they were sealed in an one-gallon glass container. The two leads of the group were extending outside the glass container and connected in series with the other three groups which were also sealed in separate containers.

Air, nitrogen, hydrogen or oxygen was then allowed to flow through each container at the pressure slightly higher than atmospheric pressure. The gases were injected at the bottom of

the glass containers and then came out at the top of the container. After coming out of the container, the gases were led with an 1/4 tube into the bottom of a one-gallon glass container filled with water. The number of bubbles coming up from the bottom of the container within a unit time was used as the guide to regulate the rate of gas flow inside the glass container.

The equipment used in the current cycling is listed in Appendix A and the set-up is shown in Fig. 3.2. Figure 3.2 shows the arrangement for temperature measurements.

3.4 Results and Discussion

The experimental data for the present current cycling test are tabulated in Appendix C. The data consisted of temperature readings for each connector at each specific cycle, and the corresponding ambient temperatures at each measurement. By subtructing the ambient temperature from the measured connector temperature, the temperature rise due to cyclic heating is obtained. However the ambient temperature was relatively constant and, therefore, the measured temperatures were used in the data analysis.

In this research the temperature of the connector was used as the criterion for the performance of the connector. Since the temperature is a direct indication of the connector resistance, a higher temperature reading for a given connector is an indication of higher deterioration of that particular connector.

Table 3.1 Connector Conditions and Testing Environments.

Connector Group	Surface Conditions	Environmental Gases	Number of Connectors	Wire AWG
Group 1	Plain surface	Air	6	12
Group 2	Plain surface	Nitrogen	6	12
Group 3	Plain surface	Hydrogen	6	12
Group 4	Plain surface	Oxygen	6	12
Group 5	Plain surface with oxidation inhibitor	Air	6	12
Group 6	Plain surface with oxidation inhibitor	Nitrogen	6	12
Group 7	Plain surface with oxidation inhibitor	Hydrogen	6	12
Group 8	Plain surface with oxidation inhibitor	Oxygen	6	12
Group 9	Teethed surface	Air	6	12
Group 10	Teethed surface	Nitrogen	6	12
Group 11	Teethed surface	Hydrogen	6	12
Group 12	Teethed surface	Oxygen	6	12

When a connector temperature reached 200 C or above. It was considered as failed and no further experimental data were taken. For the first type of connectors, plain surface connectors, all connectors failed after only 70 cycles. For the second type, plain surface with oxidation inhibitor, all connectors failed after 140 cycles. For the third type, the teethed connectors, all connectors were far below 200 C after 580 cycles except some connectors exposed to oxygen. The averaged connector life based on 200 C maximum were found to be 51, 44, 45, and 21 cycles for the plain connectors in air, nitrogen, hydrogen and oxygen respectively. The averaged life were 103, 91, 99 and 108 for the connectors with oxidation inhibitor. It should be noted that the third connector (number 45) of Group 8 was not included in this analysis due to its thermocouple failure. No averaged life were calculated for the teethed connectors, since most of the connectors were far below the 200 C level. It should be noted that the starting temperatures (which were the temperatures measured at the peak of the first cycle) were not the same due to some non-uniformity among the connectors. However to determine the perfomance of connectors, one should determine the rate of deterioration. That is to say the steeper the slope of the temperature-cycle curve the higher the rate of deterioration.

In order to determine the average rate of temperature rise for each group of connctors in a given environmental gas, the rate of temperature rise for each individual connector was

first determined and then the average rate of temperature rise for the group at that particular heating-cycle was calculated.

For example a connector at cycle Ø was at 4Ø C and at cycle 5 was 5Ø C. The rate of temperature rise is,therefore, 2 C per cycle for the heating cycles between Ø and 5. In cases where the experimental data were terminated due to the over-heating of connectors (temperature greater than 2ØØ C), the rates were assumed to be equal to that at the highest temperature. Having computed the rate at each given cycle, one could easily compute the average rate of temperature rise. Based on these rate of temperature rises, the average temperature rises (i.e. the averaged accumulated temperature increments) from the start of the heating- cycle (using Ø C at the start)) for a given group were calculated.

Figure 3.4 shows the averaged temperature rises in air environment for the three types of connectors (plain surface, plain surface with oxidation inhibitor and teethed surface). It is seen that the plain surface connectors deteriorated at the fastest rate and the teethed surface connectors deteriorated at the slowest rate. The deteriortion of the plain surface connectors with oxidation inhibitor, though, slightly at a slower rate than that of the plain surface connectors, the difference was rather small in comparison with that of the teethed connectors.

Similar results were also shown in Figs. 3.5 through 3.7 for the three types of connectors in nitrogen, hydrogen and oxygen respectively.

In order to compare the effect of the ambient gas on the performance of each type of connector, the temperature rises for connectors with plain surfaces were plotted against the number of cycles in Figures 3.8. It is seen that except those exposed with oxygen the temperature rises were essentially the same for thoses connectors exposed with air, nirogen and hydrogen. It clearly showed that for a plain surface connector in oxygen the connector deteriorated about twice as fast as those plain connectors in other gases.

In Fig. 3.9 plain connectors with oxidation inhibior were shown. Unlike those in Fig. 3.8 the connectors exposed with oxygen deteriorated at the same rate as those exposed with other gases. This was perhaps due to the fact that the existence of grease (oxidation inhibitor) betwen the connector surface and the conductor surface kept oxygen from coming into contact with these surfaces and, thus, resulted in no effect whatsoever to the exposure to the oxygen.

In Fig. 3.10 comparisons of connectors with teethed surfaces in air, nitrogen, hydrogen and oxygen were made. There were no consistent tendences or differences that could be drawn from these experimental data.

Fig. 3.11 present data for plain surface, plain surface

with oxidation inhibitor and teethed surface in air environment on a ln(temperature rise/273) v.s. cycle coordinate system. As is seen from the figure, the data for temperature rise greater than 30 C fall on a relatiely straight line. To estimate the life of a connector one may simply extend the line (as shown) until it intersects with the 180 C line which is the assumed allowable temperature rise. The estimated life cycles are 40, 100 and 1000 for plain, plain with inhibitor and teethed conectors respectively.

According to Spofford [22] the cyclic life of a connector obtained through the accelerated cyclic test is equivalent to one tenth of the actual service life of the connector. Based on this approximation, the teeth connector, for example, should last about 10,000 cycles in the actual service.

Based on these experimental analyses, the following conclusions may be made. For the connections prepared with the connectors having plain surfaces, the connections deteriorated equally fast in air, nitrogen and hydrogen (Group 1,2 and 3). The reducing properties of hydrogen did not seem to influence theconnection. Only those connectors in oxygen (Group 4) showed faster deterioration rate than others (Group 1,2 and 3).

Connections prepared with connectors having plain surface with oxidation inhibitor (Group 5 through 8) were not affected by the presence of different gases such as air, nitrogen, hydrogen and oxygen. However the deterioration rates for Group

5 through 8 were generally slower than those of Group 1 through 4.

Connections prepared with connectors having teethed surface were not affected by the gases such as air, nitrogen and hygrogen (Group 9, 1Ø and 11). Connections in oxygen (Group 12) showed higher deterioration rate after 5ØØ cycles and in most caes failed after 58Ø cycles.

4. TRANSIENT HEAT TRANSFER ANALYSIS

Thermal breakdown occurs when heat cannot be dissipated at the same rate at which it is introduced. The resulting increase in temperature leads to failure due to physical melting or decomposition. When the energy-differential mode is slight or the steady state temperature is high, chemical reactions can lead to compositional changes that alter the device or substance and render it useless.

Since the rate of deterioration of an electrical connection is a function of the temperature of the connection, theoretically even a poorly installed high resistance connection can be kept to function properly if the heat generated in the connection could be continuously dissipated away to maintain a cool joint. For example, a poor connection covered with heavy insulations tends to fail sooner than its counterpart which is exposed to a well ventilated area.

For a properly installed connection, its life can be prolonged if the connector is designed in such a way that all the aspects to increase the rate of heat transfer from the connection to the surroundings are considered. This consideration is specially important when the connector is for original equipment manufactures where the efficiency of the connector significally affects the cost and performance of the equipment. For housing industries, due to the code regulation, the connections are often confined in a box or box-like enclosure. The poor convective surroundings often causes the temperature of

the connection to increase.

Connectors installed in transformer are submerged in an oil coolant to increase the surface convective heat transfer coefficient and, thus, high heat dissipation is attained.

In accelerated test of a connector, the temperature on the connector surface is measured with a thermocouple. When the current is turned on, heat is generated primarily at the contact surface and the temperature measured increases with time. When the current is turned off, the measured temperature decreases with time. In both cases, the temperature distribution in the connector is a function of time and location. To optimise the cyclic test period, the knowledge of the transient temperature distribution in the connector is indispensible.

The crimp-type connector under investigation is made of 15-degree conical teeth as shown in Fig. 2.5. It is ,therefore, desirable to investigate analytically the transient heat transfer in the individual tooth under different rate of heat generation and heat dissipation.

The purpose of this analysis is not the study of the connector performance per se, but the study of the transient heat transfer in a conical tooth with heat generation on the tooth surface and heat convection through the tooth base.

The governing equation for transient heat transfer in spherical coordinates is solved numerically using a finite difference method based on control volume approach. The rate of heat generation on the cantact surface (i.e. the cone surface) and that of the heat convection on the sphere surface are expressed in

dimensionless parameters and the effects of these parameters on the temperature distribution in the cone are investigated.

4.1 Formulation of the Problem

The analysis is based on a sphercal coordinate system (r,θ,.) as shown in Fig.4.1 with the origin at the center of the sphere. The tooth of the connector is the part of the sphere cut out by the 30-degree-cone (i.e. $\theta_o = 15$ degrees).

The cone shaped solid is initially at a uniform temperature of t_o and heat is generated on the cone surface at constant rate per unit surface area q. This heat is transferred by conduction throughout the solid and dissipated to the ambient fluid by convection on the sphere surface having constant coefficient of convective heat transfer h. The solid material is isotropic and its conductivity k and diffusivity c are assumed to be constant. Due to the axisymmetric conditions imposed upon the solid, the transient temperature distribution in the solid is independent of the angle Ψ and is a function of time τ, the radial coordinate r and the subtended angle θ.

The energy equation in spherical coordinate system is;

$$\sin\theta \frac{\partial}{\partial r}\left(r^2 \frac{\partial t}{\partial r}\right) + \frac{\partial}{\partial \theta}\left(\sin\theta \frac{\partial t}{\partial \theta}\right) = \frac{r^2 \sin\theta}{c} \frac{\partial t}{\partial \tau} \qquad (4.1)$$

where t is the temperature

The initial condition is;

$$t = t_i \quad \text{at} \quad \tau = 0 \qquad (4.2)$$

The boundary conditions are;

$$q = k \frac{\partial t}{r \partial \theta} = \text{const.} \quad \text{at} \quad \theta = \theta_o \quad \text{and} \quad \emptyset < r < r_o \qquad (4.3a)$$

$$- k \frac{\partial t}{\partial r} = h (t_s - t_o) \qquad \text{at} \ \emptyset < \theta < \theta_o \quad \text{and} \quad r < r_o \qquad (4.3b)$$

where r_o is the radial coordinate at the spherical surface,

t_s is the spherical surface temperature

and t_o is the ambient temperature.

The energy equation is nondimensionalized as follow;

$$\sin\theta \frac{\partial}{\partial R} (R^2 \frac{\partial T}{\partial R}) + \frac{\partial}{\partial \theta} (\sin\theta \frac{\partial T}{\partial \theta}) = R^2 \sin\theta \frac{\partial T}{\partial F} \qquad (4.4)$$

where $R = \frac{r}{r_o}$, $T = \frac{h (t - t_o)}{q}$ and $F = c \tau / r_o$

The nondimensionalized initial and boundary conditions are;

$$T = \emptyset \quad \text{at} \quad F = \emptyset \qquad (4.5)$$

$$K \frac{\partial T}{R \partial \theta} = 1 \quad \text{at} \quad \theta = \theta_o \quad \text{and} \quad \emptyset < R < 1 \qquad (4.6a)$$

$$- K \frac{\partial T}{\partial R} = T_s \quad \text{at} \quad R = 1 \quad \text{and} \quad \emptyset < \theta < \theta_o \qquad (4.6b)$$

where $K = k/hr_o$ is the reciprocal of the Biot modulus.

4.2 Analysis of Solution

Three general methods of solving heat transfer problems are available: analytical, analog, and numerical. The analytical solution is exact in nature, but these solutions are almost without exception confined to linear problems and regions of simple geometry. Due to the complexity of the infinite series solutions which normally arise in analytical procedures, it is often required to employ a digital computer to evaluate the solution. However such computer programs are difficult to write; they are valid or of use for the specific solution programmed, and errors in these programs are difficult to detect. The analog method such as the conductive sheet electrical analog in the solution of two-dimensional steady state conduction is indeed very useful. However for transient heat transfer of the type under consideration, there is no such analog method available to the author. The numerical method with the use of a digital computer, which is wildly available today, has many advantages. It is capable of solving problems involving non-linear partial differential equations and complex boundary conditions.

The numerical method to be presented here is a finite difference method based on the control volume [19] approach which provides a physical insight to the process of heat transfer in each subvolume of the solid.

The tooth is divided into small control volumes and a finite difference equation for each control volume is obtained by applying the principle of the conservation of energy, which is expressed in the energy equation, and at the same time satisfying

the initial and the boundary conditions. This is accomplished by replacing the continuous domain by a pattern of discrete points within the domain and introducing finite difference approximations between the points.

The system is first subdivided into a number of small but finite subvolumes (i. e. the control volume) and each subvolume is assigned a reference number. Then each subvolume is assumed to be at the temperature corresponding to its center and the physical system is replaced by a network of fictitious heat-conducting rods between the centers, or nodal points, of the subvolumes. If thermal resistance corresponding to the resistance of the material between nodal points is assigned to each rod, the heat flow in the rod network will approximate the heat flow in the continuous system. If N points are selected, a set of N algebraic equations is obtained. The resulting set of algebraic equations is then solved by the matrix inversion method with the use of a digital computer.

For the sake of clarity, the tooth is divided into 4x1Ø (or 4Ø) control volumes (c.v.) as shown in Fig. 4.1. In the actual calculations, the tooth is divided into as many as 12x8Ø c.v. Each c.v. is assigned a reference number and is assumed to be at the temperature corresponding to its center. It is seen from the physical configuration and the boundary conditions that several different forms of difference equations can be obtained.

For example, to obtain the energy balance for the c.v.(3,9) as shown in Fig.4.2, one may integrate the energy equation (4.4) from $R = b_8$ to $R = b_9$ and $\theta = \phi_2$ to $\theta = \phi_3 = \phi_2 + \Delta\phi$

Thus;

$$R^2 \sin\theta_3 \Delta\phi \frac{\partial T}{\partial R}\Bigg|_{R=b_8}^{R=b_9} + R_9 \sin\theta \Delta R \frac{\Delta T}{R_9 \Delta \phi}\Bigg|_{\theta=\phi_2}^{\theta=\phi_3}$$

$$= R_9^2 \sin\theta_3 \Delta R \Delta\phi \frac{\Delta T}{\Delta F} \qquad (4.7)$$

$$\left[\begin{array}{l}\text{net rate of increase}\\ \text{in energy by conduction}\\ \text{in the radial direction}\\ \text{through the top and}\\ \text{bottom surfaces}\end{array}\right] + \left[\begin{array}{l}\text{net rate of increase}\\ \text{in energy by conduction}\\ \text{in the } \theta\text{-direction}\\ \text{through the side}\\ \text{surfaces}\end{array}\right]$$

$$= \left[\begin{array}{l}\text{rate of increase}\\ \text{in energy in the}\\ \text{control volume}\end{array}\right]$$

Equation (4.7) becomes;

$$b_9^2 \sin\theta_3 \frac{\Delta\phi}{\Delta R}(T_{3,10} - T_{3,9}) - b_8^2 \sin\theta_3 \frac{\Delta\phi}{\Delta R}(T_{3,9} - T_{3,8})$$

$$+ \sin\phi_3 \frac{R}{\Delta\phi}(T_{4,9} - T_{3,9}) - \sin\phi_2 \frac{\Delta R}{\Delta\phi}(T_{3,9} - T_{2,9})$$

$$= R_9^2 \sin\theta_3 \frac{\Delta\phi \Delta R}{\Delta F}(T_{3,9} - T^o_{3,9}) \qquad (4.8)$$

where T^{o} is the temperature before the time increment of F. In this analysis the angle between the centerline and the side surface of the control volume is denoted by ϕ.

Introducing;

$$B_{3,9} = b_9^2 \sin\theta_3 (\Delta\phi/\Delta R) \qquad A_{3,9} = b_8^2 \sin\theta_3 (\Delta\phi/\Delta R)$$

$$D_{3,9} = \sin\phi_3 (\Delta R/\Delta\phi) \qquad C_{3,9} = \sin\phi_2 (\Delta R/\Delta\phi)$$

and $$V_{3,9} = R_{3,9}^2 \sin\theta_3 (\Delta\phi\Delta R/\Delta F)$$

and rearranging Eq. (4.8), one finds;

$$A_{3,9}T_{3,8} - (A_{3,9} + B_{3,9} + C_{3,9} + D_{3,9} - V_{3,9})T_{3,9}$$

$$+B_{3,9}T_{3,10} = - C_{3,9}T_{2,9} - V_{3,9}T^{o}_{3,9} - D_{3,9}T_{4,9}$$

or simply by dropping the subscripts 3,9;

$$AT_{3,8} - (A+B+C+D-V)T_{3,9} + BT_{3,10} = -CT_{2,9} - VT^{o}_{3,9} - DT_{4,9} \qquad (4.9)$$

Similarly for the c.v.(2,2) the difference equation takes the form;

$$AT_{2,1} - (A+B+C+D-V)T_{2,2} + BT_{2,3} = -CT_{1,2} - V2T^{o}_{2,2} - DT_{3,2} \qquad (4.10)$$

Consider the c.v.(2,1) in Fig.4.3. Noting that there is no heat transfer between point (2,1) and the origin O, the energy balance equation becomes;

$$b_1^2 \sin\theta_2 \quad \Delta\phi \quad \frac{T_{2,2}-T_{2,1}}{\Delta R}$$

$$+ R_1 \sin\phi_2 \Delta R \frac{T_{3,1}-T_{2,1}}{R_1 \Delta\phi} - R_1 \sin\phi_1 \Delta R \frac{T_{2,1}-T_{1,1}}{R_1 \Delta\phi}$$

$$= R_1^2 \sin\theta_2 \Delta\phi \Delta R \frac{T_{2,1}-T_{2,1}^{o}}{\Delta F}$$

Introducing (and again the subscripts 2,1 for these coefficients being omitted);

$$B = \frac{\sin\theta_2 \Delta\phi}{\Delta R}$$

$$D = \frac{\sin\phi_2 \Delta R}{\Delta\phi} \quad , \qquad C = \frac{\sin\phi_1 \; R}{\Delta\phi}$$

$$V = \frac{\sin\theta_2 \Delta\phi \Delta R}{\Delta F}$$

one finds;

$$-(B+C+D+V)T_{2,1} + BT_{2,2} = -CT_{1,1} - VT^{o}_{2,1} - DT_{3,1} \qquad (4.11)$$

Note that this equation is similar to Eq. (4.1Ø) except that A=Ø. This is due to the fact that at the tip of the cone there is no surface area to contribute to the heat transfer.

In general the heat balance difference equation for a control volume with a nodal point (i,j) is given by;

$$AT_{i,j-1} - (A+B+C+D-V)T_{i,j} + BT_{i,j+1} = -CT_{i-1,j} - VT^{o}_{i,j} - DT_{i+1,j} \qquad (4.12)$$

A = (bottom suurface area of c.v.)/($2\pi\Delta R$)

B = (top surface area of c.v.)/($2\pi L\Delta R$)

C = (inside surface area of c.v.)/($2\pi R\Delta\theta$)

D = (outside surface area of c.v.)/($2\pi R\Delta\theta$)

V = (volume of c.v.)/($2\pi\Delta F$)

In particular the coefficient is A=Ø for all control volumes enclosing the origine and C=Ø for all control volumes enclosing the axis of simmetry

Table 4.1 lists the coefficients, A,B,C,D and V for all control volumes.

Thus for n x m control volumes (e.g. 4X1Ø),there are n x m equations. However, there are nxm+n+m unknowns due to extra nodal points imposed on the boundary. The rest of the finite difference

Table 4.1 Coefficients A,B,C,D AND V for the Finite Difference Equation.

c.v.	A	B	C	D	V
i,1	$\emptyset$	$b_1^2 B^*$	C	D	$R_1^2 V^*$
i,2	$b_1^2 B^*$	$b_2^2 B^*$	C	D	$R_2^2 V^*$
...	...	...	...	...	...
i,j	$b_{j-1}^2 B^*$	$b_j^2 B^*$	C	D	$R_j^2 V^*$
...	...	...	...	...	...
i,9	$b_8^2 B^*$	$b_9^2 B^*$	C	D	$R_9^2 V^*$
i,10	$b_9^2 B^*$	$2b_{10}^2 B^*$	C	D	$R_{10}^2 V^*$

where

$$B^* = \sin\theta_i \, \Delta\phi / \Delta R$$

$$C = \sin \phi_{i-1} \Delta R / \Delta \phi$$

$$D = \sin \phi_i \Delta R / \Delta \phi$$

$$V^* = \sin\theta_i \, \Delta\phi \, \Delta R / \Delta F$$

equations are obtained from the boundary conditions.

On the sphere boundary surface (i.e. the top surfase) there are n boundary nodal points (such as 1,11 to 4,11). For the nodal point (i,m+1) the finite difference equation derived from the boundary condition Eq.(4.6b) is;

$$\frac{-K(T_{i,m+1} - T_{i,m})}{\Delta R/2} = T_{i,m+1}$$

or

$$T_{i,m+1} = \left(\frac{2}{2K + \Delta R}\right) T_{i,m} \qquad (4.13)$$

Thus for n columns of control volumes, n equations are obtained.

Similar analysis on the cone surface nodal points based on the boundary condition Eq.(4.6a) gives;

$$T_{n+1,j} = R_j \Delta\phi + T_{n,j} \qquad (4.14)$$

Using Eq.(4.13) and Eq.(4.14) all of the unkown temperatures $T_{i,m+1}$ and $T_{n+1,j}$ are eliminated from the set of finite difference equations. Thus a set of n x m algebraic equations with n x m nknowns is obtained. The procedure for solving these equations is presented in the following sections.

4.3 Solution of the Algebraic Equations

The governing partial differencial equations in the analysis of steady state heat conduction problems do not contain the time dependent term and are elliptic partial differential equations. The conditions along the boundary of the regions are specified everywhere and independent of time. In contrast, the governing partial differential equations in transient heat conduction problems are parabolic equations. In addition to the boundary conditions, the initial condition,i.e. the initial temperature distribution throughout the solid must also be specified. The solution to the parabolic equations is constructed step-by-step marching forward with respect to time.

In the step-by-step construction of the solution for the parabolic equations, instability of the solution due to round off error, or the so called numerical error, may occur. The presence of instabilities stem from violations of the first and second law of thermodynamics [7]. If these laws are violated when a step forward in time is made, the answers obtained will lose their physical significance and the process may become unstable. On the other hand, if these laws are not violated, the scheme will be stable, and any round off or other error which is introduced will be damped out with time.

Stability analysis of difference equations [4.7] has shown that for the implicit method, which solves the set of algebraic equations simultaneously for the n x m unknowns, the physical laws

cannot be violated for any size time step and is unconditionally stable.

In the explicit method, the rate of change in the internal energy of the element during the time interval t to $t + \Delta t$ is based on the net rate of heat flowing to the element at time t and, thus, each finite difference equation contains only one unknown temperature and can readily be solved explicitly for the temperature of the nodal point at time $t + \Delta t$. It was found that the stable criterion for an internal node is $\Delta F < 0.25$ where F is the dimensionless time. For the boundary with heat convection and the boundary with surface heat generation, the criteria are less stringent than the internal nodes. The control volume approach employed in the present analysis is in agreement with the first law of thermodynamics and violation of the criterion is in violation of the second law (i.e. if Δt is sufficiently large, the decrease in internal energy of the element will be so large that the new temperature will be less than zero).

The truncation error, which results if the differential equation is approximated by finite difference equations, is of the order of $(\Delta F + \Delta R^2)$ for both implicit and explicit methods. The solution of the algebraic equations for the present problem is to be solved by a line-by-line method which is combination of the implicit and explicit methods and therefore the stability requirment is somewhere lied between these two methods.

In the present analysis the solid is first heated from the

room temperature by heat generation on the conical surface and then cooled down to room temperature by terminating the surface heat generation. The time increment during the heating process was $0.0001<\Delta F<.01$ for $F<1$ and $\Delta F<.1$ for $F>1$ and during the the cooling process the time increment was less than 0.01. The primary concern in this analysis was not the stability problem but the truncation error which is proportional to the time increment and, therefore, very small increments of time was employed at the initial stage of the heating. During the cooling process high incremnt of time, on the other hand, could violate the second law (in addition to the truncation error) and again small increments was employed in this analysis.

The truncation error due to space increment is proportional to ΔR^2 and $(R\theta)^2$ and, therefore, not as critical as that due to time increment. During the course of the present numerical analysis, the values of $\Delta\phi$ and ΔR were gradually decreased from 15/3.5 degrees and 1/20 to 15/11.5 degrees. This is corresponding to an increase in the number of control volumes from 4 x 20 to 12 x 80. The difference between the numerical result based on 4 x 20 control volumes and that based on 12 x 80 was less than one per cent. It was decided that calculatins using 4 x 20 would be acceptable. The results presented herein were based on 4 x 20 control-volume-analysis.

4.4 Line-by-line Iteration Method

In one-dimensional conduction problem the resulting set of algebraic equations can be solved by the standard Gaussian-elimination method. Because of the particularly simple form of the equations, the elimination process becomes a simple algorithm which is called as TriDiagonal-Matrix Algorithm (or TDMA) [19]. This is due to the fact that when the matrix of the coefficients of these equations is written, all nonzero coefficients align themselves along three diagonals of the matrix.

In two and three dimensional situations the matrix of the coefficients of algebraic equations is no longer tridiagonal. Direct methods (i.e. those requiring no iteration) for solving the algebraic equations are much more complicated and require rather large amounts of computer storage and time.

The alternative is iterative methods which start from a guessed field of the independent variable T and use algebraic equations in some manner to obtain an improved field. Successive repetitions of the algorithm will lead to the desired accuracy of the correct solution. As a matter of fact most of the computer programs for matrix inversion employs some iteration algorithm.

The Gauss-Seidel method is an iterative method in which the values of the variables are calculated by visiting each grid point in a certain order and the new temperature of the visited point is used to calculate the yet-to-be-visited neighbors. A major disadvantage of this method is that its covergence is too slow due to the slow pace of transmission of the boundary condition

information at one grid per iteration.

A convenient combination of the direct method of TDMA for one dimensional situations and the Gaus-Seidel method is the line-by-line method. To apply this method in the present analysis, the discretization equations for the control volumes along the conical surface in r-direction (i.e. column 4) are solved first. The neighboring line (i.e. column 3) are substituted from their latest values and the resulting set of equations is solved by TDMA. This procedure is carried out for next neighboring line (i.e. column 3) and continue on until the center line (i.e. column 1) is solved. This process may be employed in the other direction (i.e. O-direction). It is seen that this method provides a faster transmission of information from the boundary to the interio points and the convergnce is, therefore, faster.
To speed up the numerical integration underrelaxation was used between iterations and also between each time increment. It was also found that the temperatures near the spherical surface (i.e. the convection surface) converges to the solution first and the temperatures near the center of the sphere converges to the solution last. It was, therefore, possible to reduce the number of unknowns as the convergence proceeded towards the center of the sphere. Fig. 4.4 shows the flow chart for heating process. The flow chart for cooling process is essentially the same, except that the calculation terminates, when the temperatures in the solid become less then Ø.ØØ5 (i.e. when the solid temperature is practically equal to the ambient temperature)

4.5 Results and Discussion

In this numerical analysis of transient heat transfer the tooth of a connector is the part of the sphere cut out by a 15-degree cone and heat is generated on the conical surface at a constant intensity. The generated heat transfers through the solid by conduction and dissipates through the spherical surface by convection. Due to the choice of the dimensionless temperature, $T = h(t-t_o)/q$, in Eq. (4.4), it is seen that the present analysis is independent of the heat generation intensity q and the only variable dimensionless parameter is the reciprocal of the Biot modulus, $K = k/(hr_o)$. Thus for a given conductivity k and a convective coefficient h the temperature of the solid,t, is proportional to the heat generation intensity on the cone surface q.

In order to ascertain the convergency of the numerical analysis, two special cases may be investigated. The first case is the insulated boundary condition. The initial temperature in the solid is assumed to be uniform with T = 1 at F = Ø. This case corresponds to a one dimensional transient heat transfer in a sphere. The results were compared with Heisler's results [ref. 1 of Appendix D]. It was found that the temperature distribution in the shere cut by a 15-degree cone is indeed one dimensional and the temperature agrees with that of Heisler within 1 percent.

The second case is a solid with infinite conductivity (or K>>1). The governing equation is

$$qA_c = hA_s(t-t_o) + \rho cV(dt/d\tau) \qquad (4.15)$$

where A_c is the cone surface $\Delta r^2 \sin\phi_4$, A_s is the convective spherical surface $2\Delta r^2(1-\cos\phi)$, V is the volume of the solid, ρ is the density and c is the specific heat of the solid. The solution of this differencial equation (expressed in dimensionless form) with the initial condition that $t=\phi$ at $\tau=\phi$ is

$$T = (A_c/A_s)[1-\exp(-3F/K)] \qquad (4.16)$$

The ratio A_c/A_s for the sphere cut by a 15-degree cone is 3.798.

Comparison of Eq.(4.16) with the numerical results for K=1, 10 and 50 at $\theta=\phi$ and R=0.525 is shown in Fig. 4.5. At K=1 the transient temperature T is considerably higher than Eq.(4.16) for the negligible internal resistance and at K=10 the temperature T becomes very close to that calculated from Eq.(4.16). At K=50 the agreement between Eq.(4.15) and the numerical result is within one percent.

Another method for checking the numerical analysis is to calculate the area-averaged temperature on the convective surface at steady state. Sicnce all heat generated must be transferred through the surface convection, the area-averaged temperature at steady state is equal to A_c/A_s (=3.798). The area-aveaged temperature were found to be within one percent for K=1 through 50 and within 3 percent for K=.01 and 0.1. From the examination of the two special cases and the area-averaged

surface temperature under steady state, it is, therefore, concluded that the present analysis should give correct results.

At K=5Ø the temperature differeences within the solid under steady state condition is less than 3 percent. Thus for K greater than 5Ø, the internal resistance to heat transfer may be neglected.

Figure 4.6 depicts the transient temperature distribution on the surface of the sphere for K=Ø.1. As is seen from Fig.4.6, the temperature near the heat generating surface is consistently higher than those near the centerline. However the temperature differences decrease with increasing conductivity (or K).

Approximate expressions were found by trial-and-error method in this analysis. Figures 4.7 and 4.8 present the transient temperature at nodal point (1,21). Equation (4.17) was obtained by trial-and-error method curve fitting on these figures.

$$T = [3.8-Ø.6/(1+K+6ØK^2)]\ [1 - \exp(-F/(Ø.1+Ø.333K))] \qquad (4.17)$$

Temperatures calcuated from Eq.(4.17) are also shown in these figures with solid lines. It is seen that the approximate expression gives very good results. Figures 4.7 and 4.8 also show that the time F required for the temperature T to reach a steady state increases with increasing K. The time required to reach 99 percent steady state from Eq.(4.17) is equal to Ø.46+1.53K. Howéver the actual time ($t = F\,\rho c r_o^2/k$ where c is the specific heat of the solid), is given by $t = (Ø.46r_o/k + 1.53/h)\rho c r_o$ which indicates that the transient time decreases

with increasing conductivity. For high conductivity materials such as aluminum and copper the expression may further approximated to $t=1.53\rho cr_o/h$ which may also be obtained from Eq.(4.16). For 95 percent steady state the time required is $0.3 + K$ or $t = 0.1r_o/k + 1/h)\rho cr_o$. The corresponding transition time required for the center of the sphere as well as the heat generating surface is slightly less than those mentioned above.

Figures 4.9 and 4.10 depict the transient temperatures at the apex of the cone (nodal point 1,1) for various values of K. A similar approximated expression for T was found to be

$$T = [3.8+3.75/(K+0.01K^2)]\ [1-\exp(-F^p/(0.13+0.27K))] \quad (4.18)$$

The transient temperatures at the circumference of the convective surface (nodal point 5,21) are shown in Figs. 4.11 and 4.12. This nodal point is at the edge of the heat generating surface and the temperature is the highest on the convective surface. The approximated expression was found to be

$$T = [3.8+1.7/(1+20K+60K^2]\ [1-\exp(-F^p/(0.1+.333K))] \quad (4.19)$$

where $p=1-0.2/(1+20k)$. Temperatures calculated from Eq. (4.19) are also shown in these figures with solid lines

The temperature distribution for K=Ø.1 and 1 in the radial direction along the centerline is shown in Figs. 4.13 and 4.14 respectively. As the heating process proceeds, the solid near the heat generating surface starts to receive heat and rise its temperature. The heat continues to flow from the boundary toward the convective surface. Being closest to the heat generating surface, the temperature at the apex is the highest and that at the center of the convective surface is the lowest. The temperature distribution is relatively linear except at the beginning of the heating process. The temperature in the solid increases with decresing K.

Figure 4.15 shows the transient temperature distribution on the heat generatig surface for K=Ø.1. Except that the temperatures near the surface at $R=1$ surface are higher than those along the centerline as shown in Fig. 4.14, the distributions are very much the same. The temperature in the solid is greater for smaller value of K. In this analysis the heating process is terminated as soon as the temperature increase between each time increment is less than 1.ØE-Ø7. Thus the solid is cooled from its steady state temperature distribution at time equal to zero (F=Ø).

Figure 4.16 shows the transient temperature distribution along the centerline (Θ=Ø and Ø<R<1). The temperature distribution transforms from a relatively straight line into a curve with dT/dR=Ø at R=Ø (similar to the one dimensional cooling of the sphere) within a relatively short period of time. The temperature distribution in the solid at the start of

cooling is a strong function of R and a weak function of O. As the cooling is started, the temperature distribution becomes a function of R alone in a very short time (less than one percent difference for F<Ø.Ø2). The cooling is practically one dimensional in nature.

Using the result of the closed form analysis for sphere at long time as described in Appendix D, a closed form approximated expression for the apex temperature(nodal point 1,1) is obtained as follow.

$$T_c=[1-Ø.2/(1+K)]T_{st}\exp[-3F/\ (Ø.2+Ø.13/(1+2K)+K)] \qquad (4.2Ø)$$

$$T_{st} = [3.8+3.75/(K+Ø.ØlK^2)]$$

where T_{st} is the steady state apex temperature. This approximated expression is shown in Fig. 4.17 as solid lines and is compared with the numerical results shown as data points in the figure. The time F required to cool the solid temperature down to a temperature of $Ø.Ø5T_{st}$ is Ø.2 + Ø.13/(1+2K) + K.

In conclusion the numerical analysis has shown that the temperature in the cone is higher for smaller K and it decreases with increasing K. For K>5Ø the internal resistance of the solid may be neglected. Several approximated expressions for the transient temperature distribution in the solid have been obtained and the time reqired for the cone to be heated or cooled to a certain percent of its steady state temperature can be easily obtained. In general this transient time

required is longer for solid with smaller conductivity. In a heating process the temperature on the heat generating surface is the highest and the temperature on the centerline is the lowest. During the cooling process the temperature distribution in the solid changes from a linear distribution along the centerline into a concave downward curved temperture distribution with dT/dR=Ø at R=Ø in a very short time (F<.Ø2) and the temperature distribution in the solid is essentially one-dimensional. The temperarure at the apex is the highest and that at the surface is the lowest during heating process and cooling process as well.

5. CONCLUSIONS

This investigation was carried out to study the performance of aluminum-copper electrical connectors experimentally and to analyze the transient temperature distribution in a cone-shaped tooth.

Three types of connectors investigated were (1) plain surface, (2) plain surface with oxidation inhibitor and (3) teethed surface. These connectors were placed in four different kinds of gas environment, i.e. air, nitrogen, hydrogen and oxygen. The current cycling test showed that the connectors with plain surfaces deteriorated in less than 70 cycles in all gas environments. The connectors having plain surfaces with oxidation inhibitor lasted about twice as many cycles as the plain surface without oxidation inhibitor. After 580 cycles of accelerated testing, the teethed connectors, except those in an oxygen environment, were all at temperatures less than the break-down temperature of 200 C. Based on the data analysis, the teethed connectors were expected to last 20 to 30 times longer than the plain surface connectors. The oxygen environment accelerated the deterioration of the connectors, but the effect was not as pronounced for the teethed connectors and the connectors with oxidation inhibitor. The reducing property of hydrogen did not affect the performance of the connectors.

The numerical analysis of transient heat transfer in a

tooth made of the partof the sphere cut out by a 30-deg. cone showed that the rate of temperature rise in the solid increases with higher heat generation on the surface of the cone, and decreases with increasing surface convection as well as solid conductivity. The temperature difference in the solid is less than three percent for K = 50 and, therefore, the internal resistance of the solid may be neglected for K > 50. The time required for the solid to reach y percent of its steady state temperature in heating is given by F = (0.1 + 0.333K)ln(1-0.01y) and that in cooling is given by F = [0.2 + 0.13/(1+2K) + K] ln(1-0.01y). In both heating and cooling this transient time required is longer for smaller conductivity. The transient temperature distribution in the cone during heating can be estimated with those approximated equations 4.17 through 4.19.

In a heating process the temperature on the heat generating surface is higher with the apex at the highest and the temperature at the center of the convective surface is at the lowest. During the cooling process the temperature distribution in the solid changes from a linear distribution along the centerline into a concave downward curved temperature distribution with dT/dR=0 at R=0 in a very short time (F≤.02). The temperature distribution in the solid is essentially one-dimensional. The apex temperature during cooling for F > 0.02 may be calculated from Eq. 4.20.

The line-by-line iteration method employed in this analysis is a combination of the direct method of TDMA

(TriDiagonal-Matrix Algorithm) and the Gauss-Seidel method and have shown its usefullness in saving computer time. The control volume approach in conjuction with the line-by-line method can be easily extended to solve problems involving temperature dependent conductivity.

6. RECOMMENDATIONS

The connector provided with cone-shaped teeth and cavities has been investigated and the result indicates that it is effective in solving the problems associated with the connection between an aluminum conductor and a copper connector. The cone-shaped teeth penetrating into the conductor have served several purposes: they increase the contact surface area, the contact pressure from the normal pressure, and the heat transfer surface area. Since the shape of the penetrating tooth may be any configuration, it is interesting to investigate other geometrical configurations. Some of the concievable configurations are (1) truncated cone, (2) rectangular cross-section bar or (3) rectangular cross-section cone.

The cavities underneath the cone-shaped teeth are for compensating the expansion of the conductor. The depth of the cavity could increase the effective length of the projected member, the fin. An investigation on the performance of the connector with projected members having cavities with various depth is recommended.

Metal creep is considered to be an important factor affecting the life of a joint, and this is a function of time and temperature. It is important, therefore, not to hurry the testing of joints, otherwise the effects of creep may not be

observed. Even if 2000 cycles are sufficient to permit the effects of creep, if any, to become apparent, the time required would be too long to be practical.

In the field of theoretical analysis, the following parameters may also be investigated: the angle of the cone may be varied, and the conductivity of the solid may be a function of temperature.

REFERENCES

1. Boudart, M., " Kinetics of Chemical Processes ", Prentice-Hall, Inc, Englewood, Cliffs, N.J. 1968.

2. Bowden, F. P., and Tabor D., " The Friction and Lubrication of Solid, I ", Oxford, Clarendon Press, 1950.

3. Bond, N. T., " Aluminum Contact Surfaces in Electrical Transition Interfaces ". I.E.E.E. Transactions on Parts, Material, and Packaging, Vol. PMP-5, No. 2, June 1969.

4. Chen, R.Y. and Kuo, T.L., " Closed Form Solutions for Constant-Temperature Heating of Solids ". Mech. Engrg. News A.E.E.E., Feb.,1979, PP.20-23.

5. Chaikin, S. W., " Mechanics of Electrical Contact Failure Caused By Surface Contamination ", Electro-Technology, August 1961, PP.70-75.

6. Devins, J. C. and Sharbaugh, A. H., " The Fundamental Nature of Electrical Breakdown ", Electro-Technology, Feb. 1961.

7. Clausing, A. M. " Numerical Methods in Heat Transfer ", Advanced Heat Transfer, Editor B. T. Chao, University. of Illinois Press, PP. 157-216, 1969

8. Freudiger, E. and Jost, E.," The Kinetics and Thermodynamics of the Internal Oxidation of Silver-Cadmium Alloys and the Arc Erosion Properties of the Oxidized Material", International Research Symposium on Electric Contact Phenomena, University of Maine, Orono, Maine. (1961)

9. Greenwood, J. A., " Constriction Resistance and the Real Area of Contact ", British J. Appl. Phys., Vol. 17. 1966

10. Hakajima, K., " Properties of New Aluminum Alloy Conductor ", Wire Association, Non-ferrous Div. Meeting, April 15, 1970

11. Hoffman, R., " Terminating Aluminum Conductors ", I.E.E.E. Powre Engineering Society, 1972 Winter Meeting.

12. Holm, R., Electric Contacts ,Theory and Application, Springer- Verlag, New York,1967

13. Holm, R., "Electrical Contact Handbook", Springer-Verlag, Berlin/Gottinger/Heidelberg, (1958)

14. Jadynak, L. " Where the (Swtich) Action is ", Components, I.E.E.E. Spectrum, Oct. 1973.

15. Jones, F. L., " The Physics of Electrical Contacts ", Oxford, Clarendon Press, 1957.

16. Kuo, T. L., " Insulation Piercing Magnet Wire Connectors ", U. S. Patent, No. 3549,786. Presented at 10th Electrical Insulation Conf. Sept. 1971, Chicago.

17. Kuo, T. L. " Joining Copper and Aluminum Conductors ---- Try Cutting Tooth Connectors ". Insulation / Circuits, Vol. 19, No. 6, June 1973.

18. Naybour, R. D., Ferrell, T., " Degradation Mechanical Connectors on Aluminum Connectors " Proc. I.E.E. Vol. 120, No. 2, Feb. 1973.

19 Patankar, S. V., Numerical Heat Transfer and Fluid Flow, Hemisphere Publ. Corp., McGraw Hill Book Co. New York,1980

20. Roulier, I., " Testing of Mechanical Joints in Aluminum Conductors for Insulated Cables ". Proc. I.E.E., vol 110, No 4, April 1963.

21. Shackman, N. and Thomas, R. W., " Pressure-Type Connectors for Aluminum and Copper Connectors ", A.I.E.E. Fall General Meeting, Detroit, Mich., Oct. 15-20, 1965.

22. Spofford, T. G., " Index of Performance-Aluminum Wire Terminals ", Technical Report, The Thomas & Betts Co. Elizabeth, N.J. 1968.

23. Takano, E. and Mano, K., " Theoretical Lifetime of Static Contacts ", I.E.E.E. Trans., 1967.

24. Takano, E. and Mano, K., " The Failure Mode and Lifetime of Static Contacts ".

25. Thomas & Betts Co., Kuo T.L., Connector, U. S. Patent No. 3549,786

26. Williamson, J. B. P., " Significance of Non-destructive Tests of Compression Joints ", Proc. I.E.E., 1962.

27. Williamson, J. B. P., " Deterioration Process in Electrical Connectors " Proceedings of the 4th International Symposium on Electrical Contacts, Swansea, 1968.

APPENDIX A

EQUIPMENTS

Equipment used for the current cycling are listed as follows.

Harness installation:

1. Wire-AWG #12 solid aluminum with insulation removed.
2. Installing pump-Thomas & Betts CAT. #13610.
3. Installing tool-Thomas & Betts CAT. #13642 M
4. Installing die-Thomas & Betts CAT. #13670 A.

Current Cycling:

1. Transformer, variable, (powerstat)-Superior Electric Co. Model #3PN136B.
2. Transformer, variable motor driven, (powerstat)-Superior Electric Co. Model #30MD136B .
3. Transformer, Power-Federal Pacific Co. Model CTE ratio 1000/5 .
4. Transformer, controller-Superior Electric Co. Model #T6340.
5. Transformer, current controller-Midwest Electric Co. Model #9CT375B ratio 75/5.

6. Regulator controller - Superior Electric Co. Model #FR5Ø1BMP.
7. Meter, current 5 Amp AC-Weston Model #433.
8. Timer, 5 hour-Eagle Signal Model #HG1Ø8A6.
9. Counter, electric-Durant Model #5-SP-1-RMF.
10. Relay, 72Ø VA-Allen Bradley type "N".

Temperature Measurements:

1. Thermocouple wire, type "J"
2. Thermocouple Jack Panel-thermoelectric Model #416Ø3.
3. Thermocouple temperature indicator-Newport Laboratories Model #26ØØJC.
4. Meter, milliohm-Keithley instruments Model #5Ø3.

APPENDIX B.

GLOSSARY OF TERMS:

This glossary contains brief explanations of terms which are used in a special sense in this report, or terms which, though in general use, are possibly unfamiliar to either mechanical or electrical engineers.

1. Contact Resistance

The contact resistance is the electrical resistance at the interface between two metallic components placed in mechanical contact with one another. In practice most methods of measuring the contact resistance necessarily include the resistance of a portion of the body of each component. If this resistance can be calculated from the specific resistivities of the components and their geometries it can be subtracted from the measured resistance leaving a remainder which is the contact resistance.

2. Constriction Resistance and Contact Voltage

Electric current mostly crosses the interface between two metal components at microscopic metal to metal bridge, termed contact spots. These occur where asperities of the two contacting surfaces bear on one another with sufficient force to deform them plastically, rupturing the oxide films always present on metal surfaces in air, and extruding metal through the ruptures. The current hitherto flowing through the full cross-section of each

component has now to constrict itself to pass through these microscopic contact spots with a consequent increase in the voltage gradient in these regions.

The increased voltage drop across the interface is the contact voltage, while its ratio to the current is the constriction resistance. This resistance is usually the major part of the contact resistance, and of the oxide films on the metal surfaces are of high specific resistivity it is identical with the contact resistance. If, however, the oxide films permit the passage of current to some extent another factor, the film resistance, may contribute to the contact resistance.

3. Film Resistance

This is the total resistance of any current paths through the surface oxide films, as opposed to current paths through metal to metal bridges. If the metal to metal bridges exist in parallel with paths through the oxide films the film resistance is in parallel with the constriction resistance. With the high-resistance oxide films the film resistance tends to infinity and does not modify the contact resistance. If, however, they are conducting - even only moderately so - because of their greater area than the metal contact spots they may constitute a significant parallel term which lowers the contact resistance. There is a third case where the oxide films grow across fractured metal to metal contact spots, in which case they contribute a series addition to the constriction resistance.

4. Bulk Temperature, Supertemperature and Interface Temperature

Bulk temperature is the teperature anywhere in the bodies of the contacting components, except at the contact interface. It is assumed to be uniform throughout.

As the contact spots are regions of higher current density than the bodies of the contacting components, they generate heat at a greater rate and are at a higher temperature.

This excess temperature, which can be shown to be the same for all contact spots in a given contact, is called the supertemperature. As the rate of heat generation is determined by the electrical conductivity and the rate of heat dissipation is determined by the thermal conductivity, the supertemperature is dependent on their ratio, and also on the contact voltage. The term interface temperature is used in this report to denote the actual temperature of the contact spots and is simply the sum of the bulk temperature and the supertemperature.

5. The Wiedman-Franz-Lorenz Law

It is known that good thermal conductors are also good electrical conductors. This led us to suspect that thermal as well as electrical conduction may depend upon the activity of electrons. The relationship is brought out quantitatively by Wiedeman-Franz-Lorenz Law. If we calculate the ratio of the thermal conductivity (in calories per cm. per sec. per degree) to the electrical conductivity (in reciprocal ohms-centimeters) for a

number of metal at Ø C we get results like the following:

copper	Ø.ØØØØØ156
platinum	Ø.ØØØØØ143
lead	Ø.ØØØØØ169

The ratio appears to be nearly constant.

The Wiedeman - Franz - Lorenz Law states that the ratio of the thermal to the electrical conductivity for all metal is proportional to the absolute temperature T, and in the above units equal to $6.11 \times 10_{-9}$ T. For Ø C (273 K) this gives Ø.ØØØØØ147 calorie ohm per sec. per degree, which is very close to the observed value for platinum.

Lorenz showed that the quantity

$$L = k/oT = (\pi_2^2/3)\ (k/e) = 2.45 \times 10^{-8}\ \text{Volt}^2/\text{K}$$

where k is Boltzmann's constant, e the charge on an electron, and T the absolute temperature.

6. Plastic and Elastic Strain or Deformation

The terms strain and deformation are synonymous, the former being the more quantitative concept. When a force is applied to metal the resultant strain may consist of two parts, an elastic part which is recovered when the force is removed and a plastic part which is not recovered when the force is removerd.

7. Bulk Stress, Bulk Plastic Deformation

The term "bulk" is used here to denote properties or effects occurring in the body of the components as opposed to localised regions in or adjacent to contact spots.

8. Activation Energy

Many physical and metallurgical processes involve thermal motion of atoms, and the transition from one arrangement of atoms to another involves them breaking through some energy barrier. The "height" of this energy barrier is termed the activation energy, Q, and only those atoms with energy greater than Q can make the transition. At any instant the proportion of atoms with energy greater than Q is given by kinetic theory as exp. $-Q/kT$ where k is Boltzmann's constant and T the absolute temperature. This exponential determines the rate at which the rearrangement takes place. Stress relaxation is a process involving atomic rearrangements in which Q depends on intrinsic structural factors, together with the initial stress and the stress at the instant under consideration.

APPENDIX C

EXPERIMENTAL DATA: GROUP 1, Plain Surface(in Air)

CYCLE	AMBIENT TEMP. C	CONNECTOR TEMPERATURE C					
		1	2	3	4	5	6
0	19.75	20.00	30.00	33.00	30.00	72.00	36.00
5	20.00	52.50	57.00	33.00	80.00	91.00	63.00
10	25.00	52.75	62.00	57.00	99.00	107.50	87.50
20	27.50	62.50	77.50	93.00	117.00	139.00	100.00
25	19.75	62.50	89.00	95.00	136.00	158.00	123.00
30	26.00	72.50	105.00	149.00	155.00	201.00	124.00
35	22.50	83.00	168.00	157.50	162.50		136.00
40	17.00	123.00	178.00	150.00	196.00		161.00
45	28.00	138.00	205.00	176.00	212.00		198.00
50	27.50	133.00		190.00			202.00
55	22.50	138.00		184.00			
60	32.00	150.00		192.00			
65	20.00	164.00		224.00			
70	27.00	210.00					

EXPERIMENTAL DATA: GROUP 2, Plain Surface(in Nitrogen)

CYCLE	AMBIENT TEMP. C	CONNECTOR TEMPERATURE C					
		7	8	9	10	11	12
0	30.00	74.00	81.00	35.00	49.00	26.00	30.00
5	30.00	84.00	91.00	59.00	46.00	40.00	38.50
10	25.00	82.50	100.00	119.00	51.00	48.00	41.00
15	27.50	103.00	109.00	180.00	61.00	46.50	50.00
20	30.00	117.50	122.00	209.00	76.00	57.50	85.00
25	27.50	129.00	151.00		101.00	69.00	80.00
30	32.50	143.00	211.00		111.00	76.50	93.00
35	28.00	142.00			134.00	154.00	117.50
40	32.00	172.00			138.00	186.00	142.00
45	26.00	183.00			152.50	207.50	145.00
50	25.00	192.00			166.00		176.50
55	26.00	214.00			215.00		177.50
60	32.50						207.50

EXPERIMENTAL DATA: GROUP 3, Plain Surface(in Hydrogen)

CYCLE	AMBIENT TEMP. C	CONNECTOR TEMPERATURE C					
		13	14	15	16	17	18
0	30.00	34.50	36.00	87.50	51.00	76.00	50.00
5	25.00	37.00	40.00	87.00	91.00	76.50	50.05
10	29.50	48.00	40.00	95.00	89.00	76.50	50.00
15	22.00	48.00	54.00	103.00	106.00	84.00	67.00
20	38.00	75.50	55.00	112.00	116.00	104.00	128.00
25	33.00	82.00	87.50	137.00	137.00	149.00	128.00
30	31.50	100.00	91.50	147.00	152.00	224.00	141.50
35	30.00	120.00	96.00	160.50	214.00		205.00
40	28.50	127.00	102.50	172.00			
45	32.00	128.00	154.00	206.50			
50	37.50	142.00	186.50				
55	33.50	183.00	209.00				
60	37.50	203.00					
65	30.05						

EXPERIMENTAL DATA: GROUP 4, Plain Surface(in Oxygen)

CYCLE	AMBIENT TEMP. C	CONNECTORS TEMPERATURE C					
		19	20	21	22	23	24
0	23.00	35.05	30.00	86.00	44.00	69.00	26.00
5	23.00	54.00	35.05	101.00	46.00	84.00	70.00
10	25.00	58.50	65.05	113.00	76.00	178.00	131.00
15	23.00	157.50	119.00	131.00	81.00	224.00	186.50
20	25.05	214.00	182.50	156.50	196.00		229.00
25	28.50		202.00	176.00	231.00		
30	33.50		240.00	241.00			

EXPERIMENTAL DATA: GROUP 5, Plain Surface/Inhibitor(in Air)

CYCLE	AMBIENT TEMP. C	CONNECTOR TEMPERATURE C					
		25	26	27	28	29	30
0	23.00	30.00	28.00	34.00	49.00	25.50	42.00
5	22.50	32.00	35.00	26.00	49.05	24.50	41.00
10	23.50	33.00	34.50	36.00	50.00	28.00	42.00
15	20.50	36.00	34.00	41.05	54.00	36.00	40.00
20	24.00	32.50	40.05	41.05	55.00	36.50	50.00
25	25.00	46.00	40.00	43.50	56.00	66.00	50.05
30	23.50	55.00	40.00	44.00	58.00	67.00	52.00
35	25.00	62.00	42.00	46.00	58.00	70.00	52.00
40	24.00	61.50	45.00	52.50	64.50	75.00	57.50
45	25.05	68.50	45.00	54.00	64.50	78.00	59.05
50	22.50	79.00	44.05	55.00	71.00	84.00	75.00
55	25.00	83.00	59.05	54.00	104.00	86.05	65.05
60	23.50	87.50	61.05	57.00	114.00	99.00	69.00
65	25.00	102.00	54.00	59.05	138.00	126.00	71.00
70	23.00	102.50	58.00	64.05	157.00	182.00	72.00
75	24.00	111.00	70.05	65.05	171.00	216.00	76.50
80	24.50	119.00	66.00	78.00	220.00		72.00
85	21.50	122.00	67.50	85.05			72.00
90	24.00	132.00	80.05	91.00			85.00
95	24.00	141.00	76.00	110.00			95.00
100	25.00	164.00	81.05	144.50			100.05
105	27.00	206.00	101.00	159.50			108.00
110	27.00		146.00	219.00			128.00
115	27.00		166.00				152.00
120	25.05		207.00				166.00
125	29.00						192.00

EXPERIMENTAL DATA: GROUP 6, Plain Surface/Inhibitor(in Nitrogen)

CYCLE	AMBIENT TEMP. C	CONNECTOR TEMPERATURE C					
		31	32	33	34	35	36
0	24.05	50.00	25.00	45.00	39.00	29.00	21.00
5	26.00	50.00	27.50	45.00	39.00	22.50	32.00
10	24.00	51.00	31.00	45.00	49.00	26.00	24.00
15	27.50	54.00	36.00	49.00	44.00	41.00	30.00
20	27.00	55.00	40.00	51.00	46.00	44.00	30.50
25	23.00	51.00	43.00	45.00	49.00	67.00	35.00
30	21.00	46.00	42.50	49.00	51.00	76.00	35.50
35	21.00	61.50	46.00	60.00	51.00	76.00	40.50
40	29.00	61.00	40.00	66.00	45.00	86.00	36.00
45	27.50	69.50	51.00	74.00	62.50	99.00	45.00
50	21.00	75.00	51.00	66.50	71.00	106.50	46.00
55	28.00	75.00	57.50	78.00	83.00	125.00	51.00
60	25.00	79.00	65.00	90.00	85.00	151.50	55.00
65	27.00	79.00	84.00	102.50	121.50	188.50	66.50
70	26.05	99.00	107.50	125.50	134.00	210.00	66.50
75	23.00	101.00	127.50	122.50	201.50		66.50
80	26.00	105.00	136.00	147.50			60.00
85	25.50	108.00	161.00	217.50			70.00
90	24.50	117.50	201.00				76.50
95	27.50	155.00					80.50
100	24.00	201.00					85.00
105	24.00						91.00
110	26.05						110.00
115	24.00						136.00
120	26.00						161.00

EXPERIMENTAL DATA: GROUP 7, Plain Surface/Inhibitor(in Hydrogen)

CYCLE	AMBIENT TEMP. C	CONNECTOR TEMPERATURE C					
		37	38	39	40	41	42
0	24.00	20.00	44.00	27.50	34.00	24.00	38.00
5	26.00	20.05	40.000	45.00	34.50	24.00	57.00
10	24.00	24.00	48.00	54.00	39.00	29.00	59.00
15	27.00	24.00	55.00	49.00	44.00	29.00	61.00
20	27.00	26.50	56.00	48.50	51.00	34.00	64.00
25	23.00	30.00	58.00	51.50	49.00	39.00	65.00
30	21.00	30.00	61.00	51.50	56.00	36.50	68.00
35	21.00	40.50	71.00	59.00	56.00	36.00	77.00
40	29.00	40.00	66.00	60.00	71.00	49.00	75.00
45	27.00	45.00	81.50	64.00	75.00	51.00	75.00
50	21.00	43.00	80.00	65.00	75.50	55.00	80.00
55	28.00	44.00	85.00	69.00	91.00	55.00	80.00
60	25.00	55.00	106.00	69.00	95.00	65.00	114.00
65	27.00	52.50	116.00	76.00	101.00	70.00	110.00
70	26.00	59.00	207.50	81.00	111.00	75.00	116.50
75	23.00	65.00		85.50	121.00	95.00	116.50
80	26.00	66.50		100.00	126.00	109.00	130.00
85	26.00	70.00		115.00	121.00	127.00	135.00
90	25.00	81.00		160.00	131.00	201.50	149.00
95	27.50	83.00		180.00	166.00		209.50
100	24.00	90.00		220.00	201.50		
105	24.00	104.00					
110	26.00	120.00					
115	24.00	111.00					
120	26.00	111.00					
125	24.00	115.00					
130	24.50	143.50					
135	25.00	176.00					
140	24.00	215.00					

EXPERIMENTAL DATA: GROUP 8, Plain Surface/Inhibitor(in Oxygen)

CYCLE	AMBIENT TEMP. C	CONNECTOR TEMPERATURE C					
		43	44	45	46	47	48
0	24.05	21.00	18.00	18.00	29.00	14.00	25.00
5	26.00	20.00	21.00	15.00	29.50	17.50	25.00
10	24.00	21.00	19.00	34.00	30.00	23.00	26.00
15	27.50	21.00	31.00	36.00	44.00	23.00	27.50
20	27.00	34.00	31.00	49.00	40.00	28.00	35.00
25	23.00	57.00	40.00	51.00	46.00	30.00	35.00
30	21.00	58.00	35.00	54.00	49.00	40.00	45.00
35	21.00	55.00	45.00	64.00	59.00	40.00	50.00
40	29.00	70.00	49.00	66.50	59.00	44.00	54.00
45	27.50	87.00	69.00	80.00	76.00	51.00	64.00
50	21.00	90.00	62.00	84.00	76.50	56.00	69.00
55	28.00	107.00	67.00	89.00	84.00	59.00	93.50
60	25.00	111.00	71.50	93.00	106.00	60.00	97.00
65	27.00	134.00	73.00		109.00	64.00	104.00
70	26.05	156.00	75.00		121.00	70.00	114.00
75	23.00	242.00	79.00		124.00	85.00	120.00
80	26.00		94.00		120.00	89.00	125.00
85	25.50		95.00		144.00	101.00	134.00
90	24.50		119.00		150.00	121.00	140.00
95	27.50		129.00		154.00	120.00	147.50
100	24.00		150.00		155.00	170.00	160.00
105	24.00		165.00		176.00	204.00	170.00
110	26.05		180.00		196.00		175.00
115	24.00		190.00		198.00		198.00
120	26.00		191.50		209.00		215.00

EXPERIMENTAL DATA: GROUP 9, Teethed Surface(in Air)

CYCLE	AMBIENT TEMP. C	CONNECTOR TEMPERATURE C					
		49	50	51	52	53	54
0	20.00	30.00	34.00	34.00	39.50	30.00	34.00
10	24.00	30.00	34.50	34.00	38.00	44.00	40.00
20	26.00	38.00	34.50	32.00	46.00	50.00	42.50
30	20.50	36.00	35.00	40.00	48.00	51.00	45.00
40	29.00	44.00	40.00	51.00	51.00	54.50	50.00
50	21.00	46.50	44.00	57.00	55.00	60.00	48.00
60	25.00	47.50	45.00	43.00	62.00	65.00	56.00
70	26.05	47.50	45.50	53.00	60.00	64.50	56.00
80	26.50	48.00	54.00	45.00	69.00	74.00	62.50
90	25.00	50.00	52.00	45.00	74.00	69.50	62.50
100	24.50	50.00	48.00	54.00	72.00	75.00	64.00
120	26.50	51.50	55.50	44.00	63.00	75.00	67.50
140	24.00	53.00	50.00	42.00	76.00	80.00	68.00
160	26.00	53.00	56.00	44.00	70.00	82.00	75.00
180	26.00	54.50	58.50	44.00	86.00	90.00	74.50
200	27.50	61.00	55.00	44.00	87.00	89.50	75.00
220	24.00	64.00	60.00	73.50	85.00	90.00	78.00
240	25.00	64.50	84.00	77.50	92.50	99.00	87.00
260	24.00	84.00	86.00	81.50	94.00	101.00	89.50
280	26.00	80.00	77.50	83.50	98.00	103.00	92.00
300	21.00	75.50	80.00	86.00	99.00	106.00	94.00
320	27.00	76.50	73.00	86.00	104.00	100.00	96.00
340	24.50	76.00	80.50	96.00	110.00	105.00	92.00
360	25.00	78.50	85.00	94.00	104.50	109.00	98.00
380	25.00	80.00	85.00	94.50	109.00	105.00	98.50
400	23.00	80.00	85.00	92.00	109.00	114.00	102.50
420	23.00	84.00	89.00	98.00	114.00	109.00	103.00
440	23.00	91.00	90.00	100.00	125.00	119.00	106.00
460	26.00	95.00	95.00	105.00	125.00	128.00	111.00
480	24.00	96.00	95.00	105.00	125.00	125.00	111.00
500	23.50	98.00	100.00	124.00	130.00	129.00	115.00
520	21.50	99.00	101.00	120.00	131.00	131.00	126.00
540	22.50	102.00	106.00	124.00	136.00	137.00	132.00
550	25.00	103.50	108.00	142.00	145.00	144.00	134.00
560	25.00	103.00	115.00	140.00	151.00	139.00	133.00
570	25.00	100.00	124.00	138.00	144.00	144.00	134.00
580	25.5	100.50	126.00	135.00	154.00	144.00	132.00

END OF EXPERIMENTAL DATA: GROUP 9

EXPERIMENTAL DATA: GROUP 10, Teethed Surface (in Nitrogen)

CYCLE	AMBIENT TEMP. C	CONNECTORS 55	56	57	58	59	60
0	23.00	48.00	32.50	36.00	39.00	29.00	40.00
10	22.00	33.00	36.00	40.00	52.50	44.00	47.00
20	26.00	49.00	38.00	42.00	53.00	44.00	45.00
30	21.00	56.00	40.00	42.50	60.00	47.00	51.00
40	25.00	55.00	47.00	43.00	59.00	49.00	52.00
50	26.00	59.00	48.00	44.00	65.00	50.00	55.00
60	27.50	62.50	50.00	44.00	66.00	54.00	57.00
70	24.00	66.00	53.00	47.50	66.00	56.00	62.00
80	25.00	60.00	52.00	46.00	65.00	55.00	62.50
90	24.00	64.00	54.00	48.00	75.00	56.00	66.00
100	24.00	64.00	54.00	49.00	74.00	60.00	67.00
120	24.00	69.00	54.00	50.00	64.00	59.00	64.00
140	25.00	69.00	50.00	54.00	72.00	59.00	63.00
160	25.00	65.00	57.50	54.00	79.00	60.00	64.00
180	25.00	67.50	60.00	55.00	85.00	63.00	71.00
200	25.00	65.00	56.00	54.00	86.00	61.00	68.00
220	26.00	70.00	59.00	55.00	90.00	62.00	74.00
240	26.00	82.50	51.00	55.00	91.00	60.00	73.00
260	26.00	89.00	60.00	56.00	83.00	65.00	76.00
280	27.00	86.00	60.00	56.00	82.00	74.00	78.00
300	27.00	85.00	60.00	57.50	90.00	74.00	82.50
320	25.00	82.50	58.00	62.50	90.00	76.00	86.00
340	24.00	85.00	64.00	66.00	95.00	77.50	89.00
360	26.00	95.00	68.00	70.00	102.50	87.50	99.00
380	25.00	105.00	25.00	72.00	106.00	86.00	104.00
400	25.00	110.00	77.00	73.00	112.50	90.00	108.00
420	26.00	110.00	74.00	77.50	113.00	91.00	115.00
440	24.00	116.00	78.00	83.00	122.50	92.00	120.00
460	24.00	115.00	77.50	86.00	120.00	99.00	118.00
480	24.00	115.00	85.00	90.00	126.00	97.50	120.00
500	24.00	131.00	90.00	96.00	126.00	105.00	124.00
520	24.00	131.00	95.00	105.00	126.00	114.00	135.00
540	24.00	131.00	95.00	114.00	135.00	122.00	140.00
550	26.00	143.00	100.00	116.00	140.00	124.00	146.00
560	24.00	142.00	105.00	119.00	145.00	139.00	150.00
570	26.00	145.00	106.00	120.00	151.00	140.00	156.00
580	24.00	148.00	108.00	122.50	151.00	135.00	157.00

END OF EXPERIMENTAL DATA: GROUP 10

EXPERIMENTAL DATA: GROUP 11, Teethed Surface(in Hygrogen)

CYCLE	AMBIENT TEMP. C	CONNECTOR TEMPERATURE C					
		61	62	63	64	65	66
0	23.00	39.00	43.00	29.00	35.00	40.00	32.50
10	24.00	45.00	49.00	42.00	33.00	38.00	38.00
20	23.00	42.50	49.00	44.00	34.00	30.00	31.00
30	23.00	50.00	35.00	46.00	39.00	43.00	37.50
40	27.50	55.00	50.00	32.00	40.00	47.00	38.00
50	28.00	52.50	56.00	36.00	44.00	48.00	41.00
60	26.00	52.00	55.00	48.00	44.00	52.00	40.00
70	27.50	61.00	55.00	42.00	49.00	59.00	46.00
80	24.00	60.00	56.00	38.00	43.00	52.00	49.00
90	24.00	65.00	56.00	41.00	49.00	62.00	52.50
100	29.00	68.00	59.00	37.00	49.00	65.00	53.00
120	26.00	57.50	60.00	51.00	52.00	67.00	57.00
140	29.00	64.00	60.00	55.00	55.00	68.00	52.00
160	26.00	72.00	58.00	52.00	67.00	76.00	63.00
180	27.50	24.00	89.00	100.00	84.00	77.00	79.00
200	27.50	97.00	102.00	106.00	92.50	76.00	87.50
220	26.00	86.00	100.00	105.00	95.00	89.00	86.00
240	24.00	90.00	114.00	105.00	96.00	119.00	88.00
260	25.00	98.00	116.00	110.00	101.00	125.00	105.00
280	25.00	123.00	116.00	126.00	100.00	112.00	105.00
300	25.00	110.00	130.00	125.00	99.00	113.00	105.00
320	25.00	119.00	140.00	128.00	107.50	117.50	112.50
340	25.00	144.00	138.00	129.00	112.50	124.00	117.50
360	25.00	148.00	153.00	133.00	120.00	130.00	122.50
380	26.00	157.00	143.00	138.00	120.00	129.00	125.00
400	27.50	162.00	142.00	139.00	128.00	120.00	125.00
420	27.00	155.00	160.00	148.00	124.00	134.00	126.00
440	26.00	165.00	157.50	150.00	129.00	134.00	125.00
460	25.00	154.00	160.00	149.00	134.00	130.00	130.00
480	24.00	154.00	158.00	146.00	134.00	125.00	137.50
500	24.00	163.00	169.00	157.50	140.00	129.00	135.00
520	26.00	160.00	157.50	164.00	144.00	134.00	139.00
530	26.00	177.00	170.00	165.00	146.00	135.00	141.00
540	26.00	173.00	177.50	165.00	146.00	135.00	142.00
550	26.00	175.00	160.00	168.00	149.00	139.00	144.00
560	27.00	176.00	159.00	170.00	149.00	140.00	144.00
570	27.00	195.00	176.00	168.00	150.00	141.00	146.00

END OF EXPERIMENTAL DATA: GROUP 1

EXPERIMENTAL DATA: GROUP 12, Teethed Surface(in Oxygen)

CYCLE	AMBIENT TEMP. C	CONNECTOR TEMPERATURE C					
		67	68	69	70	71	72
0	22.00	35.00	47.00	35.00	40.00	43.00	37.00
10	19.00	40.00	54.00	41.00	46.00	47.00	50.00
20	20.00	44.00	57.00	44.00	47.00	50.00	54.00
30	21.00	45.00	57.50	45.00	50.00	47.50	53.00
40	20.00	49.00	66.00	46.00	64.00	58.00	62.50
50	20.00	42.50	59.00	44.00	58.00	55.00	63.00
60	22.00	49.00	67.00	45.00	63.00	60.00	62.50
70	20.00	46.00	67.00	46.00	59.00	63.00	66.00
80	22.00	45.00	75.00	45.00	60.00	64.00	67.00
90	19.00	45.00	73.00	48.00	64.00	66.00	70.00
100	21.00	50.00	76.00	46.00	64.00	68.00	72.50
110	22.50	47.50	79.00	46.00	66.00	70.00	75.00
120	20.00	50.00	93.00	53.00	78.00	83.00	89.00
140	21.00	51.00	94.00	53.00	76.00	82.00	90.00
160	23.00	55.00	99.00	58.00	80.00	84.00	95.00
180	24.00	57.00	100.00	59.00	82.00	87.00	95.00
200	23.00	55.00	101.00	61.00	85.00	90.00	96.00
220	21.00	58.00	107.50	66.00	90.00	94.00	102.00
240	20.00	55.00	110.00	68.00	99.00	96.00	106.00
260	22.00	58.00	115.00	73.00	102.00	98.00	110.00
280	24.00	69.00	110.00	70.00	97.00	100.00	114.00
300	23.00	69.00	123.00	74.00	109.00	103.00	120.00
320	20.00	70.00	125.00	76.00	116.00	105.00	121.00
340	20.00	72.50	128.00	89.00	122.50	105.00	116.00
360	22.00	84.00	129.00	94.00	114.00	107.50	120.00
380	20.00	86.00	130.00	100.00	120.00	115.00	123.00
400	23.00	92.50	133.00	110.00	137.00	120.00	126.00
420	20.00	94.00	136.00	114.00	134.00	124.00	130.00
440	20.00	101.00	145.00	121.00	137.00	134.00	141.00
460	24.00	110.00	152.00	128.00	143.00	140.00	146.00
480	22.00	115.00	172.00	134.00	160.00	147.50	153.00
500	22.00	122.50	180.00	140.00	163.00	162.50	170.00
520	19.00	127.00	184.00	147.50	168.00	169.00	175.00
530	19.00	131.00	186.00	150.00	163.00	172.50	177.00
540	21.00	134.00	189.00	154.00	163.00	174.00	175.00
550	24.00	138.00	189.00	155.00	169.00	179.00	184.00
560	26.00	160.00	199.00	160.00	191.00	188.00	205.00
570	18.00	185.00	214.00	162.00	193.00	208.00	205.00
580	22.50	185.00	222.00	162.00	195.00	215.00	215.00

END OF EXPERIMENTAL DATA: GROUP 12

APPENDIX D

CLOSED FORM SOLUTIONS FOR CONSTANT-TEMPERATURE HEATING OF SOLIDS

INTRODUCTION

Series solutions of constant-temperature heating of solids such as large flat plates, long cylinders and spheres have been obtained by Heisler [1], Grober [2] and Kutateladze and Borishanskii [5]. For practical applications of these solutions, charts from which the temperature distribution in solids can be found have been provided by many authors [1-5]. A survey of existing charts shows that to find the temperature or the total amount of energy transferred at given location and time, several interpolations must be made. For example, the dimensionless time, the Fourier number, and the dimensionless property parameter, inverse Biot number, may not fall exactly on the lines provided in the charts and thus interpolations of these lines by inspection are required. These interpolations will inevitably give additional inaccuracy in reading of a chart.

The purpose of this note is to develop approximate closed form solutions for constant-temperature heating in solids. These closed form solutions are simple enough to be handled by slide-rule-type pocket calculators which are available to most engineering students today. In this analysis, a plynomial

temperature profile is assumed and a proper form of sulotion for each type of solid is obtained using the Heat Balance Integral [6,7]. The paper also shows how the integral method employed in this analysis may be used to obtain an approximate fully-developed temperature profile.

ANALYSIS

For one-dimensional transient heat transfer in an infinite slab, the differential equation is given by

$$\frac{\partial t}{\partial \tau} = \alpha \frac{\partial^2 t}{\partial x^2}$$

where t is the temperature, τ the elaped time from the start, x the distance measured from the centerline of slab and α the thermal diffusivity of the slab material. The slab 2L in thickness is initially at a uniform temperature of t_i and is suddenly exposed to a fluid at t_o. Heat is transferred by convection at the interfaces with a unit surface conductance of h. Due to symmetrical temperature distribution, only half of the slab is to be considered. The initial condition and the boundary conditions can then be written

$$\tau = 0; \quad \text{at } 0 < x < L, \ t = t_i \tag{2a}$$

$$\tau > 0; \quad \text{at } x = 0, \ \frac{\partial t}{\partial \tau} = 0 \tag{2b}$$

$$\text{at } x = L, \; -k \left.\frac{\partial t}{\partial x}\right|_{x = L} = h(t_L - t_o) \qquad (2c)$$

where t_L is the surface temperature and k is the thermal conductivity.

Introducing dimensionless groups

$$T_c = (t_c - t_o)/(t_i - t_o),$$

$$T = (t - t_o)/(t_c - t_o), \qquad F = \alpha\tau/L^2$$

and $X = x/L$, Eq. (1) becomes

$$\frac{\partial}{\partial F}(T_c T) = T_c \frac{\partial^2 T}{\partial X^2} \qquad (3)$$

The boundary condition (2b) becomes

$$T_L = - K \left.\frac{\partial T}{\partial X}\right|_{X=1} \qquad (4)$$

where $T_L = (t_L - t_o)/(t_c - t_o)$ and $K = k/hL$.

During the initial phase of heat transfer, the developing temperature profile is assumed to consist of a uniform core and a third order polynomial profile. By applying the boundary conditions at the centerline $X = 0$, $T = 1$ and at the surface $X = 1$, $T_L = -K \, \partial T/\partial X$ as shown in Eq. (4) and the compatability condition that the uniform core and the polynomial profile have the same slope at their intersection i.e. $\partial T/\partial X = 0$ it can be shown that the temperature profile takes the following form

$$T = 1 \text{ for } \emptyset \leq X \leq 1 - n \tag{5a}$$

$$T = 1 - C_n[(1-B)X_n^2 + B\,X_n^3] \quad \text{for } 1-n \leq X \leq 1 \tag{5b}$$

$$\text{where } n = \frac{\text{thickness of thermal boundary layer}}{\text{half thickness of the plate L}}$$

$$C_n = \frac{n}{n + (2 + B)\,K} \quad \text{and} \quad X_n = \frac{X-1+n}{n}$$

B is a constant to be determined later.

Integrating Eq. (3) with respect to X from X = ∅ to X = 1, we find

$$\frac{d}{dF}(T_c I) = T_c \left.\frac{\partial T}{\partial X}\right|_{x=1} \tag{6}$$

$$\text{where } I = \int_o^1 T dX = 1 - nC_n(4 - B)/12 \tag{7}$$

and n is the ratio of the thickness of the thermal boundary layer (or penetration thickness) to the half thickness of the slab L. Substituting Eq. (5b) and Eq. (7) into Eq. (6), it becomes

$$\frac{4-B}{24+12B}\,\frac{2n\,[n + (2 + B)\,K] - n2}{[n + (2 + B)\,K]2}\,\frac{dn}{dF} = \frac{2 + B}{n + (2 + B)\,K} \tag{8}$$

With $n = \emptyset$ at $F = \emptyset$, the solution of Eq. (8) is given by

$$F = \frac{4 - B}{12\ (2 + B)} \left[\frac{n^2}{2} + (2 + B)nK \right.$$

$$\left. - (2 + B)^2 K^2 \ln \frac{n + (2 + B)K}{(2 + B)K} \right] \qquad (9)$$

So far we have treated the coefficient B as a constant in the developing temperature profile. The value of B may be assigned arbitrarily or determined by a constrained condition. For example, we may let $B = -1$ or zero or we may select B in such a way that the temperature profile satisfies the governing equation (3) at the intersection of the center core and the thermal boundary layer. To this end we substitute Eq (5b) into Eq. (3) and let $X = 1 - n$. Thus

$$\frac{dT_c}{dF} = - \frac{2T_c\ C_n}{n^2} (1 - B) \qquad (10)$$

Since T_c is constant for $n < 1$, we have $dT_c/dF = \emptyset$ and $B = 1$, for $n < 1$. We may also select B in such a way that the temperature profile for $n = 1$ is the fully-developed temperature profile.

Fully-Developed Temperature Profile

Let us consider the following temperature profile for $F>F_o$ where F_o denotes the value of F at which n equals unity in Eq. (9).

$$T' = 1 - C\,[(1 - B)X^2 + B\,X^3] \qquad (11)$$

where $C = 1/(1 + 2K + BK)$

Generally speaadking B in Eq. (11) is a function of F. However for a fully-developed flow B is a constant and the profile must satisfy the governing equation (3) along the centerline at Y=Ø.

$$dT_c/dF = - 2C\,(\,1 - B\,)\,T_c \qquad (12)$$

and must also satisfy the integrated equation (6) in which $I = 1 - c\,(\,4 - B\,)//2$. Thus

$$dT_c/dF = - C\,(2 + B)\,T_c/I \qquad (13)$$

Equating Eq. (13) with Eq. (12), we have

$$4 + (13 + 36K)B + (1 + 18K)B^2 = Ø \qquad (14)$$

Equation (14) is used to determine the fully-developed value of B for various K.

For K=Ø.Ø2, B is Ø.3ØØ. The other root B = - 9.79 is discarded since it gives a negative temperature region in the plate. The fully-developed temperature profile for K = Ø.Ø2 is, therefore, $T = 1 - 1.257\ X^2 + Ø.29\ X^3$. Comparison of this profile with Heisler's result [1] as shown in Fig. 4-9 of Kreit's Principles of Heat Transfer [4] is as follows:

X	1	Ø.9Ø	Ø.8Ø	Ø.6Ø	Ø.4Ø	Ø.2Ø	Ø
Heisler	Ø.Ø3	Ø.19	Ø.35	Ø.6Ø	Ø.82	Ø.95	1
Eq.(11)	Ø.Ø3	Ø.19	Ø.34	Ø.61	Ø.82	Ø.95	1

For a larger K, the result is much better. It is seen that the present fully-developed profile is very satisfactory. This method can also be applied to fluid flow problems to find fully-developed profiles and similarity profiles.

The centerline temperature for $F > F_o$ can be obtained by direct integration of Eq. (6).

$$T_c = \exp\left[\frac{(24 + 12B)(F_o - F)}{8 + 24K + B + 12BK}\right]$$

Heat Transferred

The total heat transferred Q is found from Eq. (6) to be $1 - T_c$ or

$$\frac{Q}{Q_i} = 1 - T_c \left[\frac{8 + 24K + B + 12\,BK}{12 + 24K + 12BK} \right] \quad \text{for} F \geq F_o \qquad (16a)$$

$$\frac{Q}{Q_i} = \frac{n^2 (4 - B)}{12n + 24K + 12BK} \quad \text{for } F \leq F_o \qquad (16b)$$

where $Q_i = 2AL\rho c(t_i - t_o)$, the internal energy stored initially in the slab, measured relative to the fixed boundary temperature t_o. The symbol A denotes the surface area of the slab, ρ the density and c the specific heat of the slab.

With equations (9, 11, 14, 15, 16), it is possible to obtain approximate expression for the temperature profile T, the centerline temperature T_c and the fractional heat transferred. These equations are listed below. Note the approximated value of B is obtained from eq. (14) with its sign changed from negative to positive.

Results corresponding to the above for an infinite cylinder and a sphere were obtained in a very similar way to that described above and only the results are stated below.

..... FLAT PLATE .....
****

The characteristic length is L

$X = x/L, \quad K = k/(hL), \quad F = \alpha\tau/L^2$

For the infinite slab (or flat plate) the equations are divided into Long Time and Short Time. The range of time for which each equation may be applied is indicated.

FLAT-PLATE; Long Time

(F-1a) Temperature profile for F > Ø.25

$$T = 1 - \frac{(1+B)X^2 - B\,X^3}{1 + (2-B)K}$$

(error in T < Ø.Ø1)

where $B = \dfrac{Ø.315}{1 + 2.5K}$

(F-1b) Centerline Temperature for F > Ø.25

$$T_c = \exp\left[\frac{F_o - F}{Ø.35 + Ø.Ø5\exp(-4K) + K}\right]$$

(error in T_c < Ø.Ø1)

where $F_o = Ø.167 - \dfrac{Ø.Ø67}{1 + 6K}$

(F-1c) Heat Transferred for $F > 0.1$

$$\frac{Q}{Q_1} = 1 - \left(\frac{0.63+2K}{1+2K}\right)\exp\left[\frac{F_o - F}{0.35 + 0.05\exp(-4K) + K}\right]$$

(error in $Q/Q_1 < 0.01$)

FLAT PLATE: Short Time

(F-2a) Surface Temperature T_L for $F < 0.25$

$$T_L = \frac{K(2.17 - 0.33\, e^{-K})}{(F/F_o)^{0.55} + K(2.17 - 0.33\, e^{-K})}$$

(error in $T_L < 0.006$)

(F-2b) Centerlne Temperature T_c for $F < 0.25$

$$T_c = \exp\left[\frac{F_o(F/0.25)^p - F}{0.35 + 0.05\exp(-4K) + K}\right]$$

(error in $T_c < 0.015$)

where $p=0.3+2K$ for $K<0.1$ and $p=0.5$ for $K>0.1$

(F-2c) Temperature Profile for $F < 0.25$

$$T = T_c\,(1 - X^m) + T_L\,X^m$$

(error in $T < 0.015$)

where $m = 1.4 + \frac{0.09}{F}$

(F-2d) Heat Transferred for $F < 0.5$

$$\frac{Q}{Q_i} = \left[\frac{0.376 - 0.02\exp(-80K)}{(F/F_o)^{0.5} + 2K}\right]\frac{F}{F_o}$$

(error in $Q/Q_i < 0.01$)

..... I N F I N I T E C Y L I N D E R .....

****

Dimensionless Groups are

$$X = r/r_o \ , \quad K = k/hr_o \ , \quad F = \alpha t/r_o^2$$

$$T = \frac{t - t_o}{t_c - t_o} \ , \qquad T_c = \frac{t_c - t_o}{t_i - t_o}$$

where r is the radial coordinate and r_o the radius of the cylinder.

[C-1] INFINITE CYLINDER: Long Time

(C-1a) Temperature profile for $F \geq 0.2$

$$T = 1 - \frac{(1 + B)\, X^2 - B\, X^3}{1 + (2 - B)K}$$

(error in $T < 0.01$)

where $B = \dfrac{0.595}{1 + 3K}$

(C-1b) Centerline temperature for $F \geq 0.2$

$$T_c = \exp\left[\frac{F_o - F}{0.13 + 0.04\exp(-2K) + 0.5K} \right]$$

(error in $T_c < 0.02$)

$$F_o = 0.14 - \frac{0.056}{1 + K}$$

(C-1c) Heat transferred for $F \geq Fo$

$$\frac{Q}{Qi} = 1 - \left(\frac{0.42 + 2K}{1 + 2K}\right) \exp\left[\frac{Fo = F}{0.13 + 0.04\exp(-2K) + 0.5K}\right]$$

(error in $Q/Q_i < 0.01$)

(C-2) INFINITE CYLINDER: Short Time

(C-2a) Surface temperature for $F < 0.2$

$$T_L = \frac{[2 - 0.4\exp(-2K)]K}{(F/F_o)0.7 + [2 - 0.4\exp(-2K)]K}$$

(error in $T_L \leq 0.03$)

$$F_o = 0.14 - \frac{0.056}{1 + K}$$

(C-2b) Centerline temperature for $F \leq 0.2$

$$T_c = \exp\left[\frac{F_o(F/0.2)^{0.3} - F}{0.13 + 0.04\exp(-2K) + 0.5K}\right]$$

(error in $T_c \leq 0.03$)

(C-2c) Temperature profile $F < 0.2$

$$T = T_c (1 - X^m) + T_L X^m$$

$$m = 2F^{-0.15} - 0.9 \qquad \text{(error in } T \leq 0.03\text{)}$$

.....S P H E R E.....
****

The dimensionless groups are the same as inan infinite cylinder.

(S-a) Temperature Profile; Long Time $F > 0.2$

$$T = 1 - \frac{(1+B)X^2 - BX^3}{1 + (2-B)K}$$

$$B = \frac{0.838}{1 + 3K} \qquad \text{(error in } T < 0.01\text{)}$$

(S-b) Centerline Temperature for $F \geq 0.2$

$$T_c = \exp\left[\frac{F_o - F}{(1/3)(0.20 + 0.11\exp(-1.5K) + K)}\right]$$

$$F_o = 0.14 - \frac{0.08}{1 + K} \qquad \text{(error in } T_c < 0.03\text{)}$$

(S-c) Heat Transfer for $F > 0.2$

$$\frac{Q}{Q_i} = 1 - \left(\frac{0.36 + 2K}{1 + 2K}\right) T_c$$

(error in $Q/Q_i < 0.03$)

EXAMPLES AND DISCUSSIONS

Example 1. A long rectangular wooden beam of 2 in. by 4 in. with α = .00667 ft^2/hr and k = 0.2 Btu/hr ft F initially at t_i = 60 F is exposed to gases at t_∞ = 1200°F and h = 3.0 Btu/hr ft^2 F. If the wood ignites at t = 800 F, how much time will elapse before the beam first starts burning ?

Since this is a two-dimensional body, we will use the product super-position principl (see example 4.7 of Kreith). Let L_1 = 1 in. and L_2 = 2 in. The product of surface temperatures must satisfy:

$$T_{L_1} \quad T_{L_2} = \frac{t - t_\infty}{t_i - t_\infty} = 0.35$$

Using the short time formula for the surface temperature of a slab, and noting that

$$F = \alpha\tau/L = 4\alpha\tau/L. = 4\ F_2, \text{ we have}$$

$$\frac{1.617}{\left(\frac{4\ F_2}{0.1554}\right)^{0.55} + 1.617} \qquad \frac{0.7795}{\left(\frac{F_2}{0.1473}\right)^{0.55} + 0.7795}$$

$$= T_{L_1}\ T_{L_2}$$

$$\text{or} \quad 17.11\ F_2^{1.1} + 9.288\ F_2^{0.55}$$

$$-1.26\left(\frac{1}{T_L\ T_L} - 1\right) = 0.$$

For $T_{L_1}\ T_{L_2} = 0,35$ we have $F_2^{0.55} = 0.1873$

or $F_2 = 0.0476$ which gives $\tau = F_2 L_2^2/\alpha = 0.198$ hr.

Using trial and error method on Heisler's short time chart, we have τ of about 0.2 hr. The advantage of the closed form solution in this case is that no iteration is required.

Example 2. A 1/32-in-diameter copper wire initially at 300 F is suddenly immersed in water (h = 15 Btu/hr ft^2F) at 100 F. Determine the time required to cool its centerline temperature down to 150 F (Refer to Kreith's Example 4.1).

In this case $K = k/h\ r_o = 216/(15 \times 0.001302) = 11060$. Clearly the internal resistance can be neglected. However we will use the infinite cylinder for long time to solve the problem.

$$\frac{150 - 100}{300 - 100} = \exp \frac{0.14 - F}{5530} \quad \text{or} \quad F = 7666$$

The time required is $F\ r_o^2\ \rho c/k = 7666 \times (0.001302)^2 \times 558 \times 0.091/216 = 0.003055$ hr = 11 sec. From Kreith's Fig 4.2, we find the time required is about two minutes. Due to an error in the volume per inch length the figure gives time by 12 times longer.

When K is very large, F is also very large and the approximate solution reduces to exact solution for negligible internal solution. For example, the long time solution for an infinite cylinder is

$$T_c = \exp\left[\frac{F_o - F}{0.13 + 0.04\, e^{-2K} + 0.5K}\right] \approx \exp\left[\frac{-F}{0.5\ K}\right]$$

$$= \exp\left(-\frac{\alpha\tau}{r_o^2} \Big/ \frac{0.5\ k}{h\ r_o}\right) = \exp\left(-\alpha\tau\, h/r_o k\right)$$

which is the exact solution for infinite cylinder with negligible internal resistance.

It is interesting to note that at $T_c = 0.001$, the series solution (F = 9.48) and the present solutions (F = 9.44) give the higher values of F than that shown in Heisler's chart (F= 9.0). It is possible that the original chart by Heisler may be in error for K = 1.0 from F = 4 to 9.0.

In conclusion approximate simple closed form solutions can be easily handled by a slide-rule pocket calculator and give good results for engineering applications.

REFERENCES

1. Heisler, M.P., Temperature Charts for Induction and Constant Temperature Heating. Trans. ASME, Vol. 69, No. 3, 1947, pp. 227-236
2. Grober, H., Einfuhung in Die Lehre der Warmeubertragung, Berlin, Springer, 1926.
3. Grober, H., Erk, S. and Grigull, U., Fundamentals of Heat Transfer, McGraw- Hill Book Co., New York, NY 1961.
4. Kreith, F., Principles of Heat Transfer, 3rd Ed., Index Educational Publishers, New York, 1973.
5. Kutateladze, S. S. and Borishanskii, V.M., A Concise Encyclopedia of Heat Transfer, Pergamon Press, New York, 1966.
6. Goodman, T.R., The Heat Balance Integral, Further Considerations and Refinements, J. of Heat Transfer, Trans. ASME, Series C, Vol. 83, 1961, pp. 83-86.
7. Sfeir, A. A., The Heat Balance Integral in Steady-State Conduction, J. of Heat Transfer, Trans. ASME, Series C, Vol. 98, 1976, pp. 466-470.

Note: This article was submitted to ASEE Mechanical Engineering News and was published in Feb. 1979, pp.20-23.

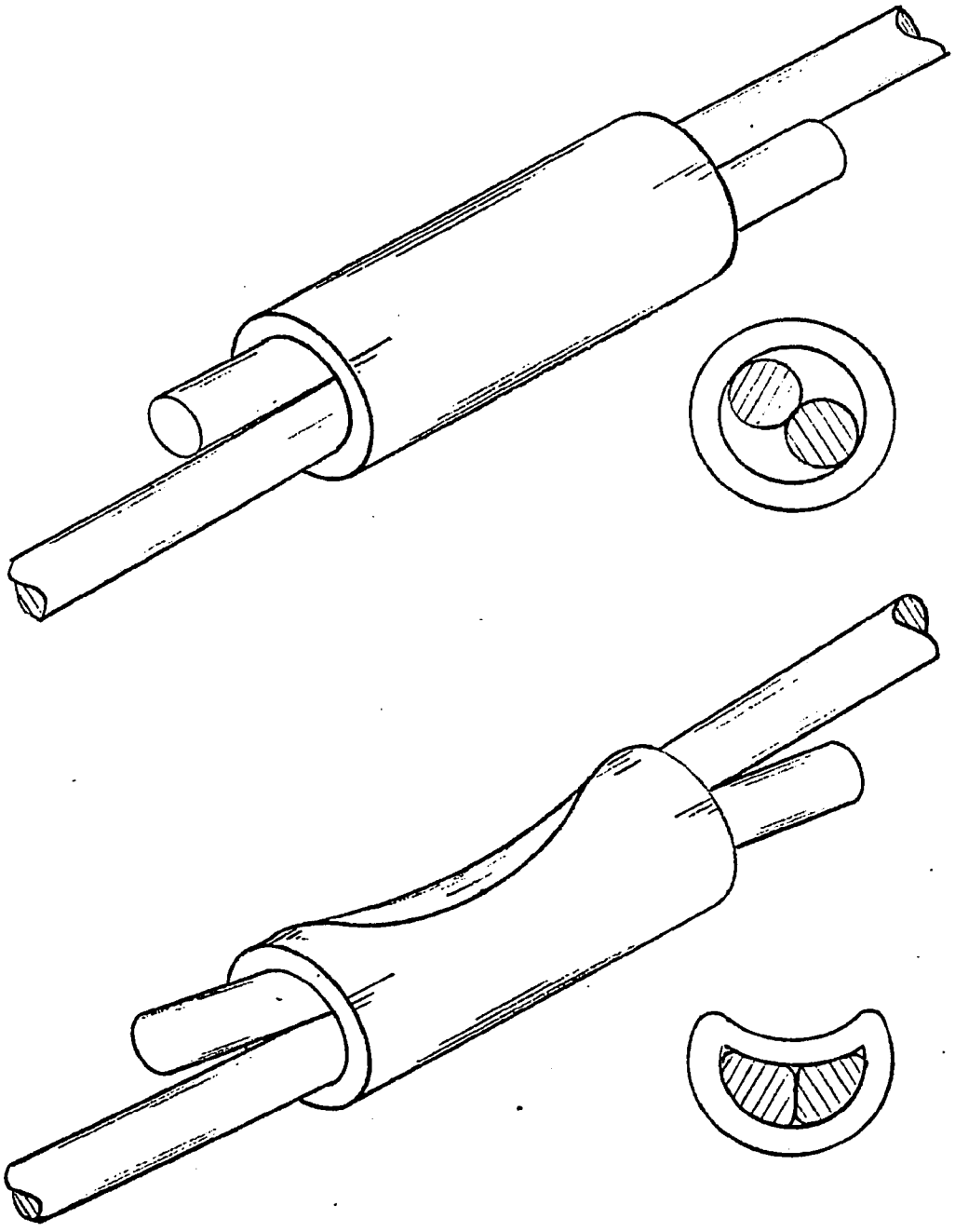

Fig. 2.1 Conventional Cylindrical Electrical Connector.

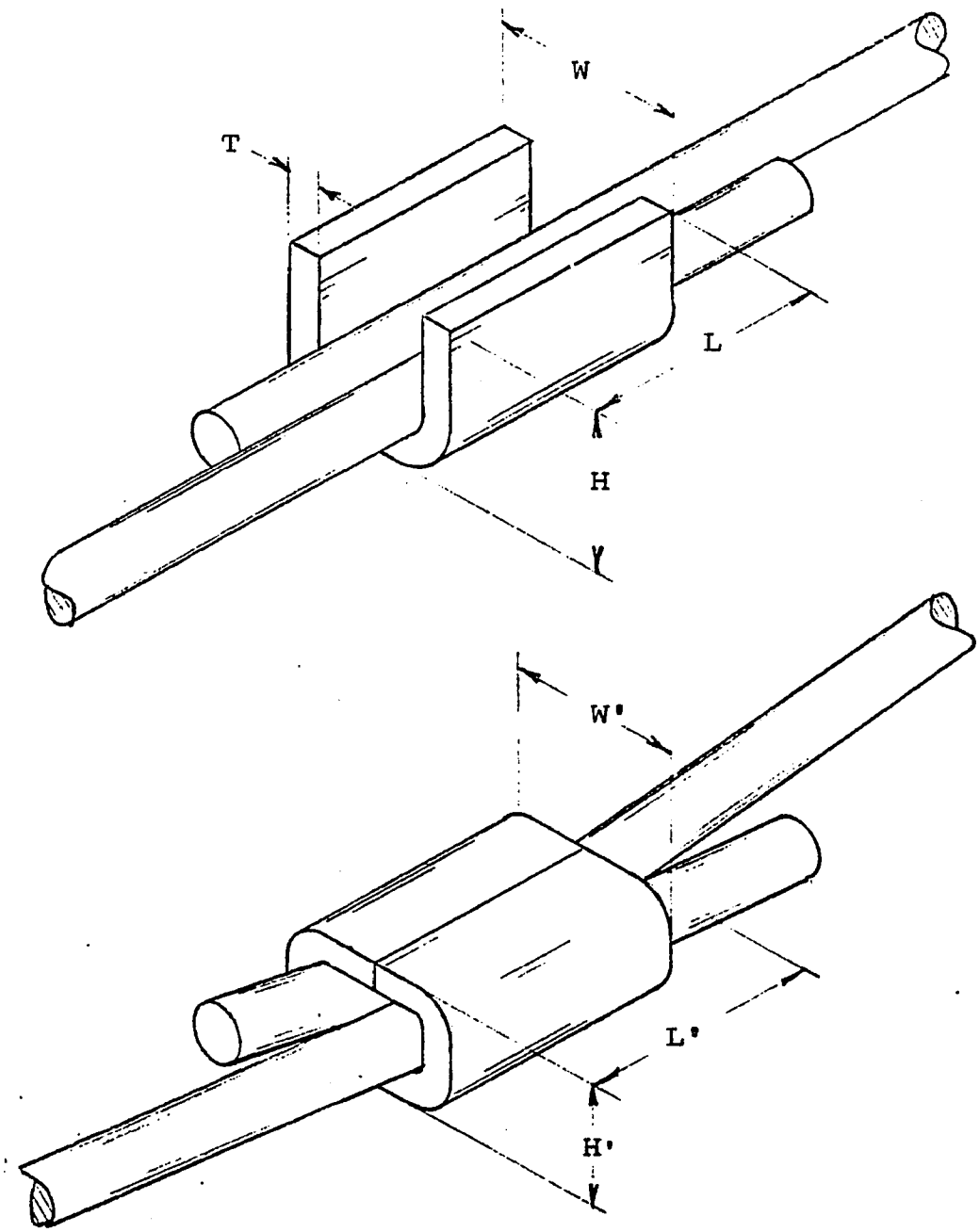

Fig. 2.2 Open-seam U-shaped Connector Used in the Test

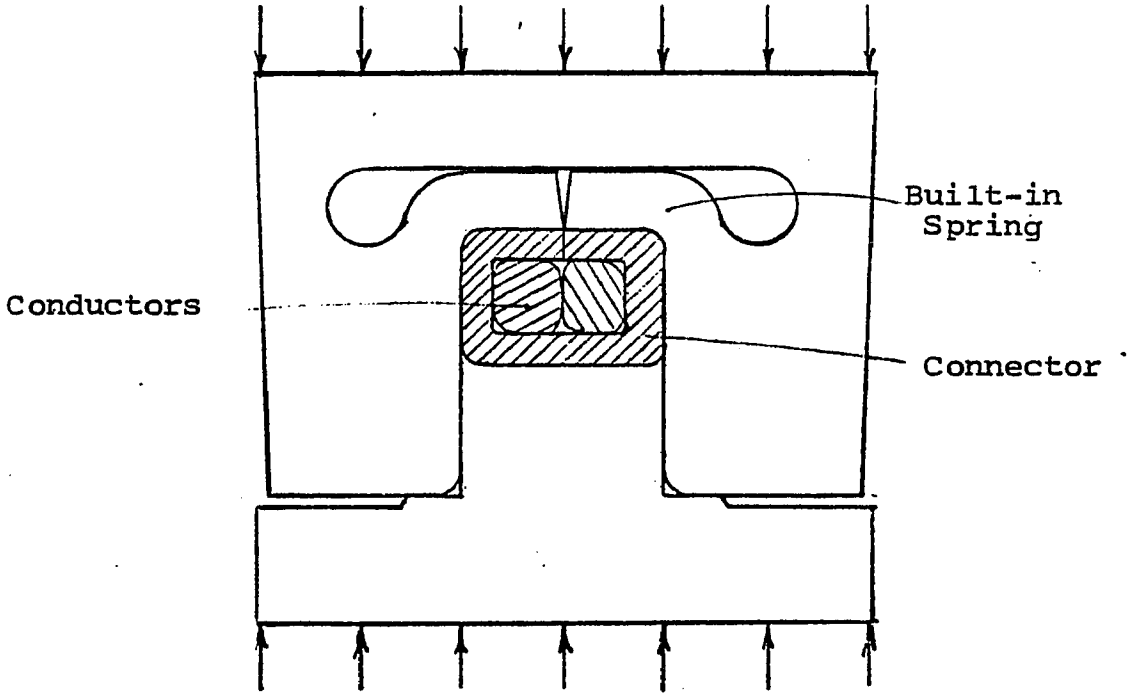

Fig. 2.3 Spring-loaded Installing Dies.

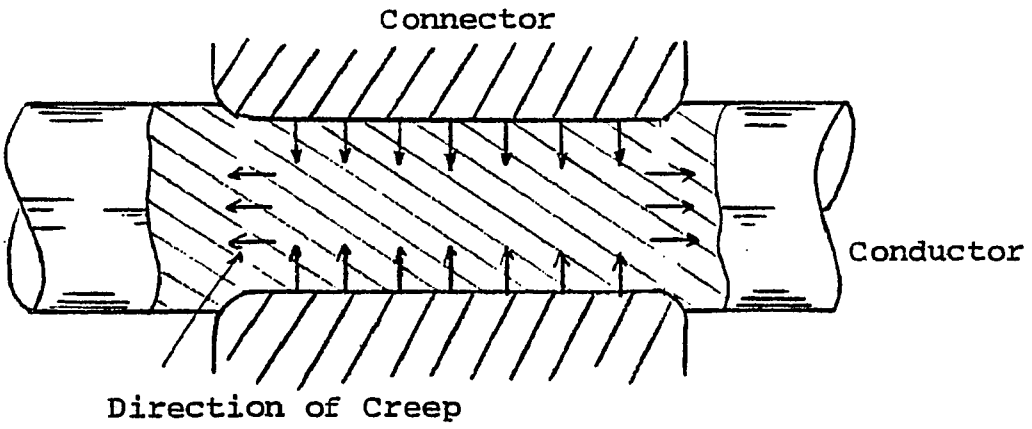

Fig. 2.4 Creep in a Connector

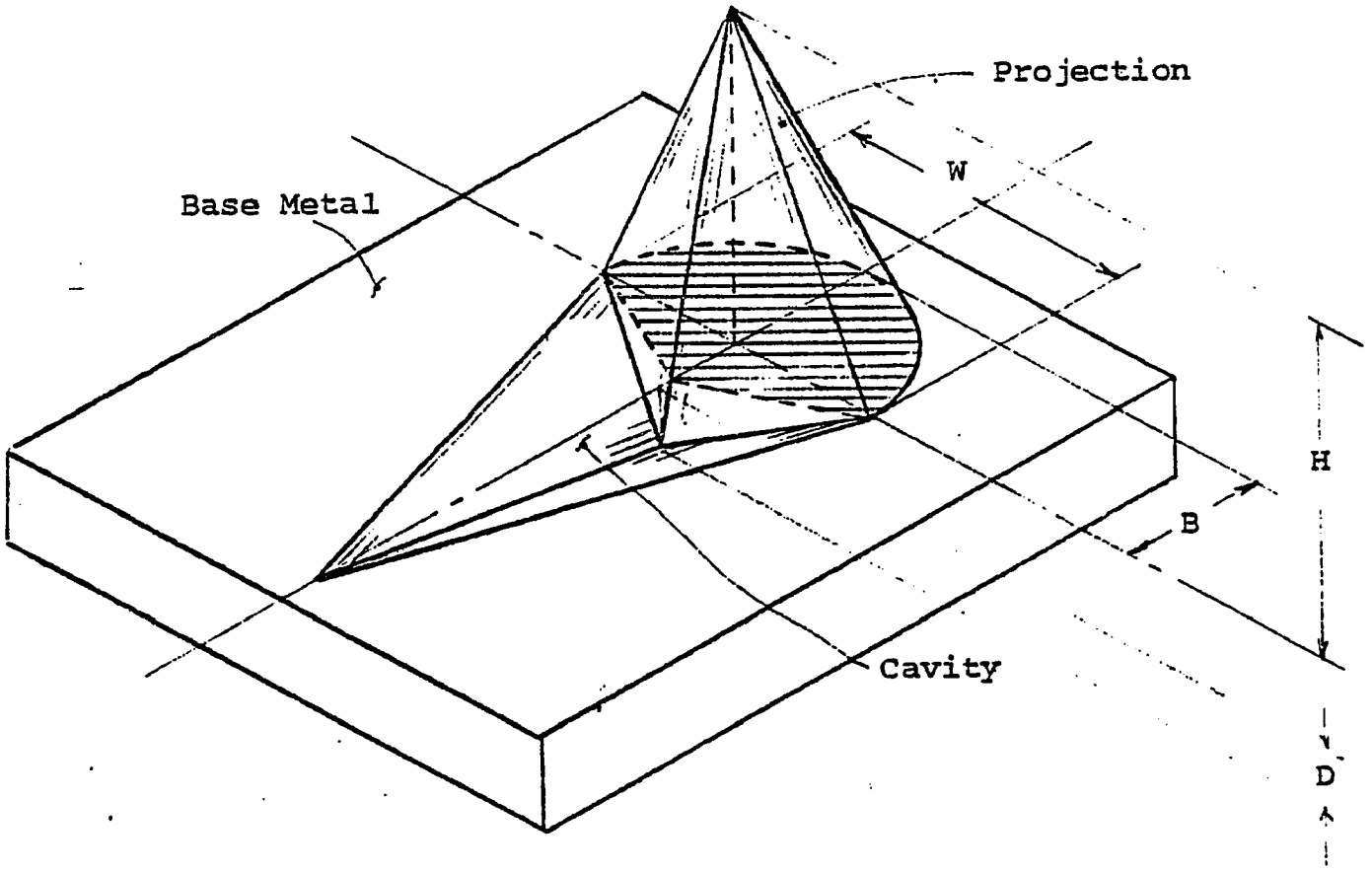

Fig. 2.5 Configuration of the Cone-shaped Projection

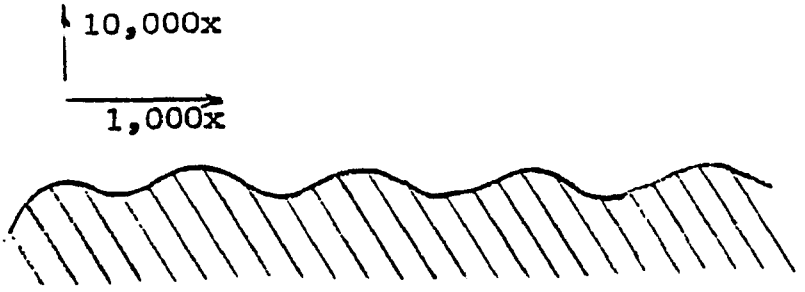

Fig. 2.6 Magnified View of the Metallic Surface.

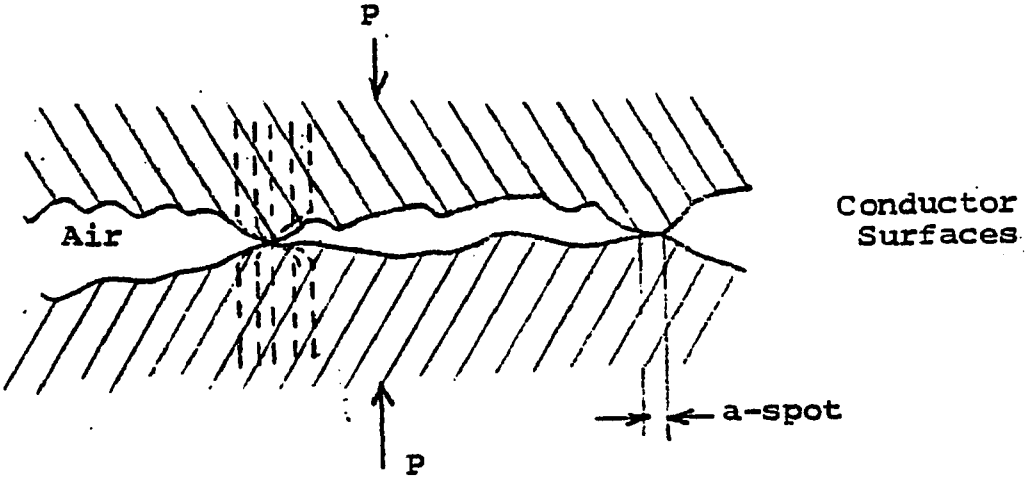

Fig. 2.7 Magnified View of the Contact Surfaces.

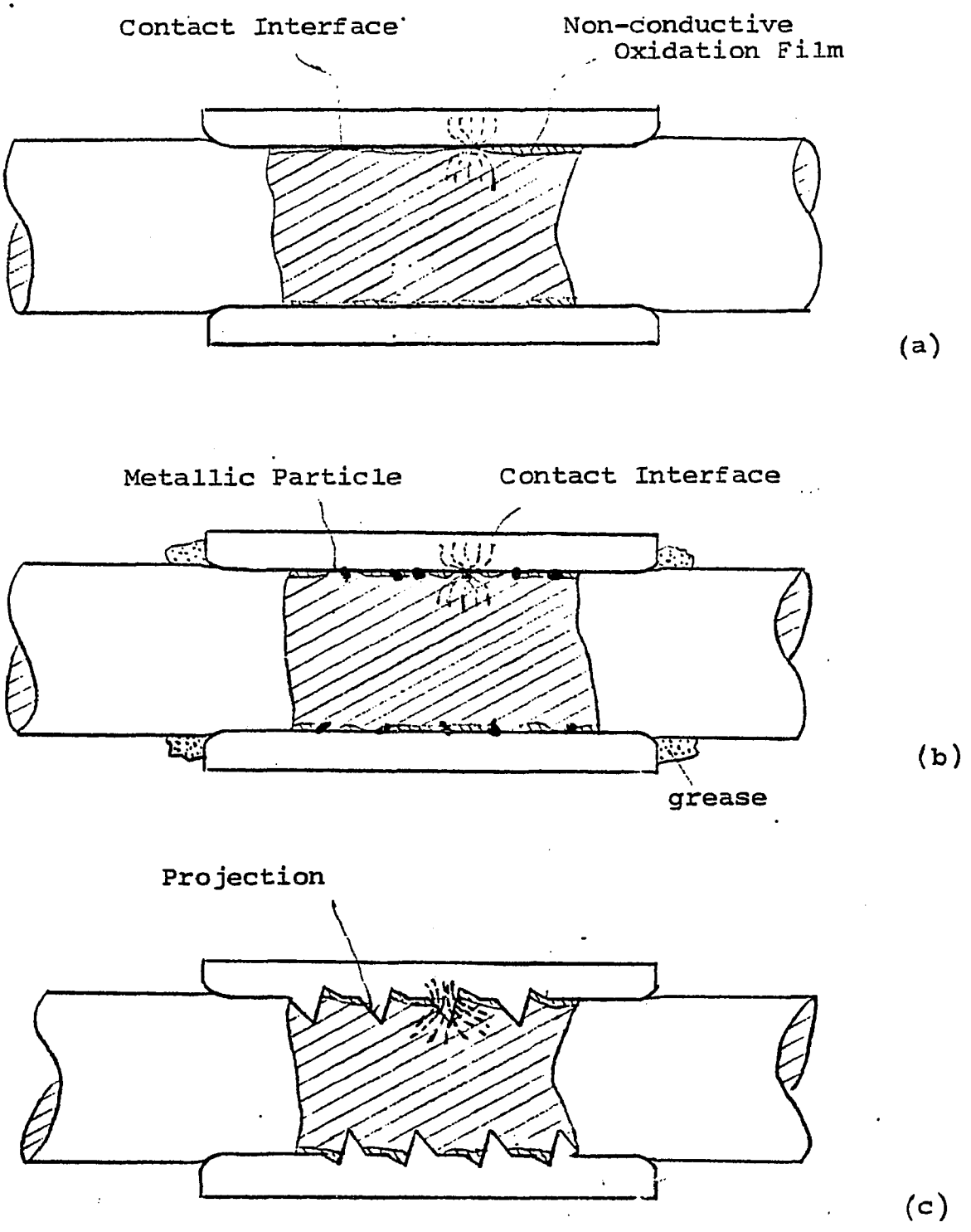

Fig. 2.8 Effect of Surface Conditions on Initial Contact Resistance.

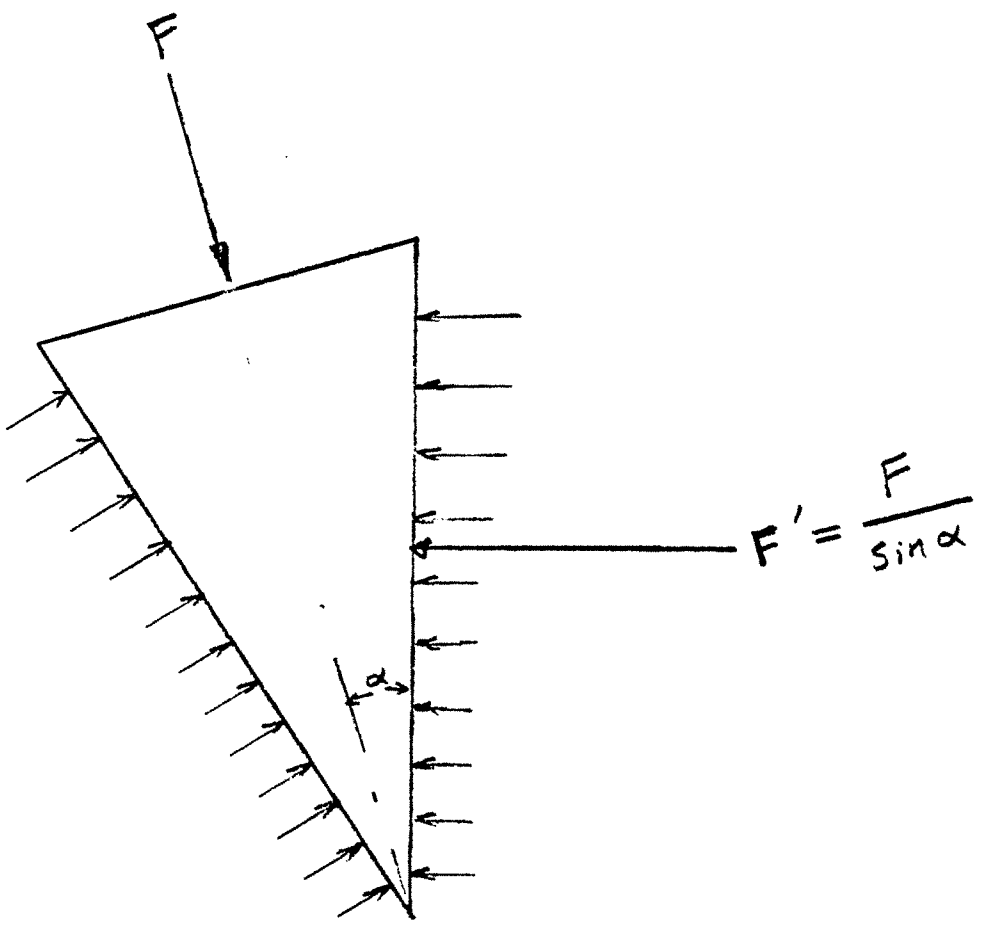

Fig. 2.9 Normal Forces on the Conical Projections.

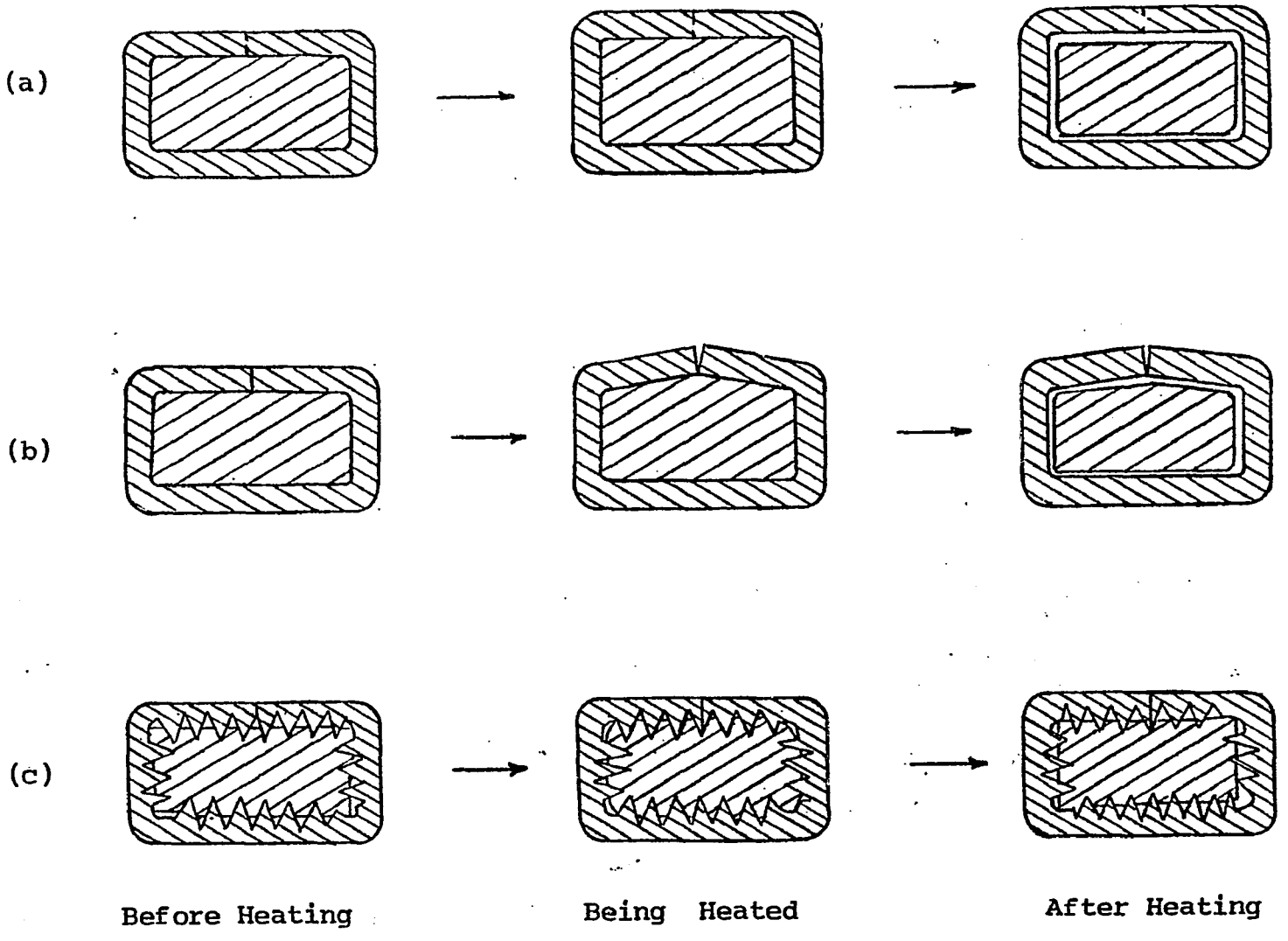

Fig. 2.10 Effects of Surface Conditions on Thermal Expansion

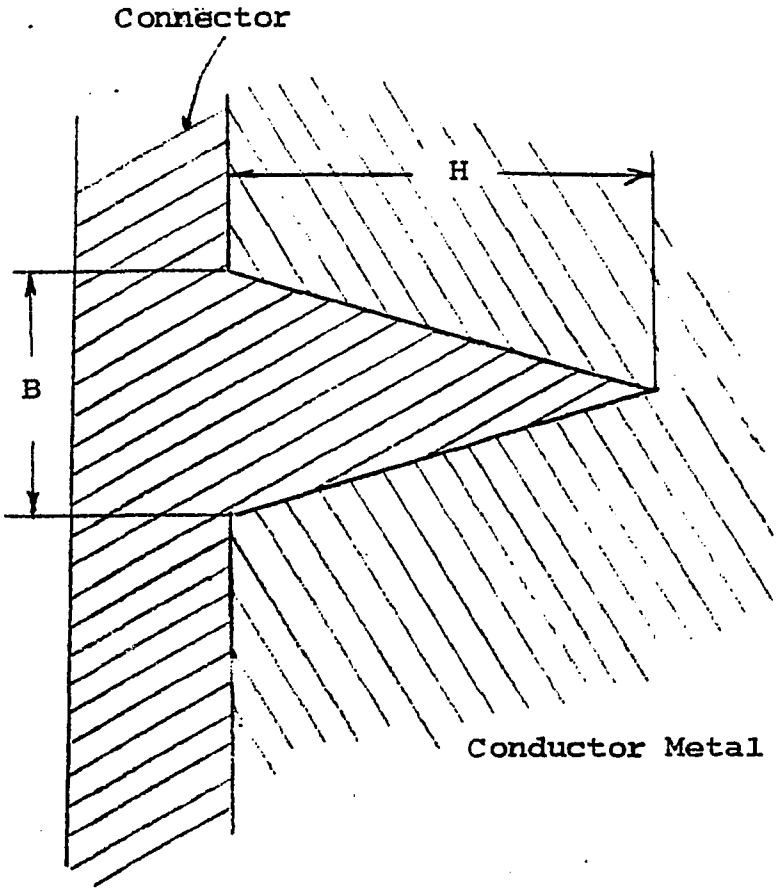

Fig. 2.11 Heat Transfer Enhancement of the Projection

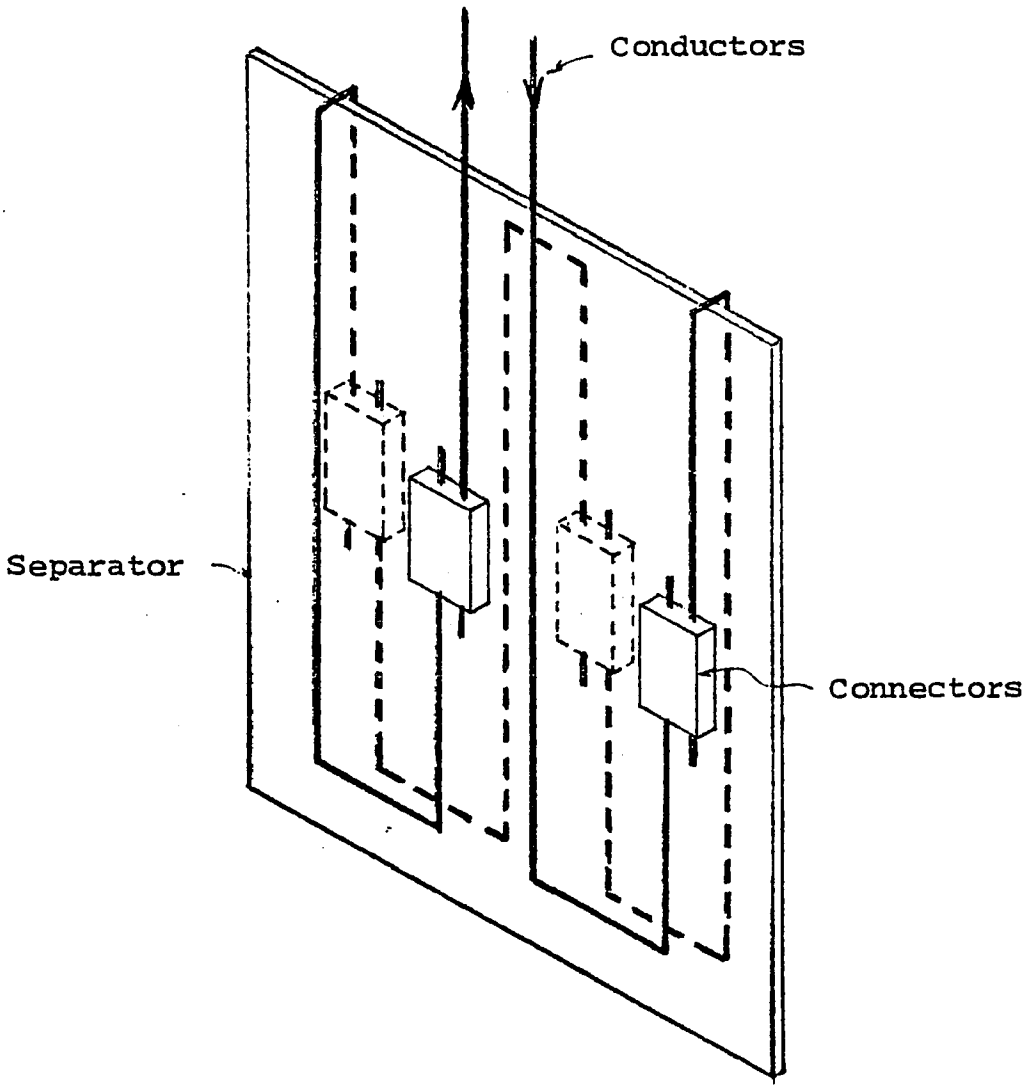

Fig. 3.1 Arrangement of Test Samples

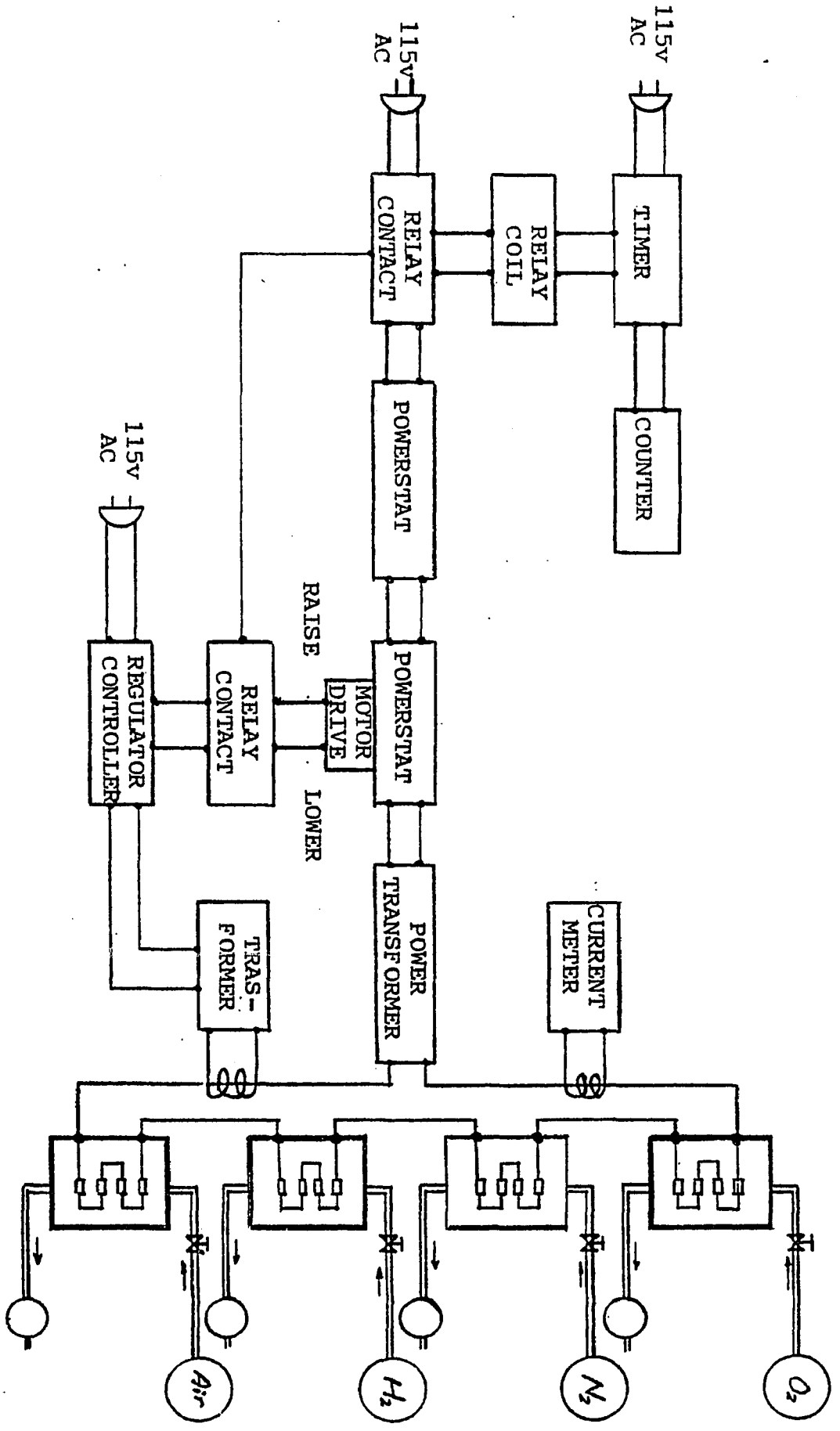

Fig. 3.2 Test Set-up

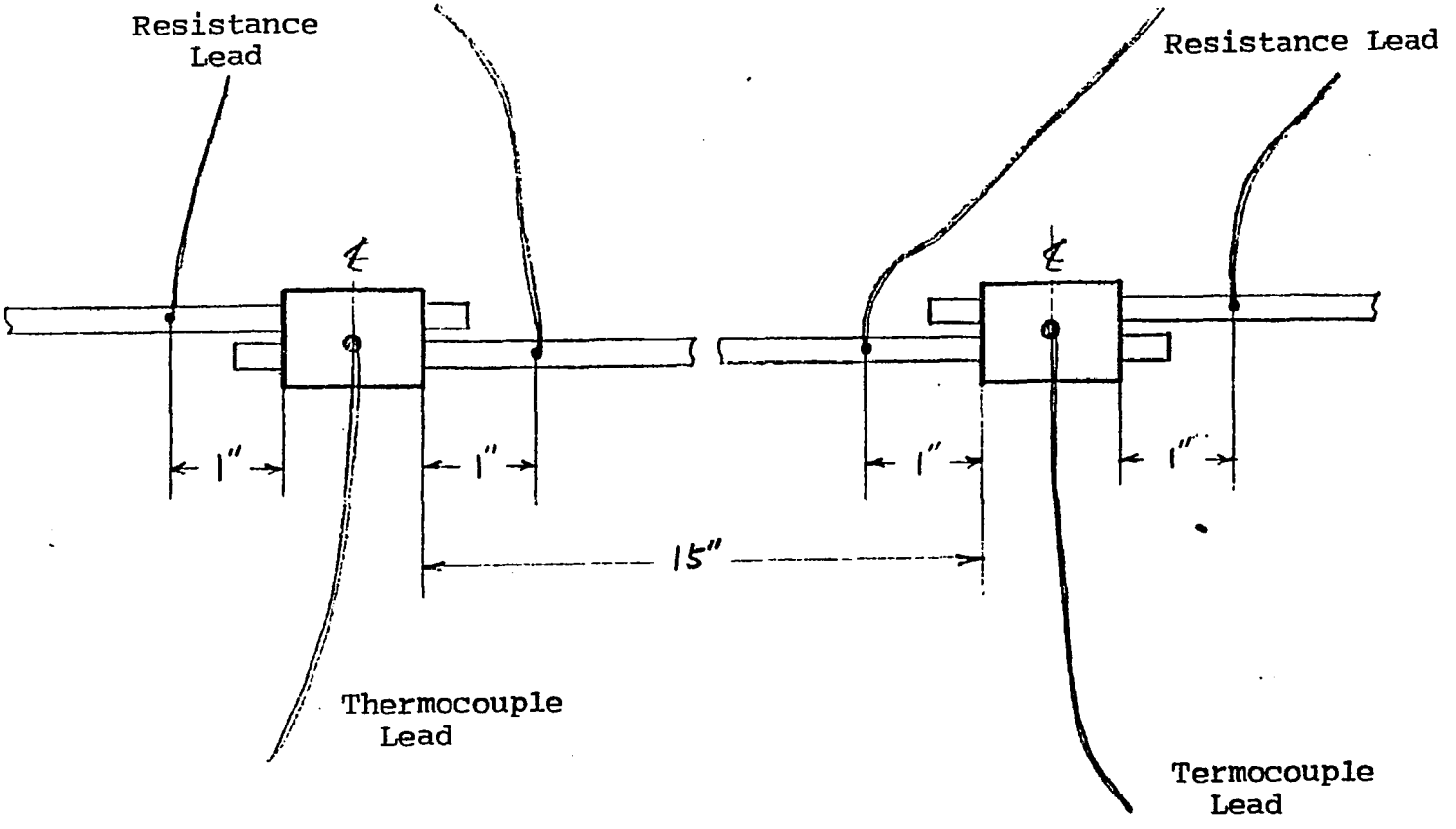

Fig. 3.3 Arrangement for Measurements

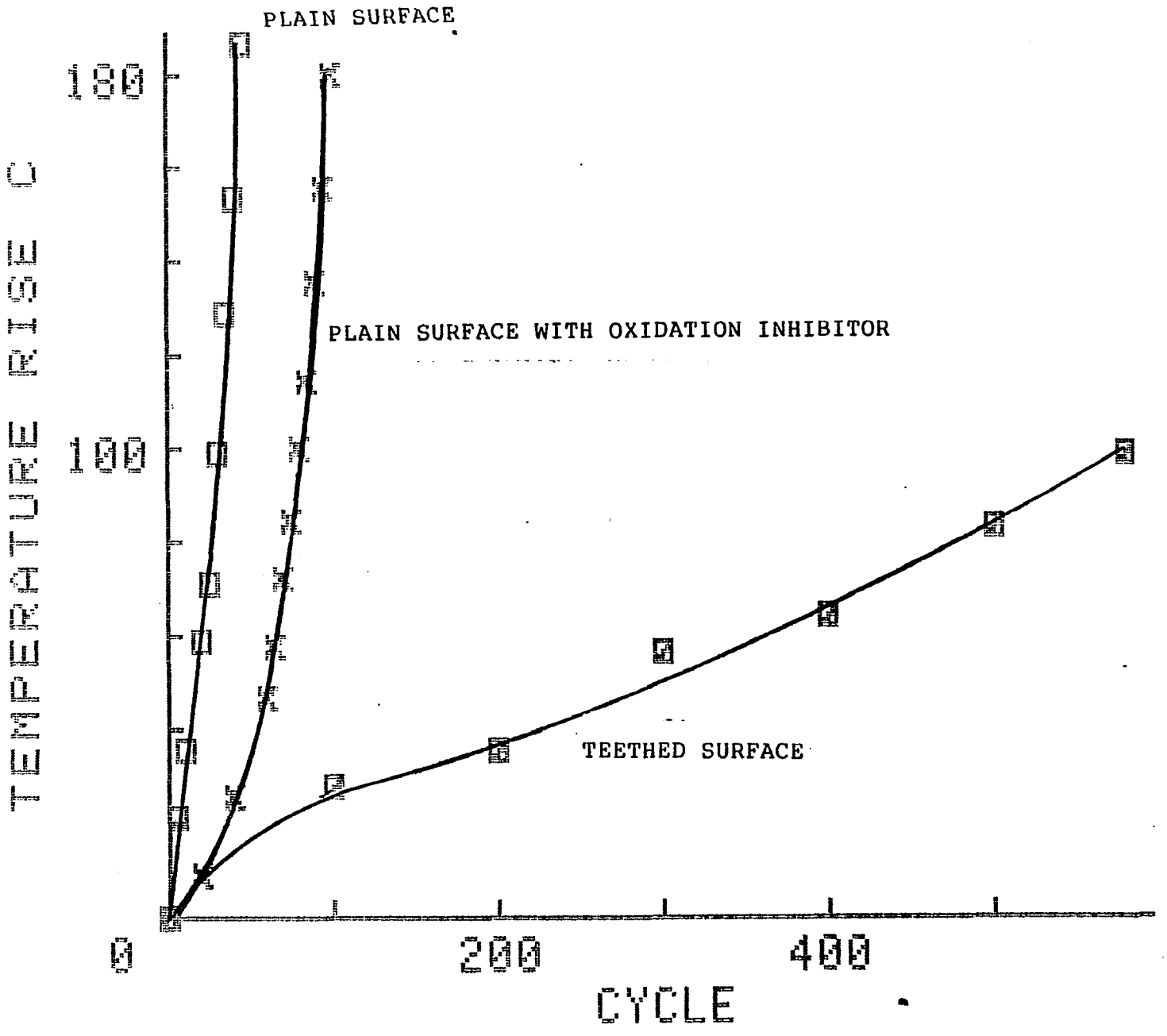

Fig. 3.4 Average Temperature Rise in Air Environment.

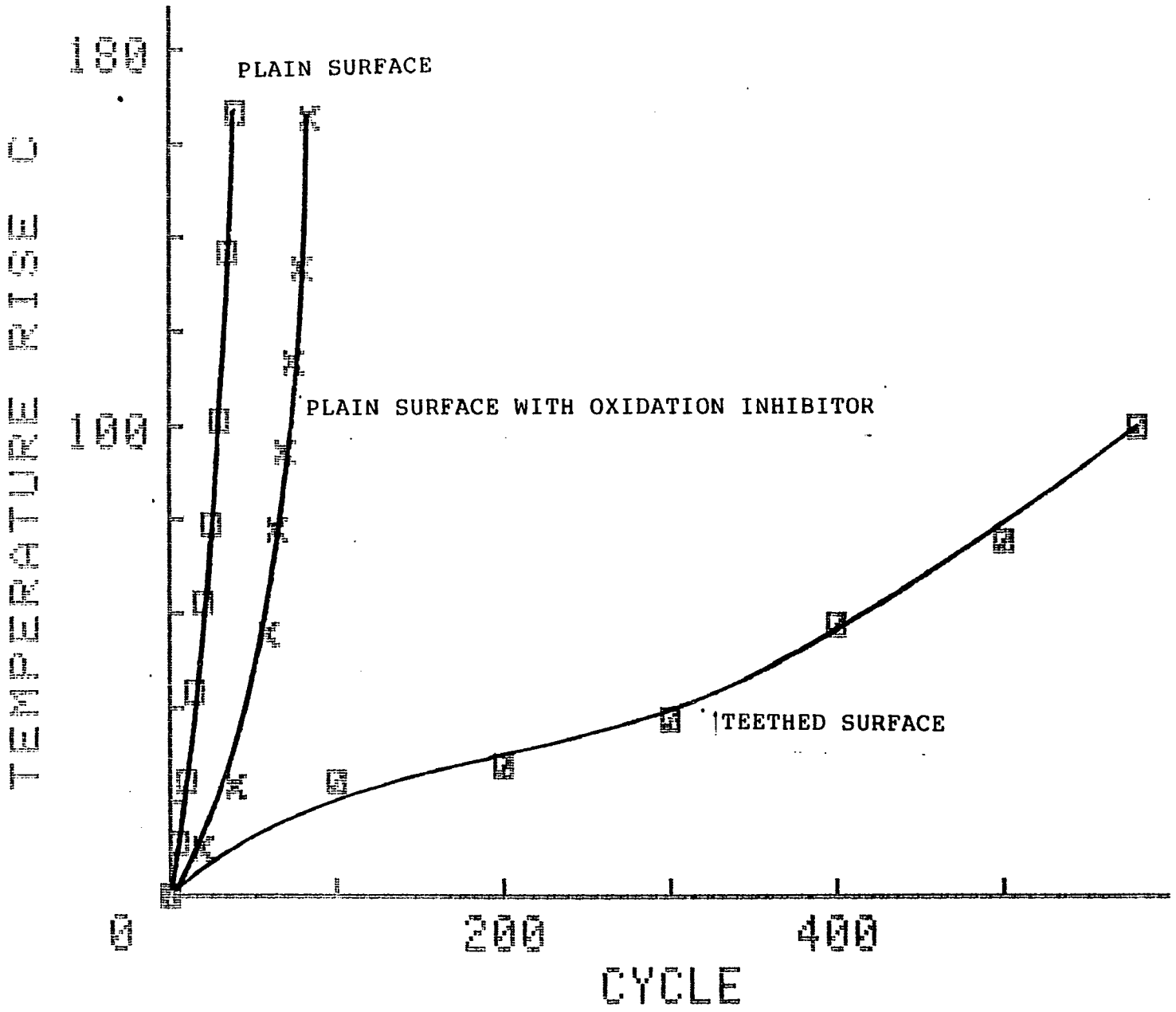

Fig. 3.5 Average Temperature Rise in Nitrogen Environment

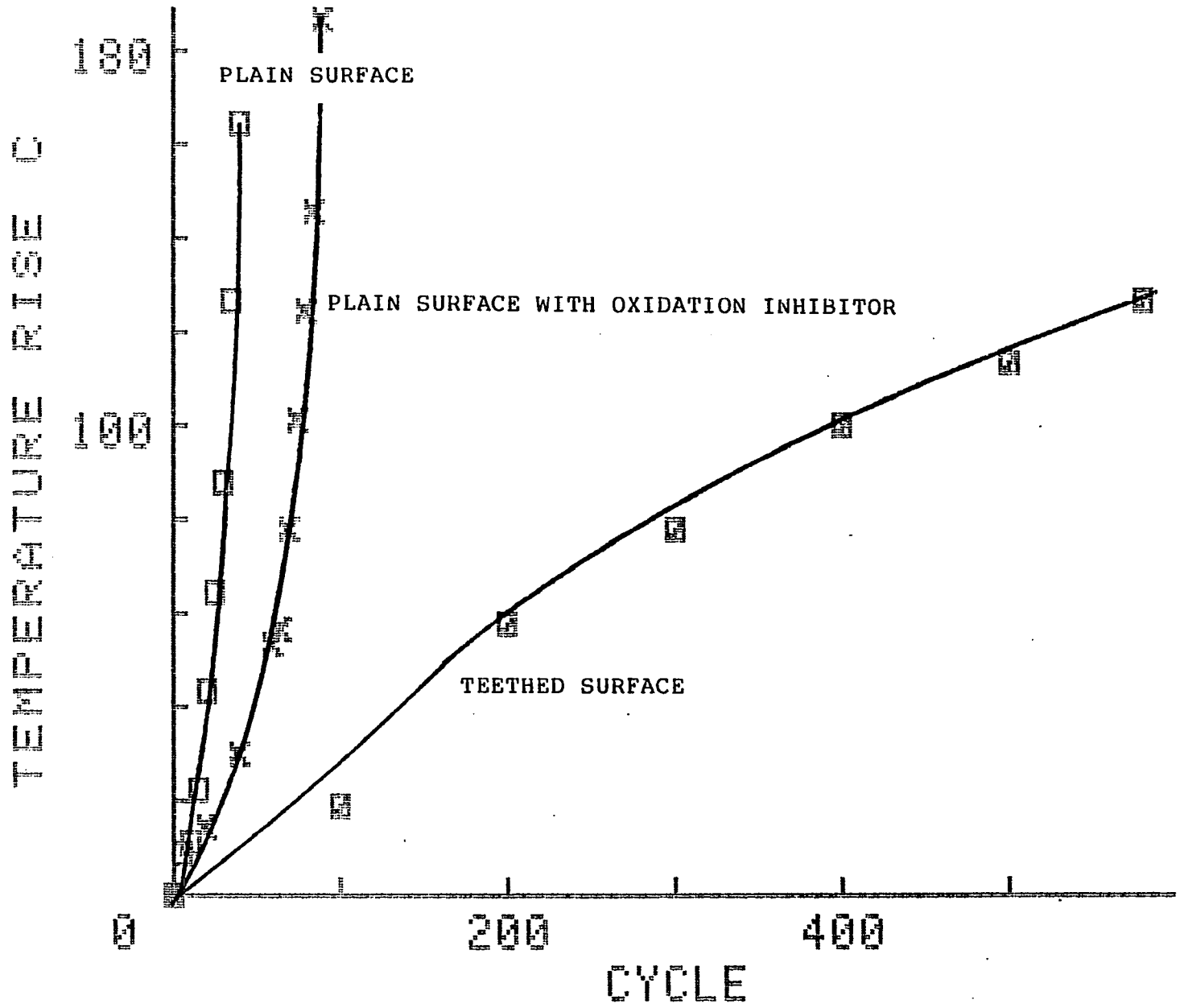

Fig. 3.6 Average Temperature Rise in Hydrogen Environment

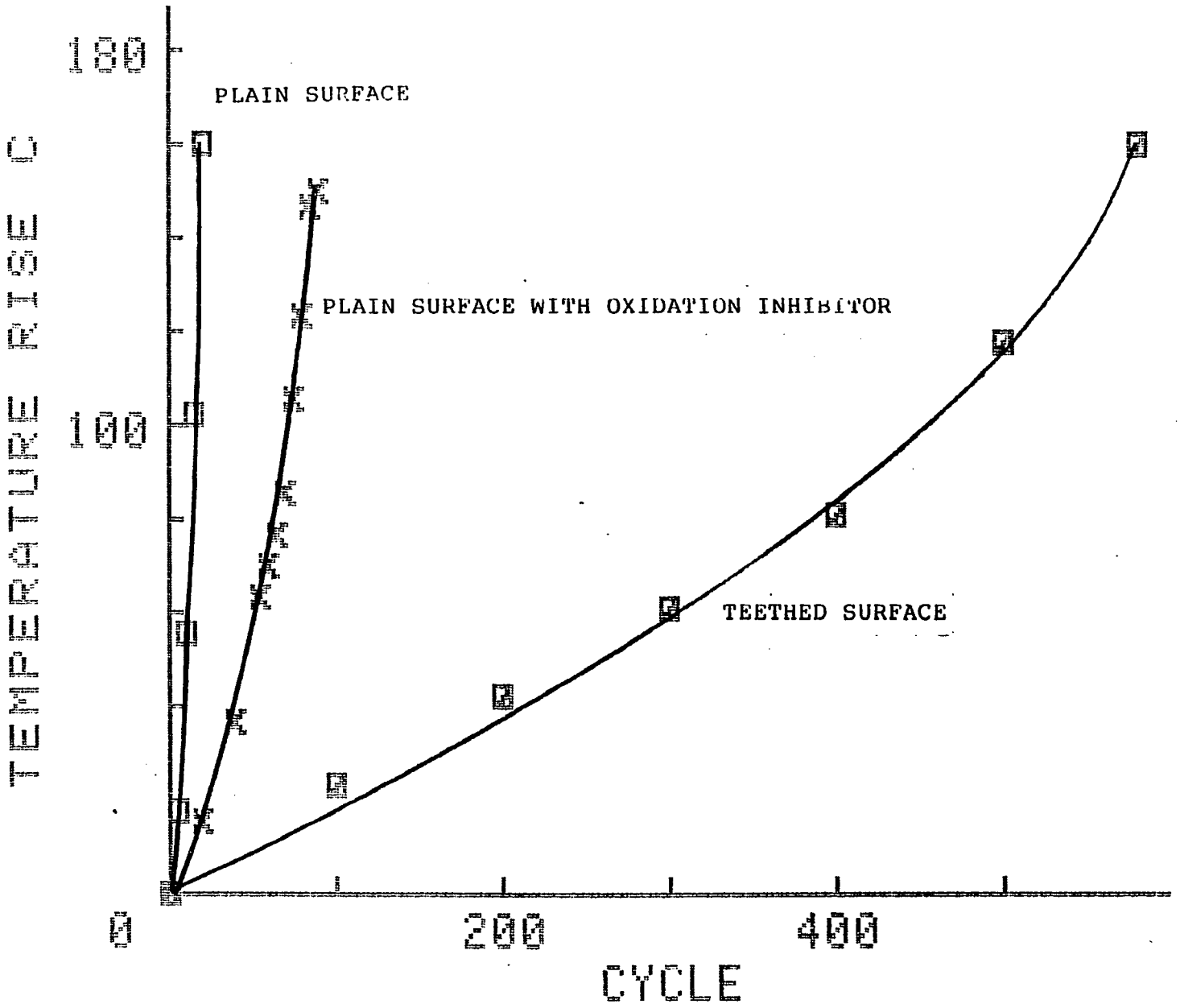

Fig. 3.7 Average Temperature Rise in Oxygen Environment

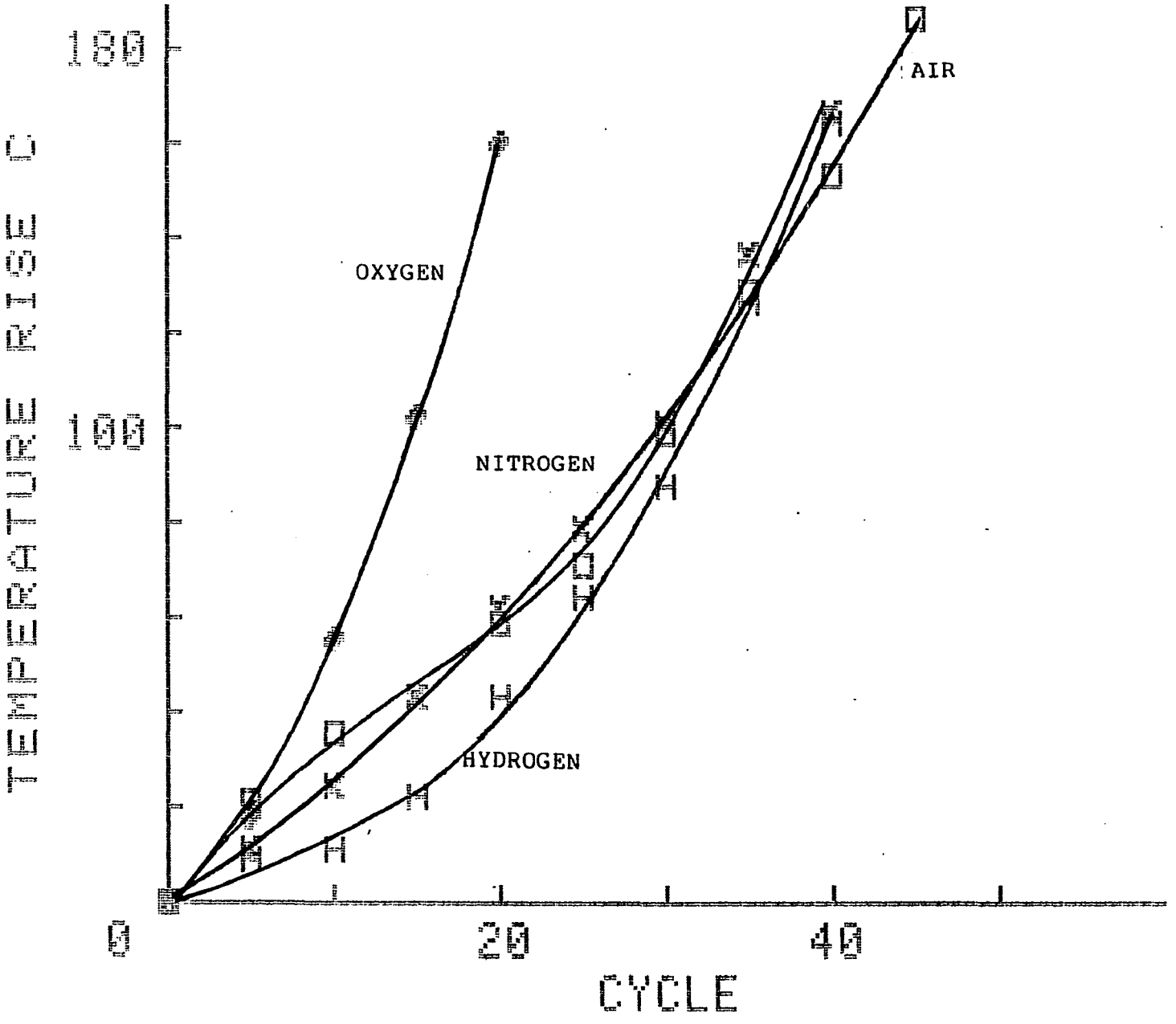

Fig. 3.8 Plain Surface Connectors in Different Gases

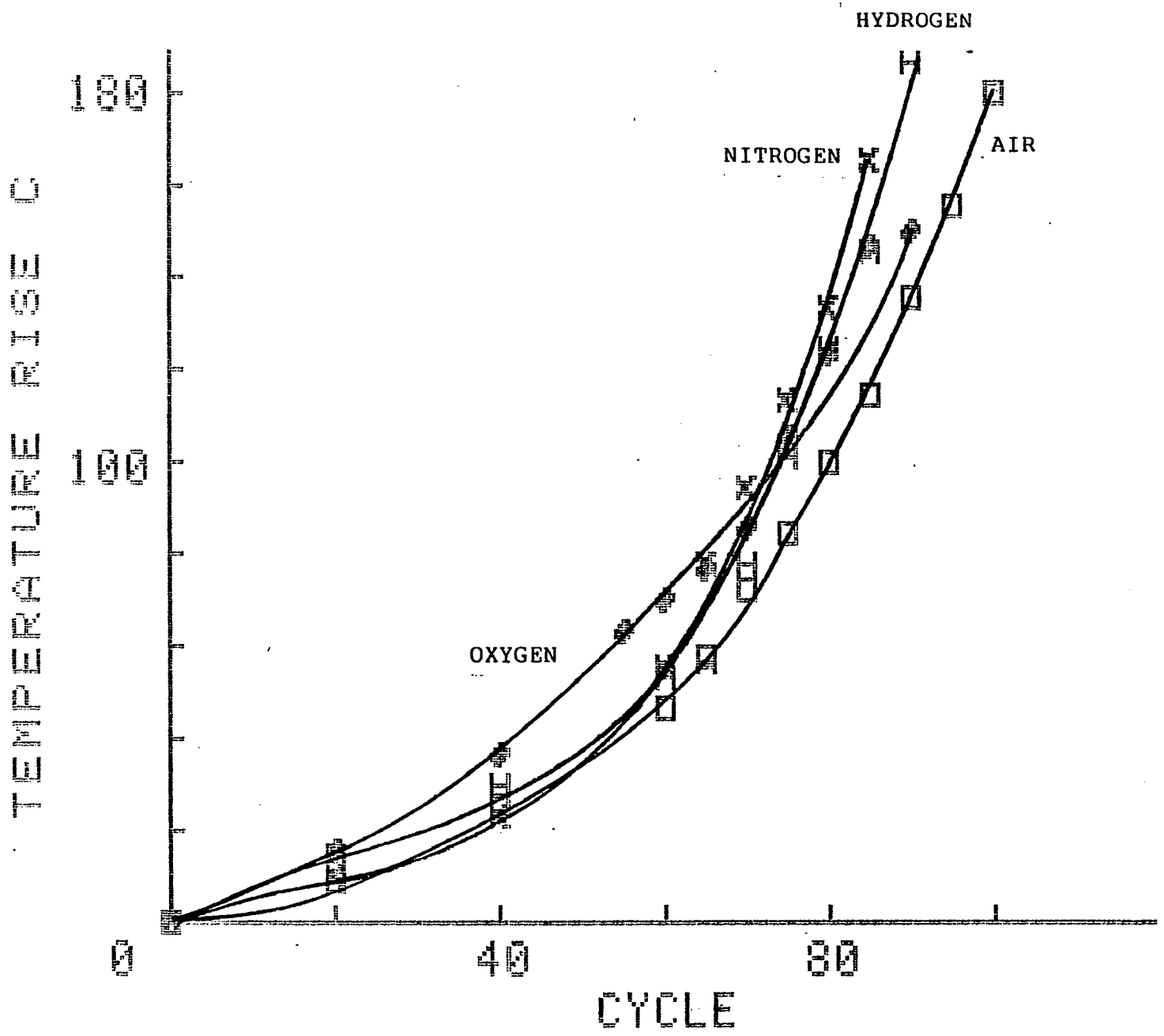

Fig. 3.9 Connectors with Inhibitor in Different Gases

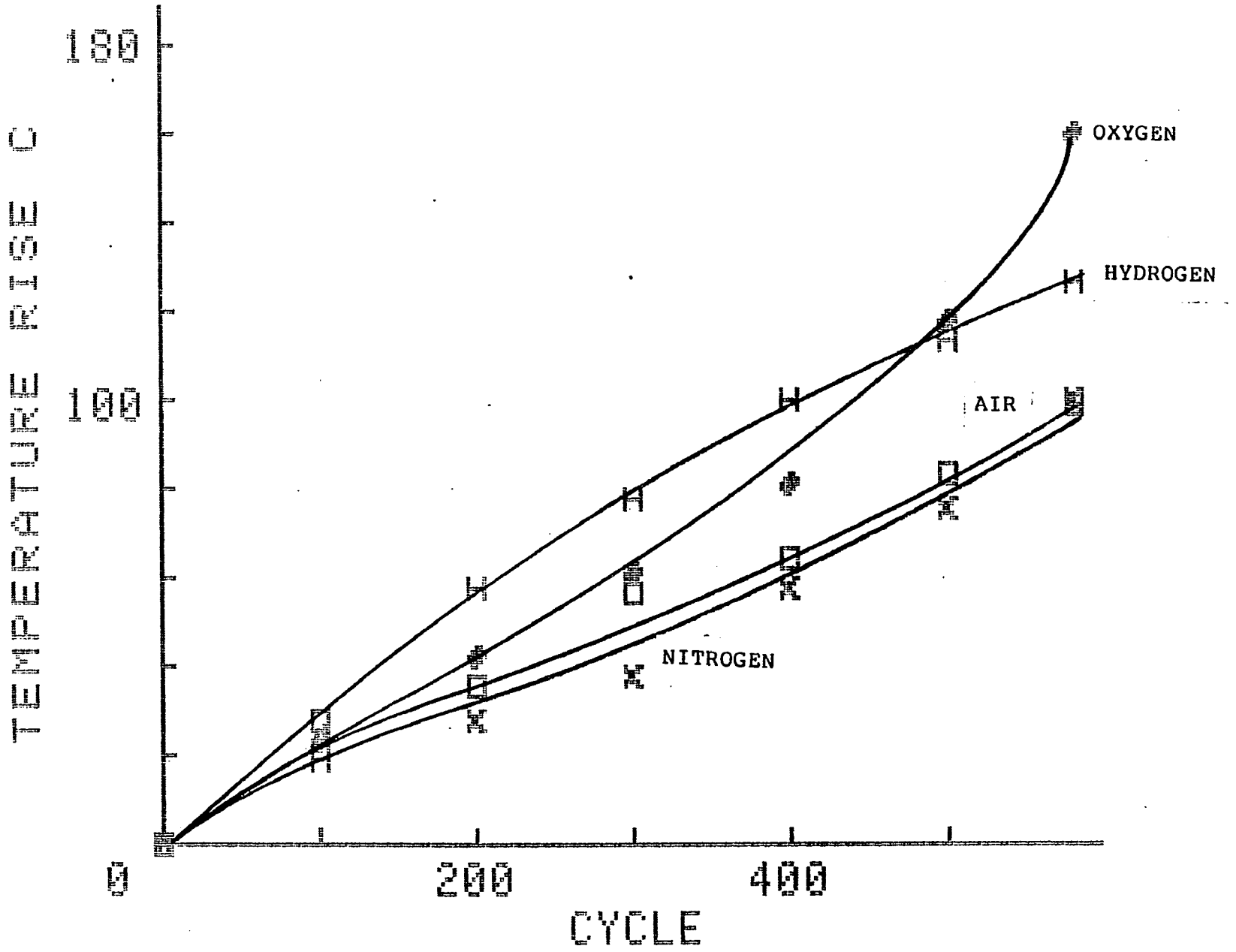

Fig. 3.10 Teethed Connectors in Different Gases.

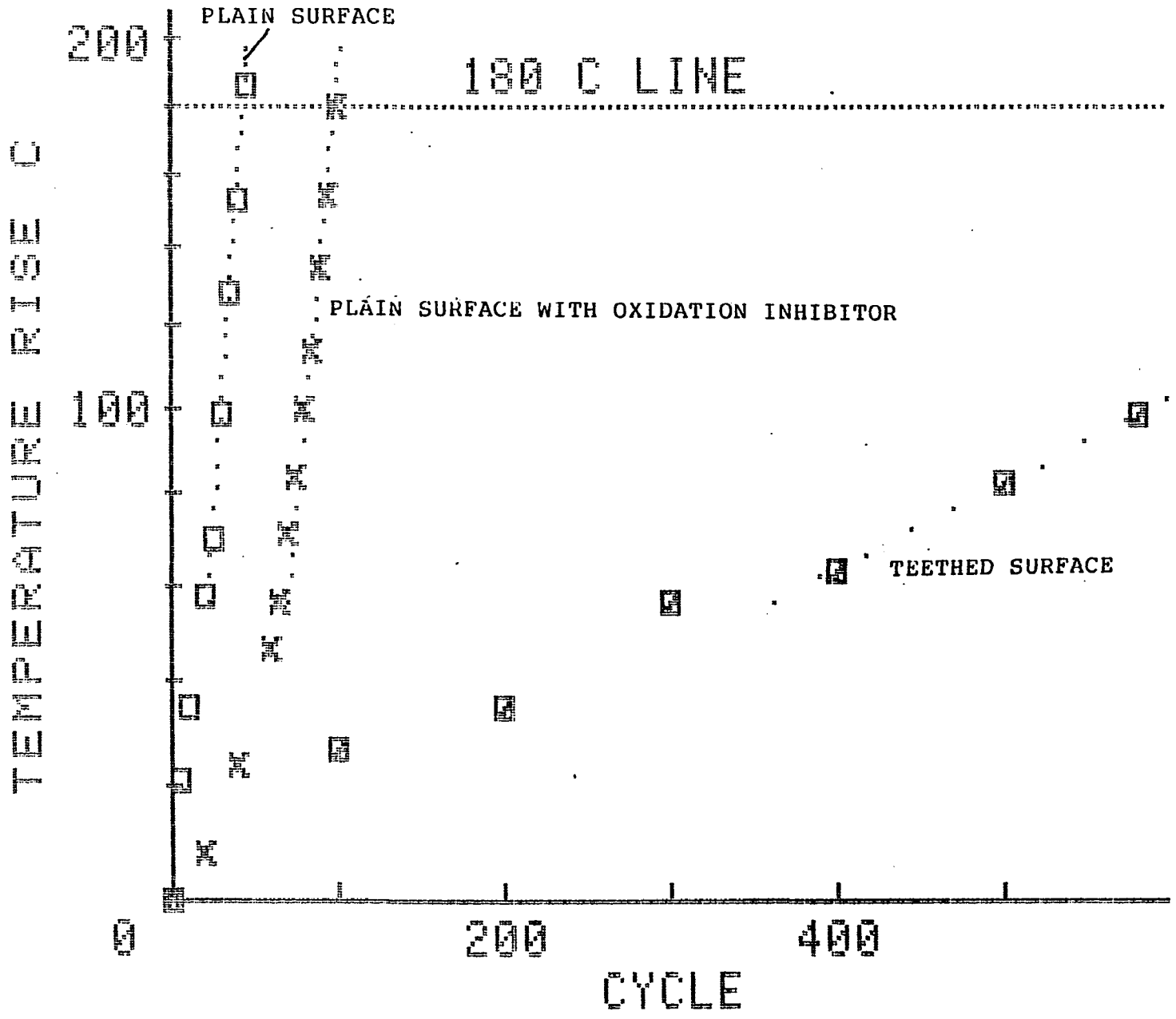

Fig. 3.11 Determination of the Connector Life in Air

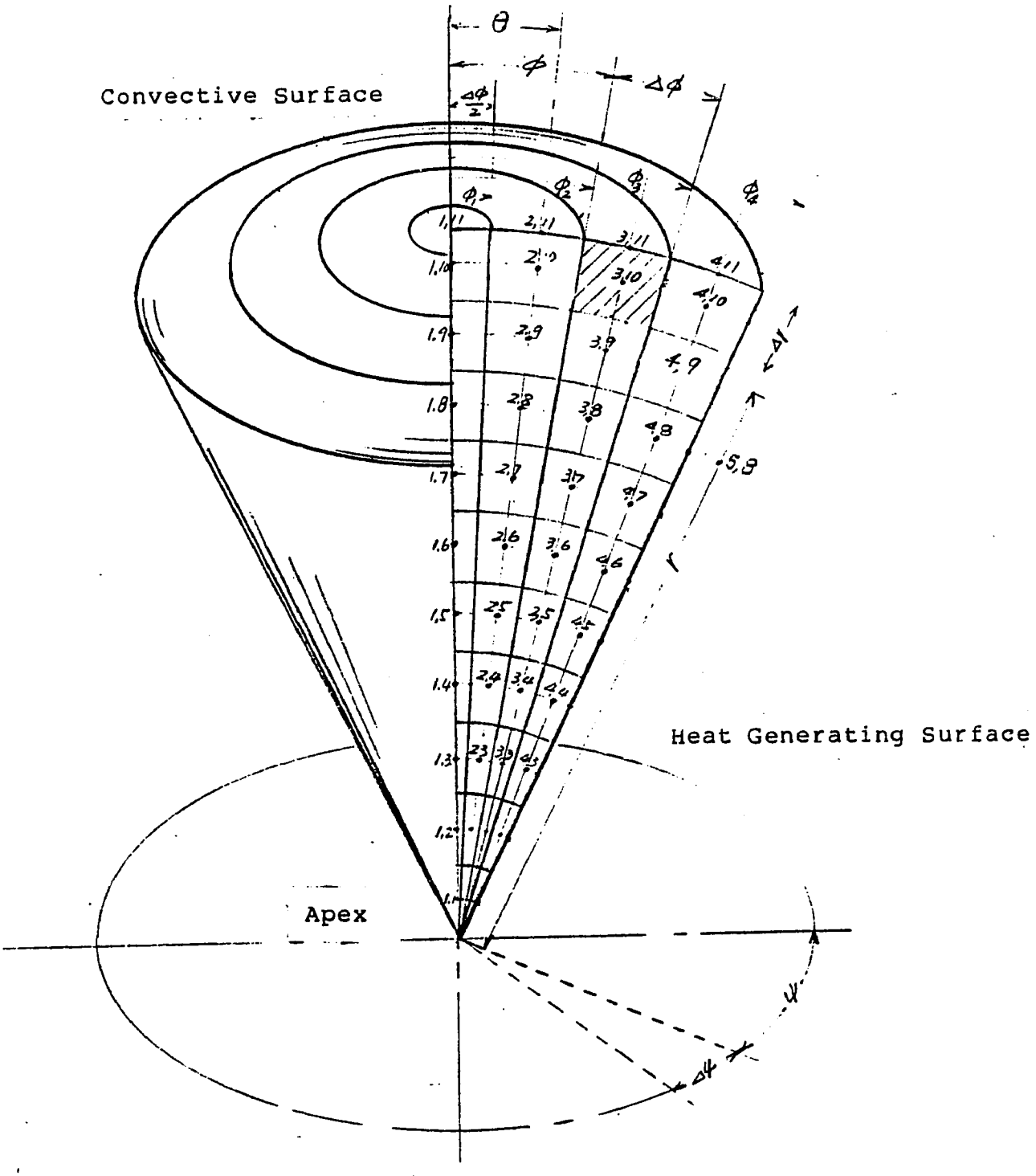

Fig. 4.1 Spherical Coordinate System and 4x10 Control Volumes for the Sphere Cut by a 15-degree Cone.

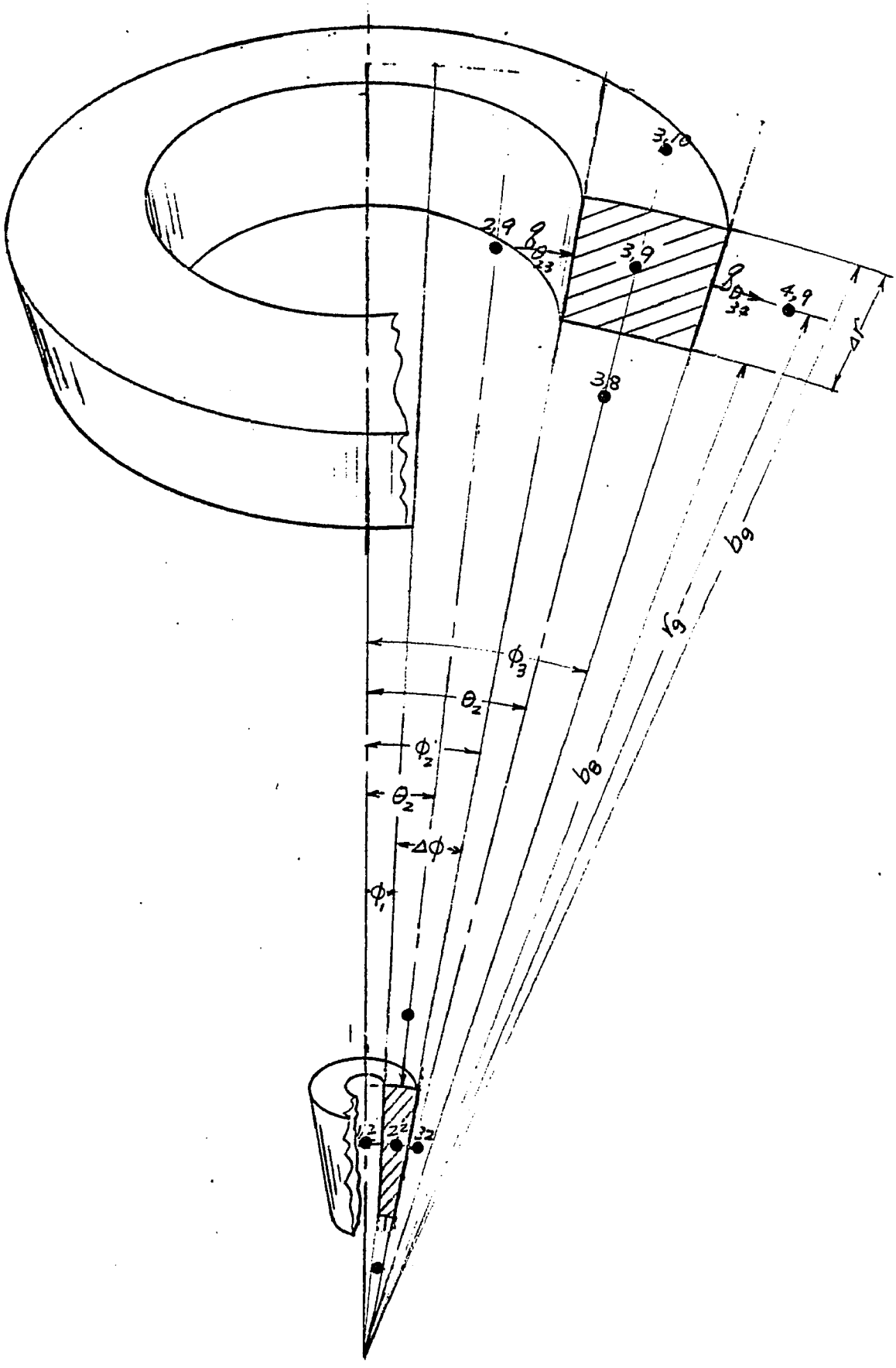

Fig. 4.2 Interior Control Volume (3,9)

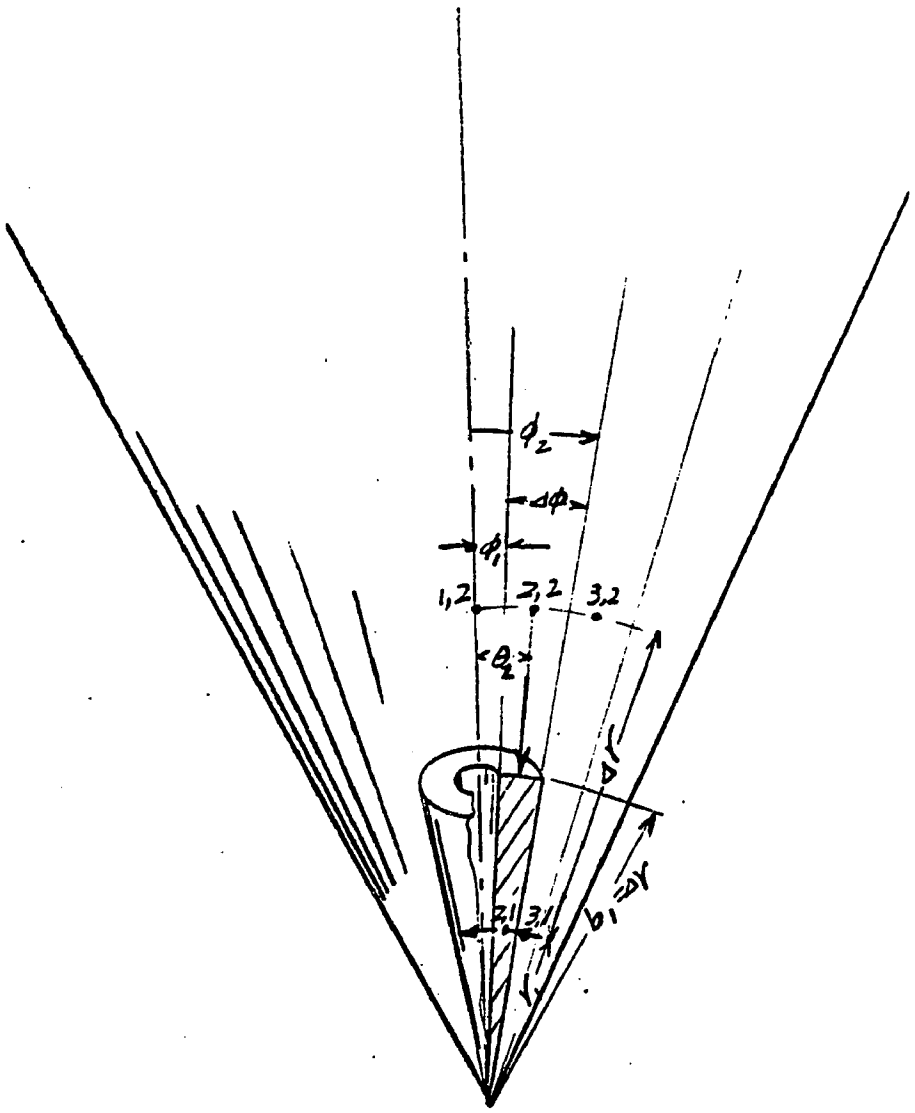

Fig. 4.3 Control Volume at the Center of the Sphere (or Apex)

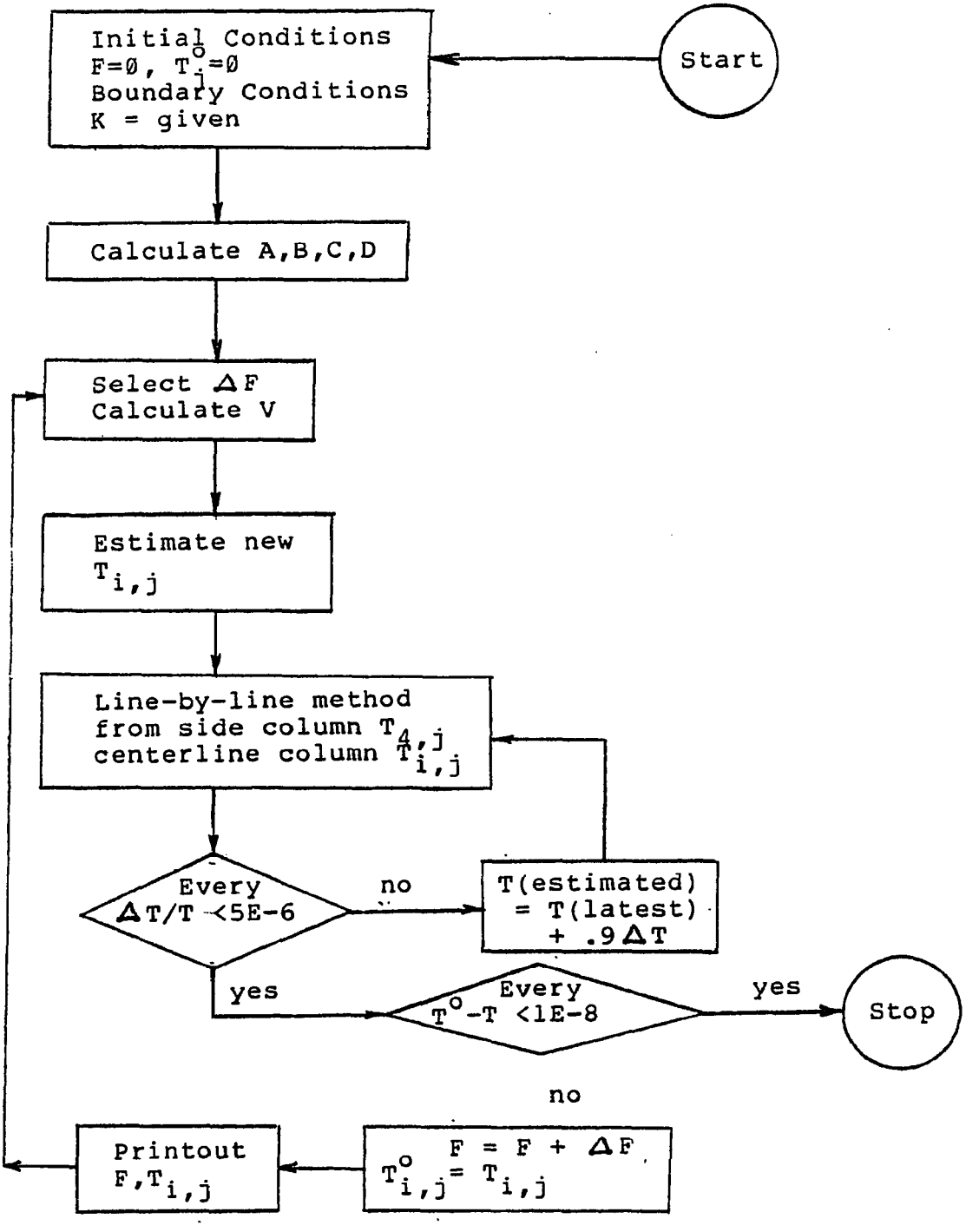

Fig. 4.4 Flow Chart for the Computer Program

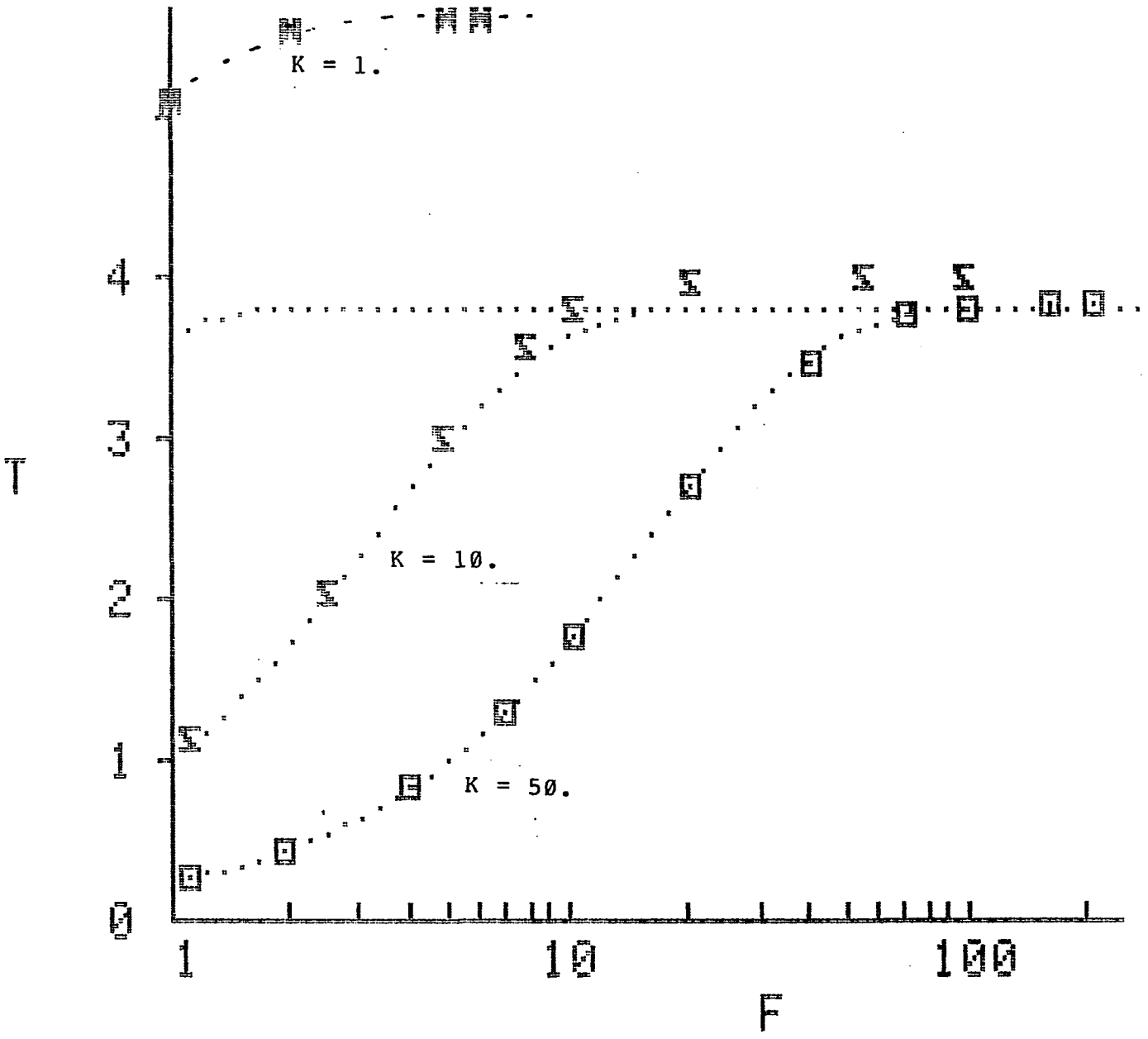

Fig. 4.5 Comparison with the Solution for Negligible Internal Resistance

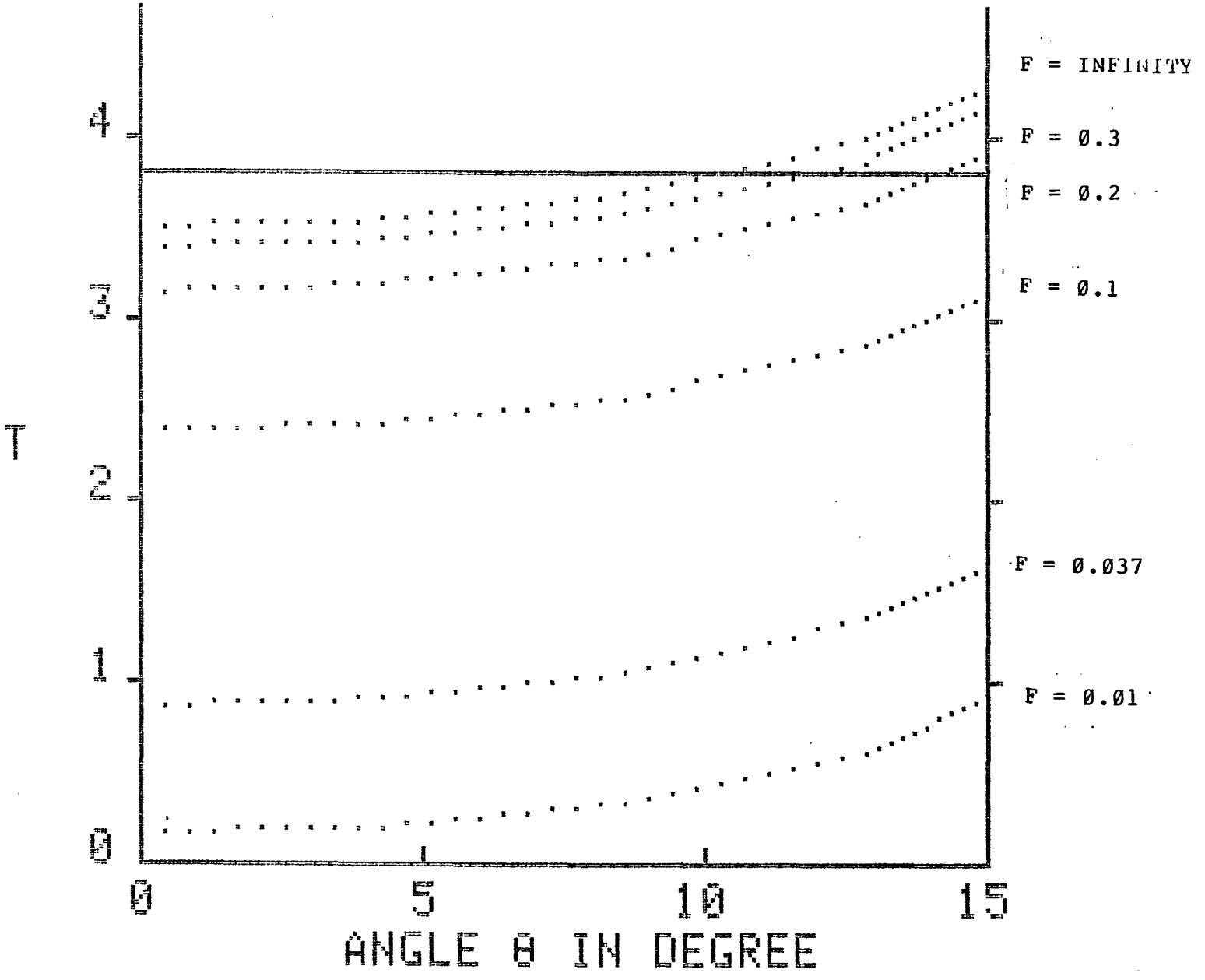

Fig. 4.6 Transient Temperature on the Convective Surface for K=Ø.1

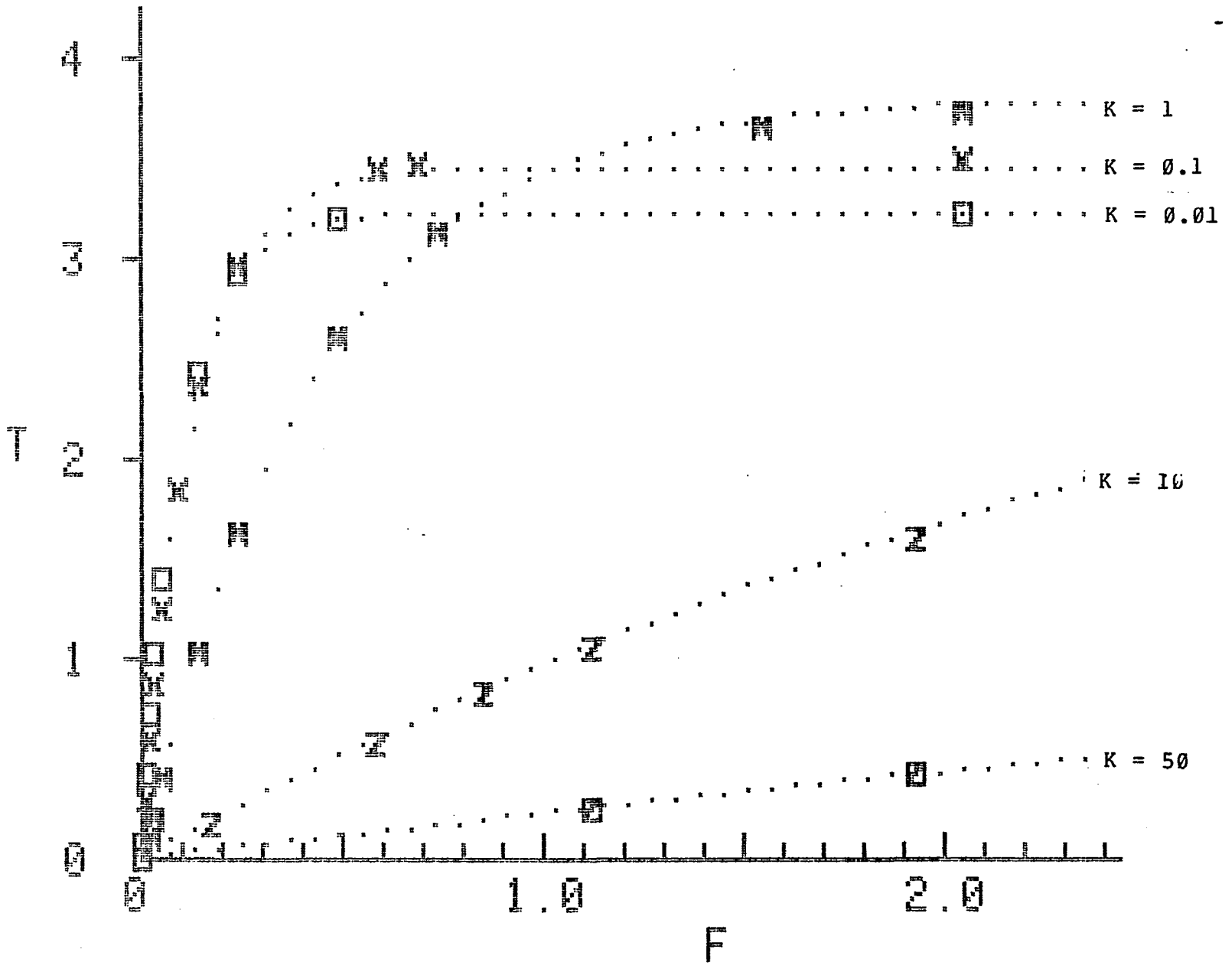

Fig. 4.7 Transient Temperature at the center of the Convective Surface for 0<F<2 and K=0.01 Through 10

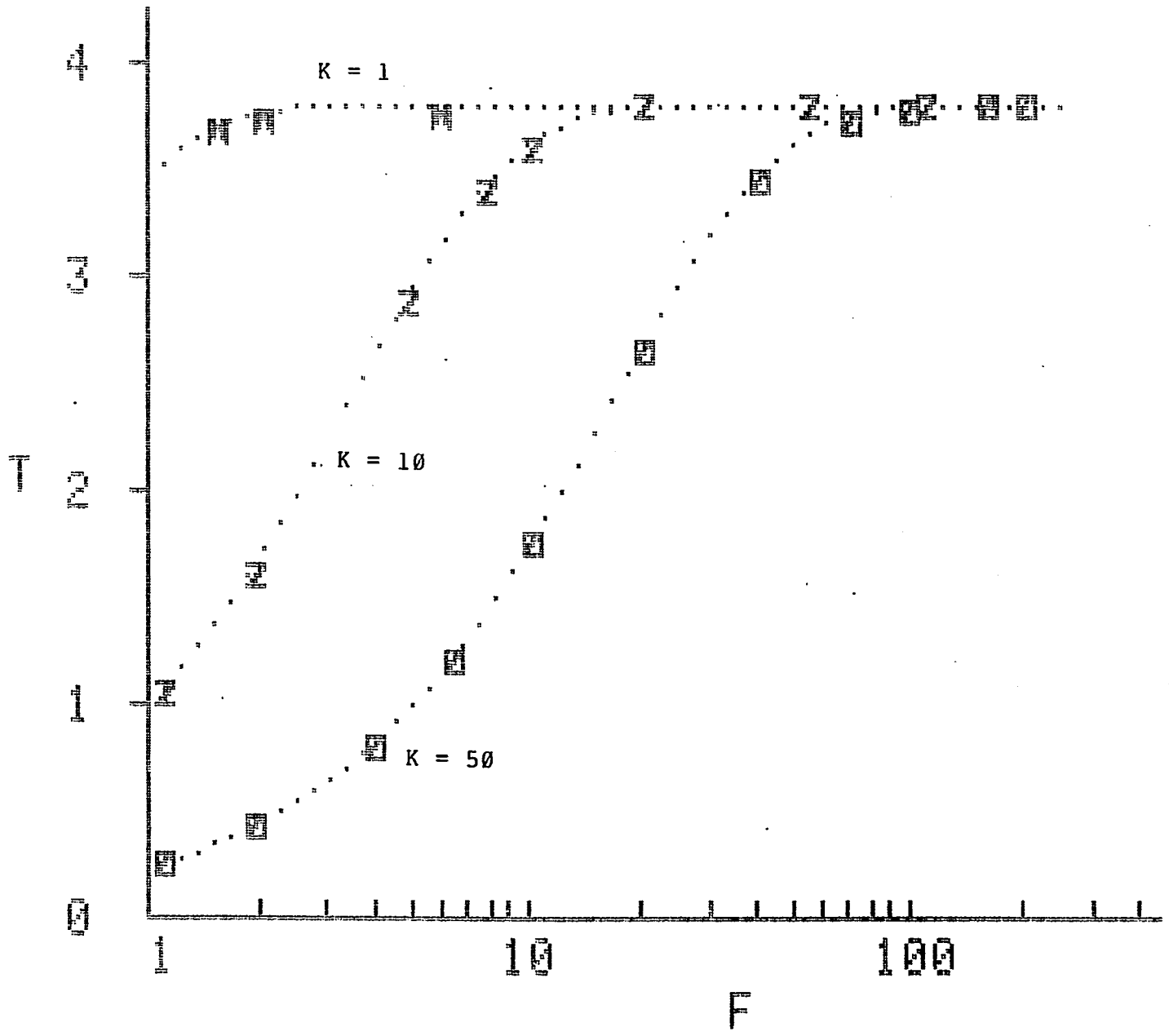

Fig. 4.8 Transient Temperature at the Center of the Convective Surface for 1<F<200 and K=1 Through 50

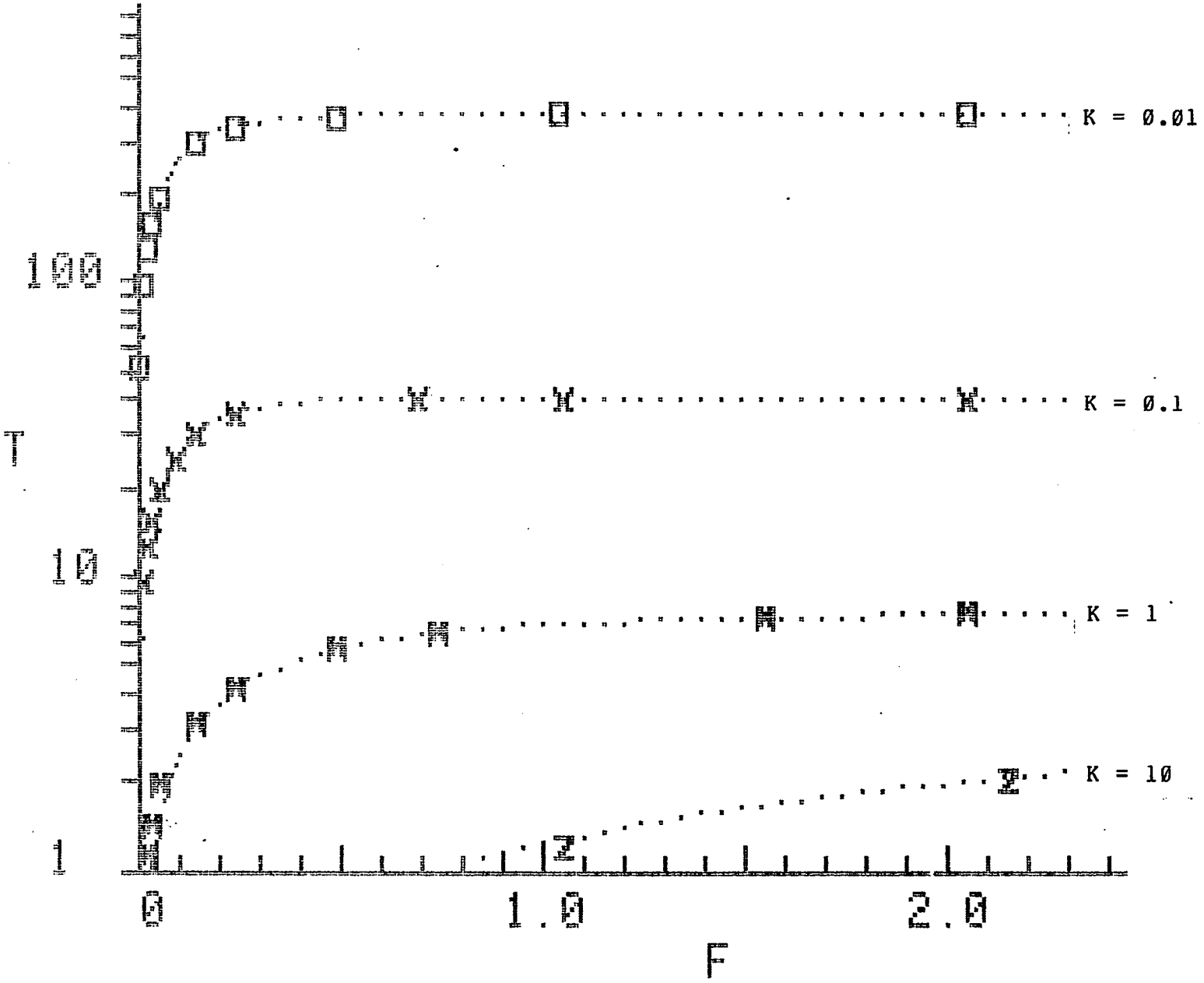

Fig. 4.9 Transient Temperature at the Apex, Nodal Point (1,1), for 0<F<2

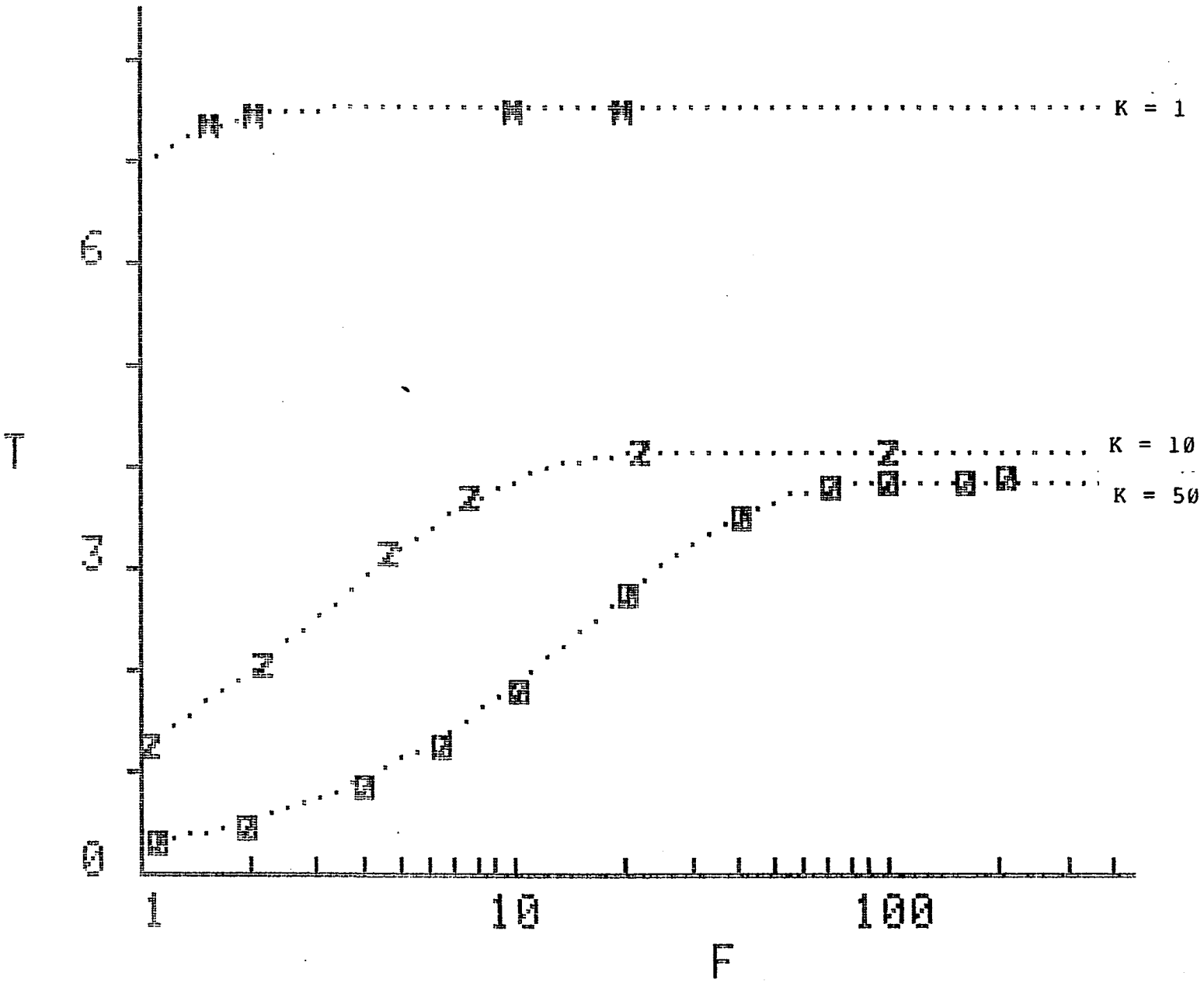

Fig. 4.10 Transient Temperature at the Apex for 1<F<300 and K=1 Through 50

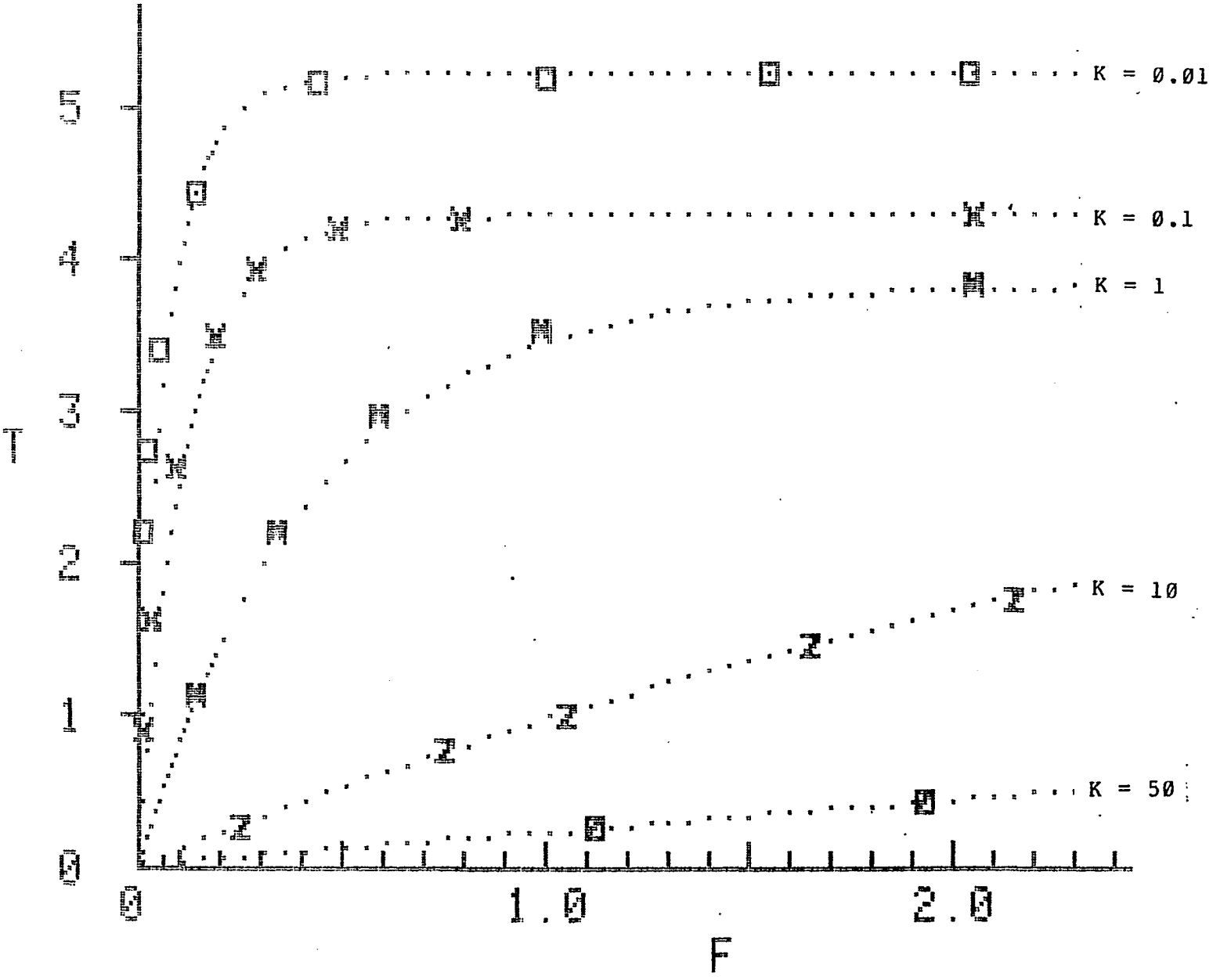

Fig. 4.11 Transient temperatures along the Circumpherence of the Convective Surface for 0<F<2

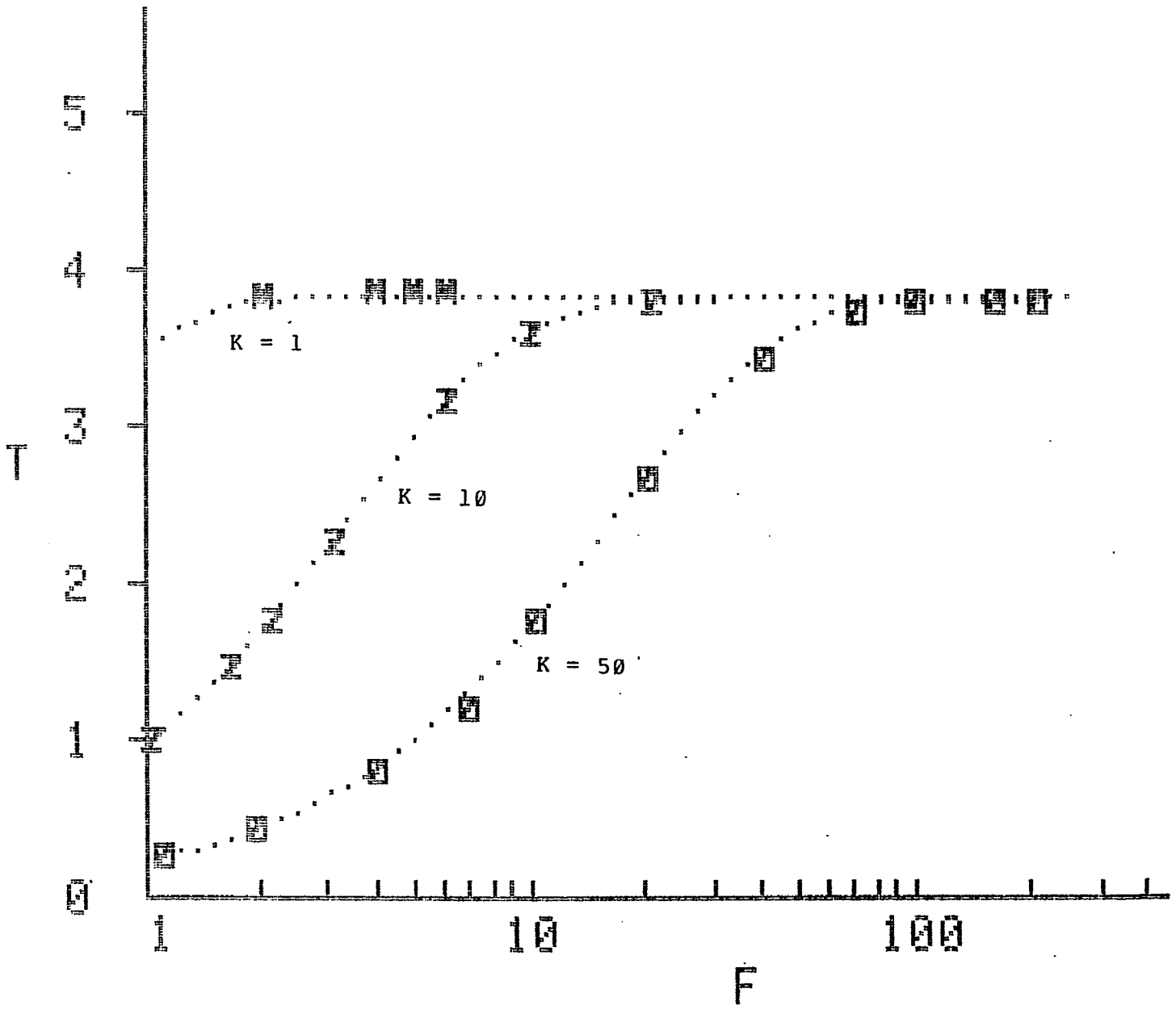

Fig. 4.12 Transient Temperature along the Circumpherence of the Convective Surface for 1<F<100 and K=1 Through 50

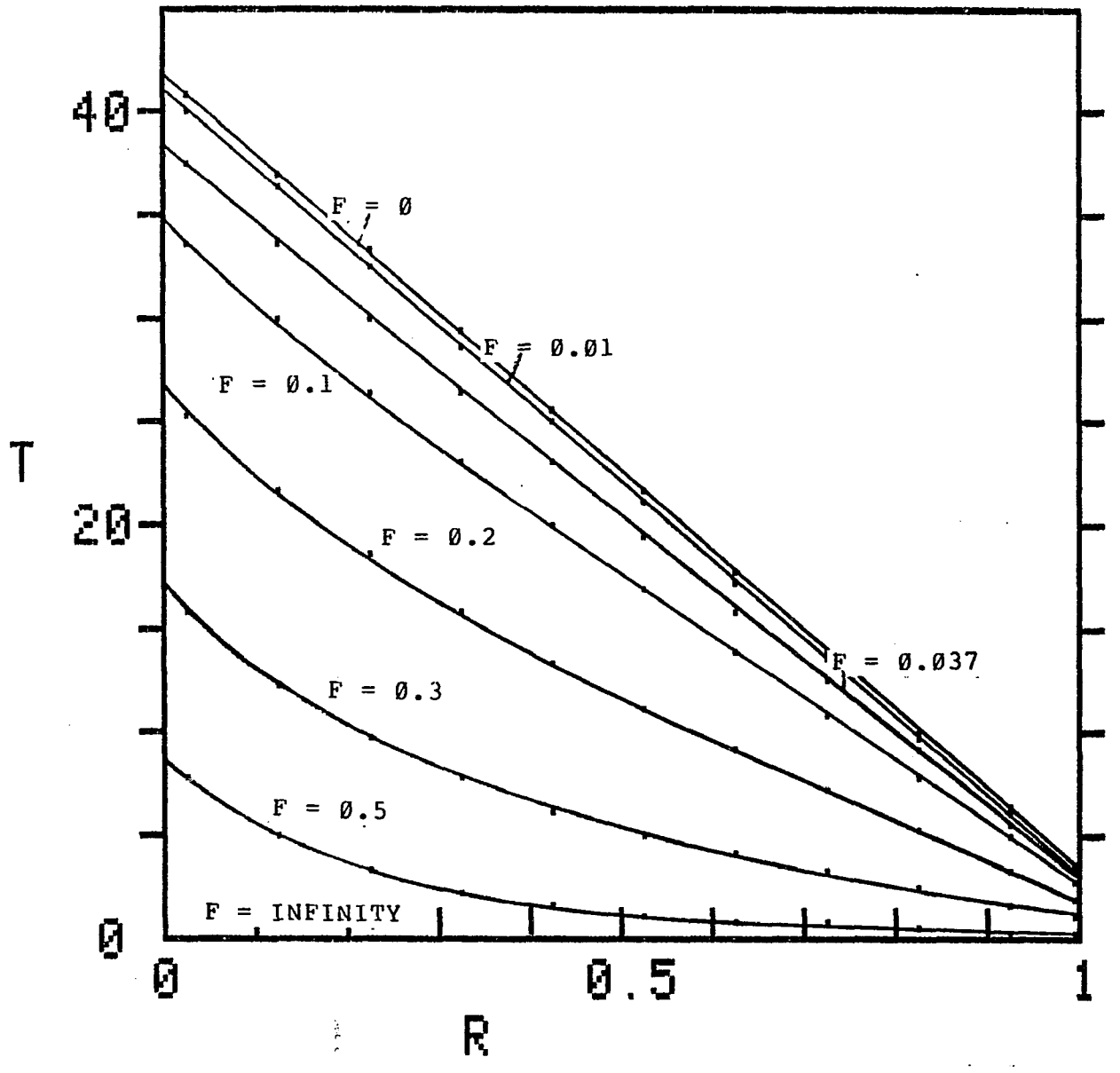

Fig. 4.13 Transient Temperature Distribution along the Centerline for K=0.1

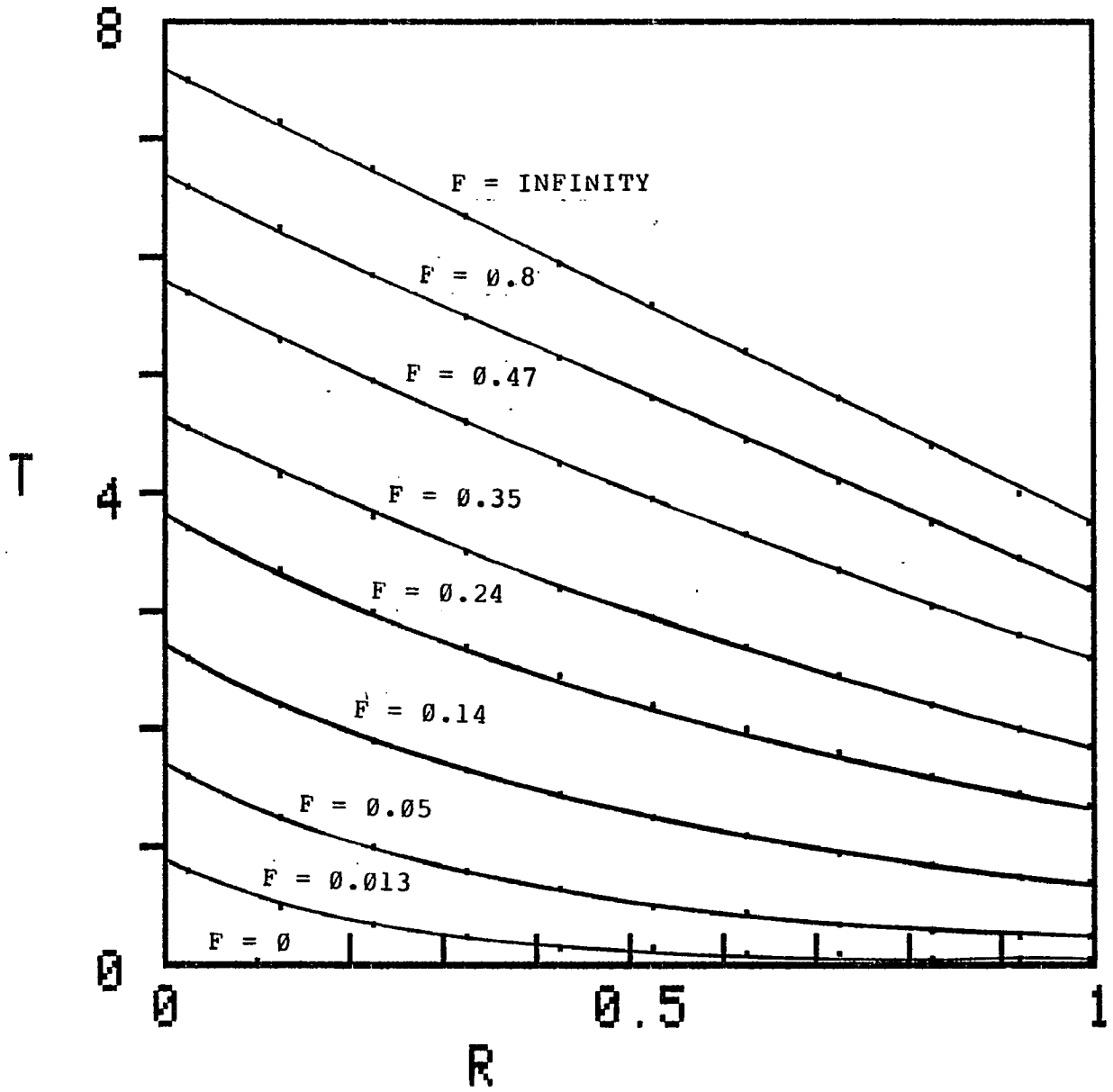

Fig. 4.14 Transient Temperature Distribution along the Centerline for K=1

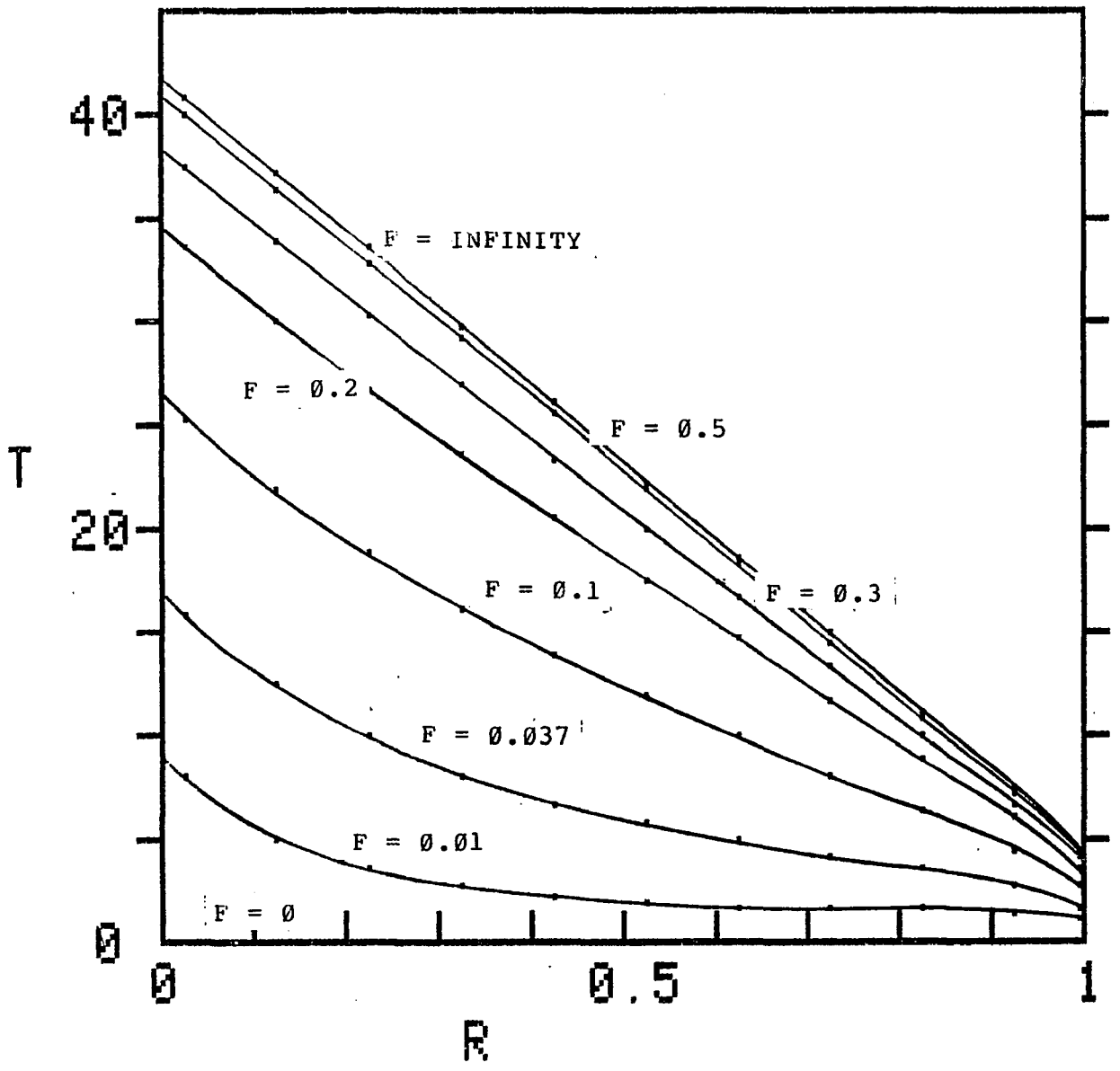

Fig. 4.15 Transient Temperature Distribution on the Heat Generating Surface for K=Ø.1

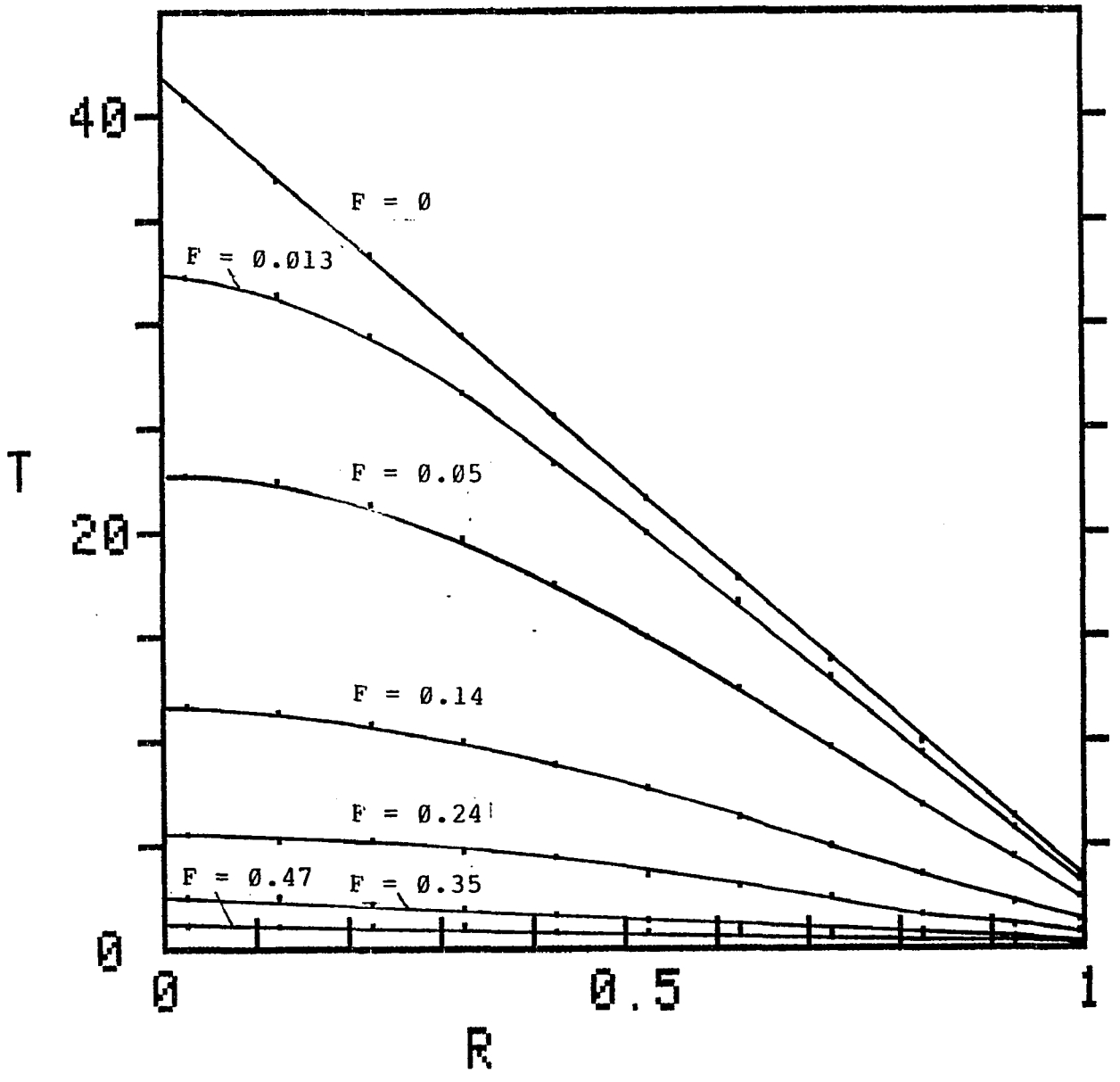

Fig. 4.16 Transient Temperature Distribution During Cooling Process alongthe Centerline for K=0.1

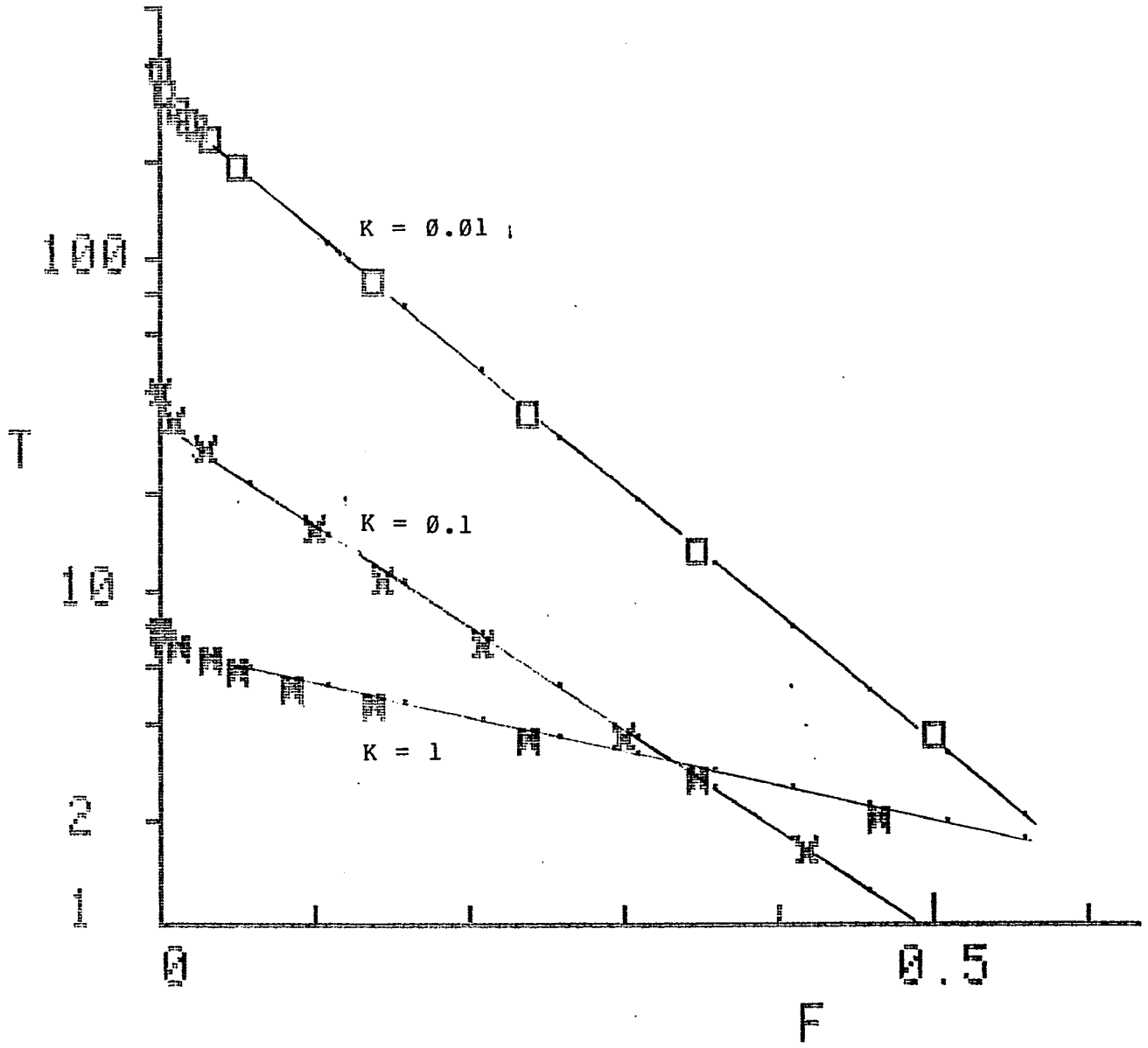

Fig. 4.17 Transient Temperature During Cooling at the Apex, Nodal Point (1,1), for Ø<F<Ø.5 and K=Ø.Ø1 Through 1

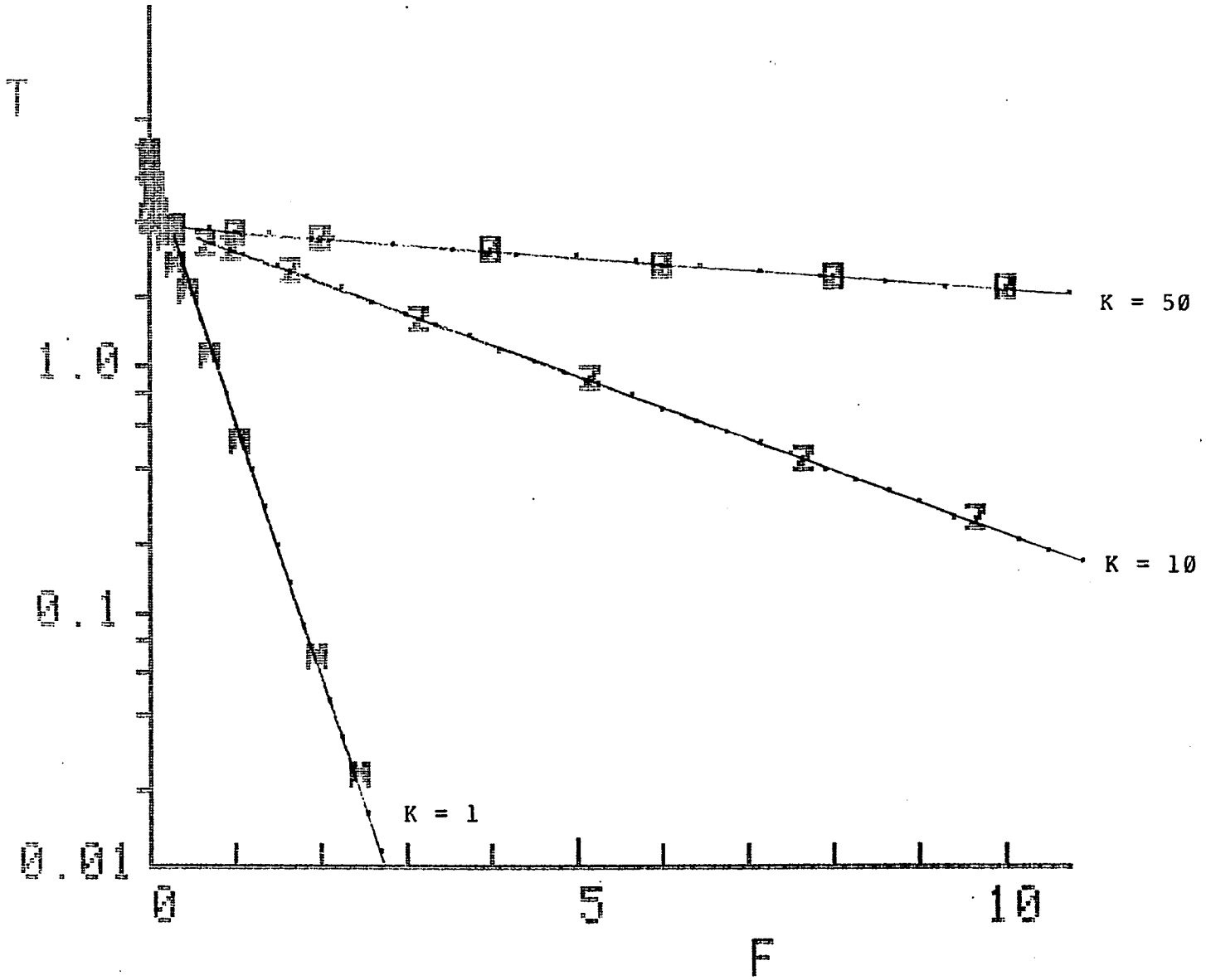

Fig. 4.18 Transient Temperature During Cooling at the Apex, Nodal Point (1,1), for 0<F<10 and K=1 Through 50

VITA

Name: Ted Lai-Che Kuo

Education:

New Jersey Inst. of Tech.	D.Sc.	1982
Kansas State University	M.S.	1966
Waseda University	B.S.	1963

Major: Mechanical Engineering

Experience: Fellow Engr., Thomas & Betts Co.

Publications:

1) Closed Form Solutions for Constant-Temperature Heating of Solids. ASEE Mechanical Engineering News, pp. 20-23 Feb. 1979

2) Joining Copper and Aluminum Conductors? - Try Cutting Tooth Connectors. Insulation/Circuits, Vol. 19 No. 6, June 1973

3) Insulation Piercing Magnet Wire Connectors. Published and Presented at 10th Electrical Insulation Conference, Chicago, Sept. 20-23, 1971

Patents:

Inventor(s)	Title	Patent No.	Issue Date
Weinmann Kuo	Method of Connecting Flat Electrical Cables	4,249,304	02/10/81
Weinmann Kuo Greenwood	Method for Electrical Connection of Flat Cables	4,249,303	02/10/81
Kuo Piasecki Grundfest	Installation Kit for Undercarpet Wiring System	4,258,974	03/31/81
Kuo	Flat Cable and Installing Method	4,219,928	09/02/80
Piasecki Kuo	Multiconductor Cable	4,283,593	08/11/81
Kuo	Self-Locking Clamp Member	4,248,493	02/03/81
Kuo	Bearing Means for a Rotatable Member	4,081,643	03/28/78
Kuo	Wiring Device	4,076,364	02/28/78
Kuo	Electrical Splice	3,846,577	11/05/74
Kuo	Inspectable-Corrosion Resistant Electrical Connector	3,805,221	04/16/74
Kuo	Method of Making an Electrical Connection between an Aluminum Conductor and a Copper Sleeve	3,956,823	05/18/76
Kuo	Foil Connector	3,752,901	08/14/73
Kuo	Multi-Orificed Electrical Connector	3,728,473	04/17/73
Kuo	Modular Connector	3,950,064	04/13/76
Piasecki Kuo	Die Set	3,616,674	11/02/71
Kuo	Multicompartment Connector	3,715,705	02/06/73
Kuo	Insulation Piercing Connector	3,549,786	12/22/70
Kuo	Insulation Piercing Connector	3,514,527	05/26/70
Kuo	Connector for Electrical Conductors with Deformable Side Panels for Contact with Such Conductors	3,515,795	06/02/70

Inventor(s)	Title	Serial No.	Filing Date
Greenwood Piasecki Kuo	Undercarpet Wiring System Installation Kit (Allowed 07/29/81)	42,539	05/25/79
Weinmann Kuo Greenwood	Method for Electrical Connection of Flat Cables (Reissue of 4,249,303)	287,463	07/27/81